Universidade de Aveiro
2019

Departamento de Química

DIOGO RAFAEL PACHECO RIBEIRO

SEPARAÇÃO DE COMPOSTOS BIOATIVOS RECORRENDO À TECNOLOGIA DE LEITO MÓVEL SIMULADO

BIOACTIVE COMPOUNDS SEPARATION WITH SIMULATED MOVING BED TECHNOLOGY

Universidade de Aveiro
2019

Departamento de Química

DIOGO RAFAEL PACHECO RIBEIRO

SEPARAÇÃO DE COMPOSTOS BIOATIVOS RECORRENDO À TECNOLOGIA DE LEITO MÓVEL SIMULADO

BIOACTIVE COMPOUNDS SEPARATION WITH SIMULATED MOVING BED TECHNOLOGY

Dissertação apresentada à Universidade de Aveiro para cumprimento dos requisitos necessários à obtenção do grau de Mestre em Engenharia Química, realizada sob a orientação científica do Doutor Carlos Manuel Santos da Silva, Professor Associado do Departamento de Química da Universidade de Aveiro e co-orientação do Doutor José Pedro Salgado de Castro Aniceto, bolseiro de Pós-Doutoramento da Universidade de Aveiro.

o júri

Presidente

Profª. Doutora Maria Inês Purcell de Portugal Branco
Professora auxiliar do Departamento de Química da Universidade de Aveiro

Doutor António Augusto Areosa Martins
Investigador de Pós-Doutoramento no Laboratório de Engenharia de Processos, Ambiente, Biotecnologia e Energia da Faculdade de Engenharia da Universidade do Porto

Doutor José Pedro Salgado de Castro Aniceto
Bolseiro de Pós-Doutoramento da Universidade de Aveiro

agradecimentos

Em primeiro lugar, agradeço ao meu orientador, Doutor Carlos Silva, por toda a sabedoria transmitida, pelo contínuo acompanhamento e preocupação que precede a minha matrícula em Engenharia Química e pela boa disposição do costume. A todas as pessoas ligadas de alguma forma ao grupo EgiChem, pela facilidade de adaptação e por todo o apoio. Ao José Pedro Aniceto, por acompanhar o trabalho e se mostrar sempre pronto a ajudar. Ao Ivo Azenha, por toda a paciência e esforço, por me acompanhar ao longo deste semestre e por estar sempre disponível. À Doutora Mónica Valéga, por me auxiliar sempre que necessário.

Agradeço também à Universidade de Aveiro e a todos os professores que de certa forma me influenciaram. A todos os amigos que fiz durante a minha Licenciatura em Química. A todas as pessoas que me acolheram e que fizeram parte da minha vida após a minha integração em Engenharia Química. A todos os meus amigos, que tornam a minha vida muito mais interessante.

À minha tia Alcina, por me proporcionar esta oportunidade, à minha avó, por ter tomado sempre conta de mim, à minha tia, por toda a dedicação ao longo da vida e às minhas primas, porque sem elas não tinha ninguém para me chatear a cabeça. Ao meu avô, porque quem não sabe ler vê os bonecos.

Por fim, à Rita, por estar sempre presente na minha vida, nos bons e maus momentos, pelo apoio, amizade e compreensão.

palavras-chave

ácidos triterpénicos, adsorção, cromatografia líquida de alta eficiência, curvas de rutura, isotérmica, leito móvel simulado

resumo

A indústria farmacêutica tem manifestado um crescente interesse em compostos naturais com propriedades biológicas e nutricionais. Os ácidos betulínico e oleanólico são dois ácidos triterpénicos que ocorrem naturalmente na natureza e que possuem tais características. Estes dois compostos podem ser extraídos de recursos naturais, tais como da casca do *Eucalyptus globulus*. No entanto, a sua separação é difícil, pois os compostos apresentam estruturas muito semelhantes (são isómeros constitucionais).

Neste trabalho estudou-se a separação cromatográfica de uma amostra representativa dos extratos de *E. globulus* dos ácidos betulínico e oleanólico. Inicialmente foram realizados testes cromatográficos em cromatografia líquida de alta eficiência, recorrendo à fase estacionária Acclaim C30. Através destes ensaios determinou-se que a fase móvel metanol/acetonitrilo 50/50 (%, v/v) é a mais adequada para a separação destes ácidos triterpénicos.

De modo a averiguar as constantes de equilíbrio (H_i) e os coeficientes globais de transferência de massa (K_{LDF}), foram determinadas as curvas de rutura dos ácidos puros (soluções unárias). Estes parâmetros foram correlacionados recorrendo a dados experimentais e posteriormente validados pela simulação da curva de rutura de uma mistura binária contendo a mesma proporção de ácido betulínico e oleanólico encontrada no *E. globulus*. Os dados advindos deste ensaio foram modelados pela solução analítica de Carta. Paralelamente, foi também usado o método dos momentos para obter os parâmetros de transporte. Os resultados obtidos foram consistentes.

Por fim, estudou-se a separação dos ácidos betulínico e oleanólico por leito móvel simulado (SMB), realizando simulações utilizando os parâmetros de transporte obtidos anteriormente pela modelação das curvas de rutura. Foram adotadas duas configurações diferentes (1-1-1-1 e 2-2-2-2) e diferentes comprimentos de coluna (variando dos 10 aos 25 cm), usando os parâmetros de transporte obtidos. Foi concluído que usando uma unidade SMB é possível separar os ácidos betulínico e oleanólico com purezas superiores a 99 % tanto no extrato como no rafinado para todos os cenários apresentados.

Posteriormente, foi analisada a recuperação dos ácidos triterpénicos das correntes de extrato e rafinado de um futuro processo, tirando vantagem da sua baixa solubilidade em água. Por conseguinte, a solubilidade de cada ácido triterpénico em misturas de solventes com o aumento da concentração de água foi medida e discutida.

keywords

adsorption, breakthrough curves, high performance liquid chromatography, isotherm, simulated moving bed, triterpenic acids

abstract

The pharmaceutical industry is developing a growing interest in natural compounds with biological and nutritional properties. Betulinic and oleanolic acids are two naturally occurring triterpenic acids, which possess such characteristics. These two compounds can be extracted from natural resources, *i.e.*, from the bark of *Eucalyptus globulus*. However, their separation is difficult because these compounds present similar structures (they are constitutional isomers).

In this work, the chromatographic separation of betulinic and oleanolic acids from representative extracts of *E. globulus* was studied. High performance liquid chromatography (HPLC) assays were initially performed using an Acclaim C30 column as stationary phase. Through these tests it was found that the mobile phase methanol/acetonitrile 50/50 (%, v/v) is the most suitable for the separation of both triterpenic acids.

In order to determine the equilibrium constants (H_i) and the global linear driving force mass transfer coefficients (K_{LDF}), several breakthrough experiments of pure acids (unary solutions) were carried out. The two parameters were correlated using experimental data and then validated by simulating the breakthrough curve of a binary mixture containing the same proportion of betulinic and oleanolic acids found in *E. globulus* extracts. The outcomes of all experiments were modeled using Carta's analytical solution. In parallel, the method of moments was also used to obtain the transport parameters. The results were consistent.

Lastly, the separation of betulinic and oleanolic acids by simulating moving bed (SMB) has been studied, carrying out simulations using the transport parameters obtained before from the breakthrough assays. Two different column configurations (1-1-1-1 and 2-2-2-2) and column lengths (from 10 to 25 cm) were adopted. It was concluded that using an SMB unit is able to separate betulinic and oleanolic acids with purity higher than 99 % both in extract and raffinate for all the scenarios presented.

Posteriorly, the recovery of both triterpenic acids from the extract and raffinate streams of a future process was also investigated, taking advantage of their low solubility in water. Accordingly, the solubility of each triterpenic acid in solvent mixtures of increasing water concentration was experimentally measured and discussed.

Nomenclature

List of abbreviations

A	Asymmetry
AARD	Average absolute relative deviation
ACN	Acetonitrile
b_i	Equilibrium constant of the compound
BA	Betulinic acid
C^*	Liquid phase concentration in equilibrium with q*
C_i	Concentration of component *i* in the fluid
C_i^F	Feed (upstream) concentration
CSS	Cyclic steady state
d_i	Internal diameter of the column
d_p	Particle diameter
D_{ax}	Axial dispersion coefficient
DoE	Design of Experiments
EE-SMB	Enriched Extract operation
E. globulus	Eucalyptus globulus
EtOH	Ethanol
H_i	Equilibrium constant
HETP	Height equivalent to a theoretical plate
HPLC	High performance liquid chromatography
k'	Retention factor
K_{LDF}	Global linear driving force driving force mass transfer coefficient
L	Column length
LDF	Linear Driving Force
$LW_{5\%}$	Left peak width at 5% of peak height
MeOH	Methanol
m_j	Ratio between fluid and solid flow rates
N	Theoretical plate number

N_{LDF}	Number of global mass transfer units
OA	Oleanolic acid
Pe	Peclet number
Prod	Productivity
PuR	Purity of raffinate
PuX	Purity of extract
Q	Flow rate
Q_A	Adsorbent capacity
Q_j	Volumetric flow rate in section j for TMB unit
Q_j^*	Volumetric flow rate in section j for SMB unit
Q_S	Solid flow rate
q^*	Solid phase concentration in equilibrium with liquid phase
R	Resolution
RecR	Recovery of raffinate
RecX	Recovery of extract
$RW_{5\%}$	Right peak width at 5% of peak height
SC	Solvent consumption
SFE	Supercritical fluid extraction
SF-SMB	Supercritical SMB
SMB	Simulated moving bed
t	Time
t^*	Switch time interval
t_0	Dead time of the column (for total liquid hold-up)
$t_{0,int}$	Dead time of the column (for interstitial liquid hold-up)
$t_{elution}$	Duration of elution period in Carta's solution
t_{feed}	Feed pulse duration in Carta's solution
t_{plant}	Dead time of the plant without column
$t_{r,i}$	Retention time of compound i
$t_{r,i,net}$	Retention time of compound i
$t_{ref,peak}$	Retention time of the reference peak

t_{total}	Total dead time
TMB	True moving bed
q_i	Solid phase concentration
u_i	Linear velocity
u_{inst}	Interstitial velocity
u_{solid}	Solid velocity in the TMB
u_0	Superficial velocity
UV	Ultraviolet
UV/Vis	Ultraviolet-visible spectroscopy
v	Heterogeneity parameter
v	Interstitial velocity of the fluid in the TMB
v^*	Interstitial velocity of the fluid in the SMB
V_c	Column volume
V_{loop}	Volume of the loop
w_h	Peak width at half height
$w_{h,ref,peak}$	Peak width at half height of the reference peak
z	Position variable

Greek letters

α	Selectivity
β	Safety margin
ε	Bed porosity of the column
ε_p	Particle porosity
ε_t	Total porosity of the column
λ	Wavelength
μ_i	i^{th} central moment in moment analysis method
μ_f	Fluid viscosity
ξ_i	Capacity parameter
ρ_f	Fluid density
σ^2	Variance

τ	Space time

Subscripts and superscripts

A	More retained compound
B	Less retained compound
calc	Calculated
E	Solvent, eluent or desorbent
exp	Experimental
F	Feed
i	Compound
j	Column
R	Raffinate
X	Extract
I, II, III, IV	SMB and TMB sections

Index

Objectives and structure of the thesis

The interest of pharmaceutical industry in natural products possessing a wide range of biological and/or nutritional properties is increasing. The fact is inducing researchers to investigate alternative sources for such compounds, mainly from biomass. Accordingly, the main objective of this dissertation is to study the separation of a binary mixture composed by two natural occurring triterpenic acids – betulinic acid and oleanolic acid – through simulated moving bed (SMB).

To research plan towards the separation of triterpenic acids were selected the mobile and stationary phases, determined and validated the transport parameters and performed the SMB simulations. In order to obtain the equilibrium constant and the global linear driving force mass transfer coefficient of both compounds, two methods were used. In the first one, the parameters were obtained fitting a chromatographic model to the experimental breakthrough curves, while in the second one they were determined through the method of moments. The results were compared in order to assess the methods viability and then used to perform the SMB simulations.

Additionally, aiming at the recovery of the pure molecules (betulinic and oleanolic acids) from the SMB raffinate and extract streams, respectively, a solubility study was experimentally performed. The compounds were dissolved in the chromatographic mobile phase and increasing amounts of water were added. Since water decreases the solubility of the two acids, their recovery can be easily accomplished by precipitation and subsequent filtration/centrifugation from the raffinate and extract streams of a future SMB unit.

In terms of structure, this thesis is divided into five chapters. The first chapter presents a review of the reported theoretical concepts. The second chapter contemplates several aspects of the modeling of the adsorption system, which are the basis for the study of the preparative chromatographic processes investigated in this work. The third chapter refers to the materials, equipments and methods used for the execution of laboratory experiments. The fourth chapter presents all obtained results, including their detailed analysis and discussion. Finally, the fifth chapter encloses this work by gathering its conclusions and future perspectives.

Chapter 1

Introduction

Fossil fuel usage to produce energy is the main reason behind climate changes. The high dependence on non-renewable energies and anthropogenic climate change are two wired problems.[1] The overexploitation of fossil energy leads to the decay of its reserves, which compels researchers to seek new sustainable resources. Among sustainable resources, biomass is one of the most promising, hyped and heavily subsidized renewable energy source.[2] Biomass is the organic material derived from living plants and through biorefinery it is possible to convert it into biofuels, high added-value chemical products and biomaterials.[3] Besides being easily available in nature, biomass only emits carbon dioxide that has been previously absorbed by plants (emission balance is null). However, the increased use of biomass for energy production may threat conservation areas, cause deforestation and pollute water resources, since liquid biofuel contributes to the acid rain formation and decreases food security.[2]

A biorefinery is an industrial facility that converts biomass in bio-based products (*e.g.* food and chemicals) and bioenergy (*e.g.* biofuels, power and heat). In biorefinery, almost all types of biomass raw materials can be converted into different classes of biofuels and biochemicals. Ultimately, the priority is to use resources, methods and techniques with reduced impact to the environment and to obtain green and sustainable final products.[4]

Besides being an interesting primary resource, biomass is widely used for the extraction of other molecules, known as natural products. These compounds represent an important source of drugs, considering the wide diversity of molecules with medicinal potential.[5] Until a few years ago, they have been forgotten, mainly because the key compounds present in natural products are often in small concentrations.[6] Terpenes are the largest class of natural products and their characteristics depends on physical, chemical and biological properties. They are mostly used in the industry as flavours, cosmetic products, fragrances, and pharmaceuticals.[7]

This dissertation will focus on a subgroup of terpenes, more specifically triterpenic acids, compounds that are abundant in the nature. The main goal is the separation of a binary mixture of two triterpenic acids, betulinic acid (BA) and oleanolic acid (OA), through high performance liquid chromatography (HPLC) techniques, in order to perform their isolation by simulated moving bed (SMB) technology.

1.1. Triterpenic Acids

Terpenes are organic compounds produced mainly by plants which are widely abundant in nature. In mammals, terpenes are involved in the stabilization of cell membranes and in metabolic pathways as regulators of enzymatic reactions. The biotransformation of terpenes allows the production of stereoselective compounds, that may be considered as natural products.[8] Triterpenic acids are terpenes with six isoprene units that can be found in several plants, fruits and vegetables.

In Portugal, *Eucalyptus globulus* is the most dominant forest species, covering 812 thousand hectares.[9] Even though its timber is widely exploited as a fiber source by the paper and pulp industry, the remaining parts of this tree – such as the bark, branches and leaves – are treated as residues. These by-products, especially the bark residues, contain circa 5.2 to 24.6 g of triterpenic acids per kilogram of bark.[10] The major components of the outer bark extract are triterpenic acids with lupane, ursane and oleanane skeletons, namely, betulinic, betulonic, 3-acetylbetulinic, oleanolic and 3-acetyloleanolic acids.[11]

Betulinic (3β-hydroxy-lup-20-en-28-oic) and oleanolic (3β-hydroxyolean-12-en-28-oic) acids have been increasingly explored in the last decade due to their pharmacological and nutritional properties.[12] While betulinic acid has shown anticancer[13], antimicrobial[14], anti-inflammatory[15], antimalarial[16], antioxidant[17], anthelmintic[18] and anti-HIV (human immunodeficiency virus)[19,17] activities, oleanolic acid presents low toxicity, anticancer[20], antimicrobial[21], anti-inflammatory[22] properties, as well as hepatoprotective effect, one of the most important properties credited to this triterpenic acid.[23]

Betulinic and oleanolic acids, as shown in Figure 1.1, are constitutional isomers. Their properties, allied to the difficulty of their separation, results in elevated prices especially when they present a higher purity (reaching 620 €/g for betulinic acid with 98 % of purity and 885 €/g for oleanolic acid with 97 % of purity).

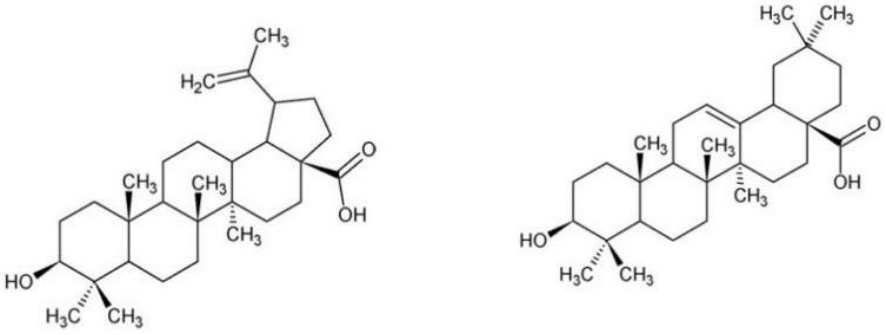

Figure 1.1 – Chemical structures of betulinic acid (on the left) and oleanolic acid (on the right).

These triterpenic acids can be extracted resorting to several methods, such as supercritical fluid extraction (SFE), ionic liquids extraction and can be analysed qualitatively and/or quantitatively by thin layer chromatography and high performance liquid chromatography (HPLC), allied to ultraviolet (UV) and mass spectroscopy detection systems.[7,24]

1.2. Preparative Chromatography

Chromatography, originally applied at the beginning of the 20th century, is now a well-established technique widely used in the industry. This technique is common in the analytic field, however, it is also expanding as a preparative process for the commercial scale production.[25] HPLC is a batch chromatography technique and the separation is achieved by injecting pulses of the solute mixture into a stream of mobile phase flowing through a stationary phase, the chromatographic column. This technique is based on the difference of affinities between the solute and the stationary phase. According to their affinities, solutes migrate through the column at different speeds which enables their separation. While the less retained compound will depart the column earlier, the more retained compound takes longer to exit the column. The principle of adsorption chromatography is depicted in the Figure 1.2.

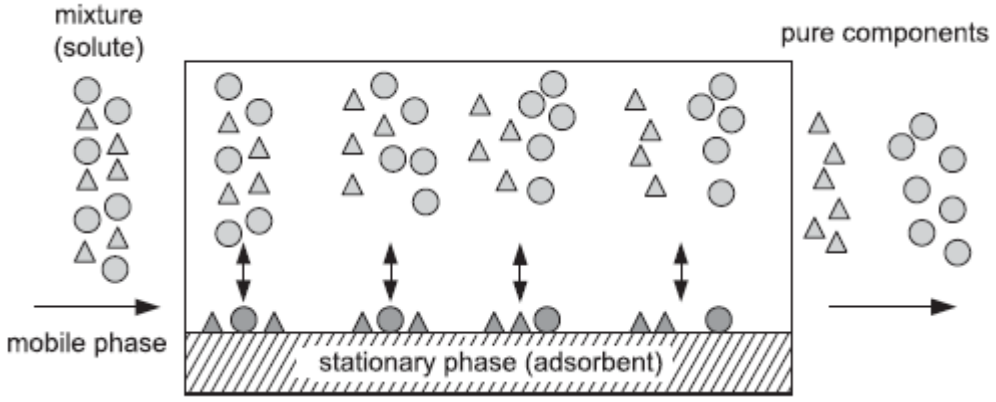

Figure 1.2 – Principle of adsorption chromatography (adapted from Schmidt-Traub[25]).

Non-retained tracers, which are compounds that do not interact with the stationary phase, exit the column first, originating the total dead time (t_{total}). These compounds enable the determination of the total porosity (ε_t), bed porosity (ε) and particle porosity (ε_p). Two examples of non-retained tracers on C30 columns (silica-based stationary

phases), are uracil and blue-dextran. Uracil can be used to determine the total porosity, since it is small enough to penetrate the particle pores. Regarding blue-dextran, this molecule can be used to determine the bed porosity, since it is not capable of penetrating the particle pores due to its size.[7] The time each component takes to elute from the column is called retention time (t_r), and it can be determined by analyzing a chromatogram, as shown in Figure 1.3.

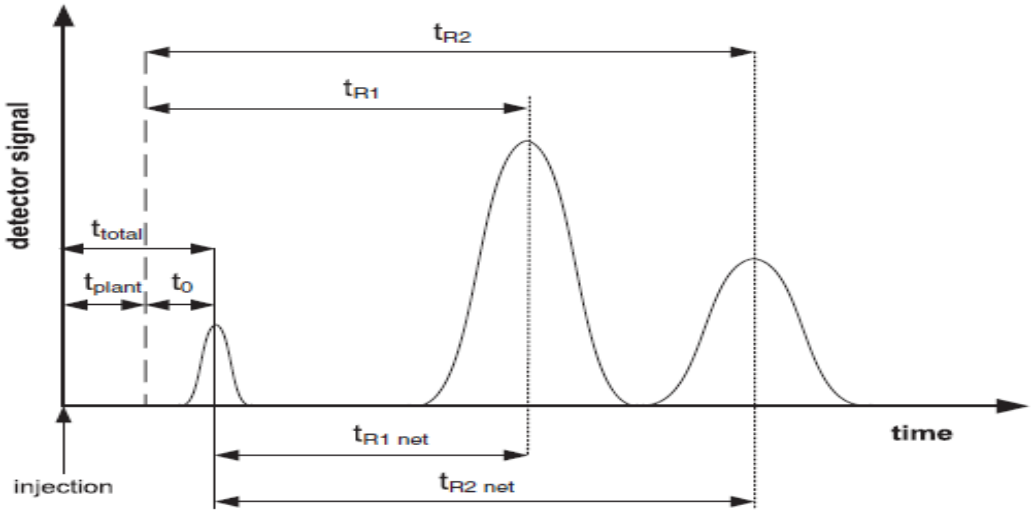

Figure 1.3 – Representative chromatogram (adapted from Schmidt-Traub [25]).

The retention time is determined from the maximum peak in case of symmetrical peak shapes. In case of asymmetric peaks, the retention time has to be calculated from the first central moment by moment analysis method.[25] The overall retention time of a retained compound ($t_{r,i}$) is the sum of the dead time (t_0) and the net retention time ($t_{r,i,net}$). The net retention time represents the time during which a compound is adsorbed onto the surface of the adsorbent. The dead time of the plant (t_{plant}) has to be determined to obtain the correct dead time of the column. The retention time of a compound depends on the mobile phase, the flow rate and the column geometry. Then, the retention behavior has to be normalized. The retention factor, that depends only on the distribution of the component of interest between the mobile phase and the stationary phase and that represents the ratio of time a compound is adsorbed to the time that is in the fluid phase, can be defined according to Equation (1.1)[25]:

$$k_i' = \frac{t_{r,i} - t_0}{t_0} \tag{1.1}$$

The main purpose of every chromatographic process is to separate dissolved compounds, therefore the distance between the peaks in a chromatogram is of great importance. The selectivity (α) of the separation of two compounds is determined according to:

$$\alpha = \frac{k'_B}{k'_A} = \frac{t_{r,B} - t_0}{t_{r,A} - t_0} \tag{1.2}$$

By convention, the more retained compound is in the numerator, so the selectivity of two components is always higher than the unity.[25]

As this technique is a batch technique, it means the process is not continuous, requires large amounts of solvent and makes an inefficient use of the column through separation, being the productivity limited.[26] A. Rajendran et al.[27] used an analogy where they consider a group of cats and turtles, see Figure 1.4, for understanding elution and countercurrent chromatography. In Figure 1.4 (a), for elution chromatography, the cat, representing the less retained compound, moves faster than the turtle (more retained compound), which leads to a separation since the less retained compound exits first. Relatively to Figure 1.4 (b), the cat and the turtle are running against the current through a conveyor belt that moves in the opposite direction. Since the cat runs at a higher velocity than the velocity of the conveyor belt, it will be sent to the right side, while the turtle will be sent to the left side of the belt, because its speed is smaller than the speed of the conveyor belt. The less retained compound (represented by the cat) and the more retained compound (represented by the turtle) will be separated. The continuous countercurrent chromatography is outlined in Figure 1.4 (c), where both the fluid and solid flow in opposite directions. This continuous technique is more efficient and consumes less solvent than batch elution chromatography, being critical in production costs. Continuous systems also offer more flexibility, capability of automatic operations and constant product quality. In this context, the true moving bed (TMB) technology, and its practical application, the SMB technology, were developed.

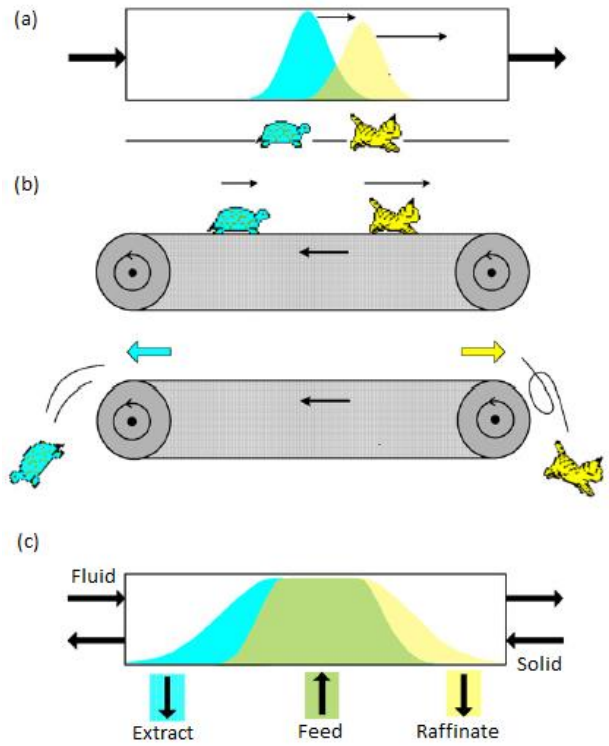

Figure 1.4 – Cat-turtle analogy for understanding elution and countercurrent chromatography: (a) Schematic and analogy for elution chromatography; (b) Analogy for countercurrent chromatography; (c) Schematic for countercurrent chromatography (adapted from A. Rajendran et al[27]).

1.3. True Moving Bed and Simulated Moving Bed

TMB technology is a continuous chromatographic technique capable of offering higher separation performance, higher productivity and smaller production costs in comparison to batch chromatography, even when selectivities approach the unitary value. In TMB, both phases flow simultaneously in countercurrent, allowing higher mass transfer driving force since none of the phases is stationary.[26] In Figure 1.5 it is represented a TMB mechanism that is divided into four sections or zones. The feed, that is constituted by a binary mixture of A and B, is constantly introduced between zone II and zone III and the mobile phase (solvent) is introduced unceasingly into zone I. The extract (rich in the more retained compound, A) and raffinate (rich in the less retained compound, B) are gathered at the outlet of zones I and III, respectively. The solid phase is recycled from zone IV to zone I after regeneration and the mobile phase, properly purified, is recycled to zone I. However, TMB technology has a serious disadvantage, the flow of the solid is hard to execute causing mixing, attrition, mechanical erosion of the adsorbent and wearing of the equipment, resulting in high maintenance costs.[27,28]

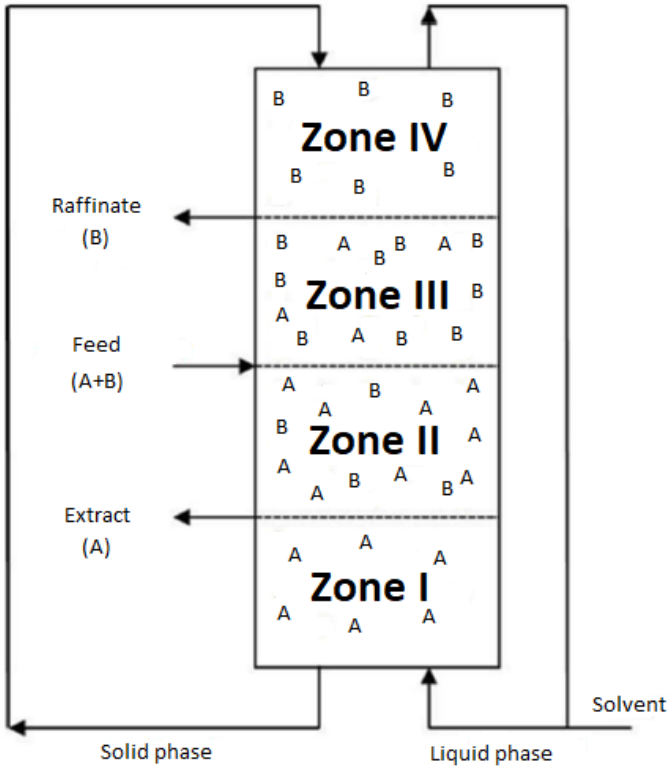

Figure 1.5 – Schematic representation of a TMB unit (adapted from Aniceto, J. P. S. et al[28]).

Due to this TMB technology problem, it has emerged a necessity to develop a more practical approach. In 1961, it was introduced by Broughton and Gerhold[29] the concept of SMB as a practical implementation of the TMB process. The first applications of SMB arise from petrochemical industry but nowadays they are also spreading to numerous binary separations of enantiomers.[30] The main differences between SMB and TMB technologies is that in SMB there are several smaller fixed bed columns and the inlet and outlet streams are periodically displaced in the direction of the fluid flow, contrary to the single TMB column, simulating, in a discontinuous way, the continuous countercurrent movement of the solid phase.[27] After several cycles, the SMB unit achieves a periodic steady state.[30] The higher the number of SMB columns and the smaller the switch times, the most it will be similar to TMB process. The limit situation is to have an infinite number of SMB columns and an infinitesimal switch time. In this case, SMB is identical and equivalent to TMB process.[26]. A schematic representation of a SMB unit with a 3-3-3-3 column configuration for the separation of a binary mixture (A and B) is shown in Figure 1.6.

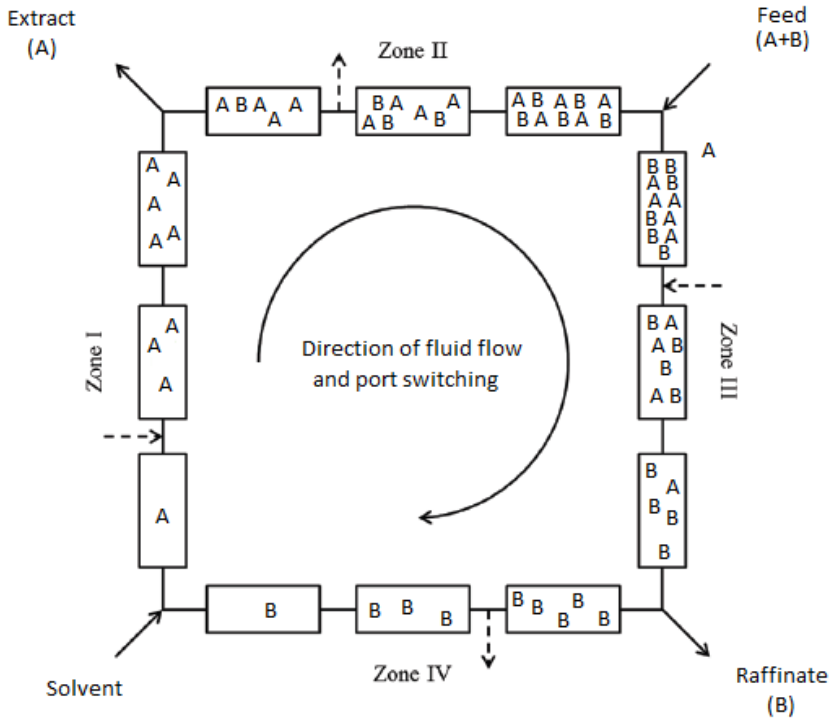

Figure 1.6 – Schematic representation of a SMB unit (adapted from Aniceto, J. P. S et al. [26]) for the separation of a binary mixture of A (more retained compound) and B (less retained compound).

The SMB unit shown in Figure 1.6 is divided into four separation zones, two inlet streams (feed and solvent) and two outlet streams (extract and raffinate). Each section or zone is delimited by the position of the external streams in each cycle and have distinct roles. In zone I the adsorbent is regenerated. Zone II desorbs the less retained compound (B) and zone III adsorbs the more retained compound (A). In zone IV the solvent is regenerated. The inner arrow in clockwise direction shows the movement of the external streams positions around the SMB unit every t^* seconds, being the switch time (t^*) a critical parameter for obtaining high purity and productivity that represents the equivalent solid velocity in TMB model[31]. There are numerous methods that lead to the parameter determination and prediction of internal concentration profiles, some more intricate and some easier. One of the simplest ways for the determination of operating parameters is the triangle theory, specified in the next chapter, which is only based on adsorption equilibrium considerations.

All this interest in SMB technology led to the formulation of new concepts and the design of non-conventional SMB operation modes[31], such as the Varicol process[32] notorious for the implementation of asynchronous inlet and outlet ports shifts; the PowerFeed technique[33] known by the modulation of the feed flow rate; the Modicon

process[34,35] where the feed concentration is varied; the M3C process[36,37], also known as Enriched Extract operation (EE-SMB)[38] in which a portion of extract product is concentrated and then re-injected in the SMB process at the same collection point; the semi continuous two-zone SMB/chromatography[39,40]; the one-column chromatography with recycle analogous to a four-zone SMB[41,42]; MultiFeed operation[43,44] based on the introduction of multi feed streams (using knowledge in distillation for the optimum location of multiple feeds); the Outlet Swing Stream[45] where the more and less retained compounds are collected non-continuously; the Pseudo-SMB process[46,47] (also known as JO process) which consists in two steps, in the first one the feed and desorbent enter the system, operating as a fixed bed, while the intermediate product is recovered and in the second step the feed stops and the unit works as a standard SMB unit where the less and more retained compounds are collected; the Supercritical SMB (SF-SMB)[48] making possible to tuning the elution strength of the mobile phase in different zones of the SMB unit, optimizing the separation performance; Gradient SMB[49] manipulating both solvent or temperature.

Chapter 2

Modeling

2.1. Modeling Fundamentals

Mathematical modeling is indispensable and essential for the accurate control and optimization of any process and chromatography is no exception. In general, to represent a generic chemical engineering process it should be taken into account a set of equations including material, energy and momentum balances, equilibrium relations, kinetic laws, along with initial and boundary conditions.[26]

This chapter will focus on the solid-liquid chromatographic separation of triterpenic acids mixtures. Many sophisticated theories have been developed to describe the adsorption of solutes in the whole concentration range, unfortunately, this problem is far from being solved and most equations used in this area are empirical and approximate. All models should consider the thermodynamic equilibrium, being this parameter complemented with others, such as the convective transport through the column, external and internal mass and eventually heat transfer limitations and axial dispersion.[26,50]

The most featured models in the literature are the equilibrium model, the equilibrium dispersive model, the lumped kinetic model, and the general rate model.[26,27,51] The equilibrium model only takes into account the thermodynamic equilibrium and convective transport along the bed, while the equilibrium dispersive model considers not only the two assumptions mentioned, but also the effect of axial dispersion. The lumped kinetic model is used to relate the rate of variation of the local concentration of solute in the solid phase and the extent of the local deviation from equilibrium. Last, the general rate model uses the concepts of mass transfer kinetics and the thermodynamic and material balance equations. All the models embody the following assumptions: isothermal process, uniform bed, no radial concentration gradients in the column, constant mobile phase velocity, negligible mobile phase compressibility and stationary phase composed by particles of uniform size.[26, 27]

2.2. Adsorption Isotherms

Adsorption equilibrium isotherm describes the distribution of solutes between interacting phases. The adsorption isotherms can be determined resorting to several techniques, some more accurate than others.[26,52] There are the classical static methods, like the batch and the adsorption-desorption methods, and the dynamic methods, that contain frontal analysis, perturbation method, elution by characteristic point, exploiting

characteristic peak features, peak fitting method and influence of applied porosity.[52] These dynamic methods are faster and more accurate than static ones.[53]

The linear isothermal model can be described as a particular case of the Langmuir equation by[26]:

$$q_i = H_i C_i \tag{2.1}$$

where q_i represents the solid phase concentration and C_i the concentration of component i in the fluid.

However, in preparative chromatography, the operating conditions allow working in a wide range of high concentrations which leads to deviations to the linear model. The competitive Langmuir isotherm for a binary mixture is represented by[26]:

$$q_i = \frac{Q_A b_i C_i}{1 + b_1 C_1 + b_2 C_2} \qquad i = 1, 2 \tag{2.2}$$

where Q_A signifies the adsorbent capacity and b_i the equilibrium constants.

In some cases, the superposition of a linear term with slope H_i to the Langmuir model can improve the fitting to experimental data.[26] So, the combination of Equation (2.1) and Equation (2.2), results in:

$$q_i = H_i C_i + \frac{Q_A b_i C_i}{1 + b_1 C_1 + b_2 C_2} \qquad i = 1, 2 \tag{2.3}$$

This combined model considers that the adsorbent has nonselective sites, represented by H_i, and selective sites, described by the Langmuir contribution.[26]

There are other and more complex models that can be used, such as the bi-Langmuir isotherm. This model contains two competitive Langmuir terms which can be represented by[26]:

$$q_i = \frac{Q_A b_i C_i}{1 + b_1 C_1 + b_2 C_2} + \frac{Q_A b_i' C_i}{1 + b_1' C_1 + b_2' C_2} \qquad i = 1, 2 \tag{2.4}$$

Langmuir-Freudlich isotherm is another model used for binary mixtures, represented by Equation (2.5).[26,54]

$$q_i = \frac{Q_A b_i C_i^{n_i}}{1 + b_1 C_1^{n_1} + b_2 C_2^{n_2}} \qquad i = 1, 2 \tag{2.5}$$

When $n_1 = n_2 = 1$, Equation (2.5) results in Equation (2.2), the previous competitive Langmuir model.

Finally, another isotherm used when Langmuir-type models do not provide an appropriate fitting is the Toth isotherm. This model assumes that the solid surface has a continuous and unimodal adsorption energy distribution and it can be represented by[26]:

$$q_i = \frac{Q_A b_i C_i}{[1 + (b_1 C_1)^v + (b_2 C_2)^v]^{\frac{1}{v}}} \tag{2.6}$$

2.3. Equilibrium Model

The most simplified chromatography theory is based on a simple equilibrium model for a fixed-bed column. This model assumes plug flow, negligible axial dispersion, mass transfer resistances and pressure and temperature gradients, as well as diluted systems. The mass balance of species *i* in a volume element of the column is given by[26,55,56]:

$$u_i \frac{\partial C_i}{\partial z} + \frac{\partial C_i}{\partial t} + \frac{1 - \varepsilon}{\varepsilon} \frac{\partial q_i^*}{\partial t} = 0 \tag{2.7}$$

where u_i is the linear velocity, ε represents the bed porosity of the column and q_i^* is the solid phase concentration in equilibrium with the liquid phase.

The adsorption equilibrium isotherm is generically represented by:

$$q_i^* = f(C_i) \tag{2.8}$$

Combining the previous two equations and using a cyclic relation between partial derivatives, the velocity of propagation of a concentration C_i can be expressed according to Equation (2.9), where $f'(C_i)$ is the slope of the adsorption isotherm.[55,56]

$$u_{C_i} = \left(\frac{\partial z}{\partial t}\right)_{C_i} = \frac{u_i}{1 + \frac{1 - \varepsilon}{\varepsilon} f'(C_i)} \tag{2.9}$$

The previous equations are the basis for the study of the dynamics of percolation columns and the concepts of compressive and dispersive waves. Three cases with practical interest are depicted in Figure 2.1.

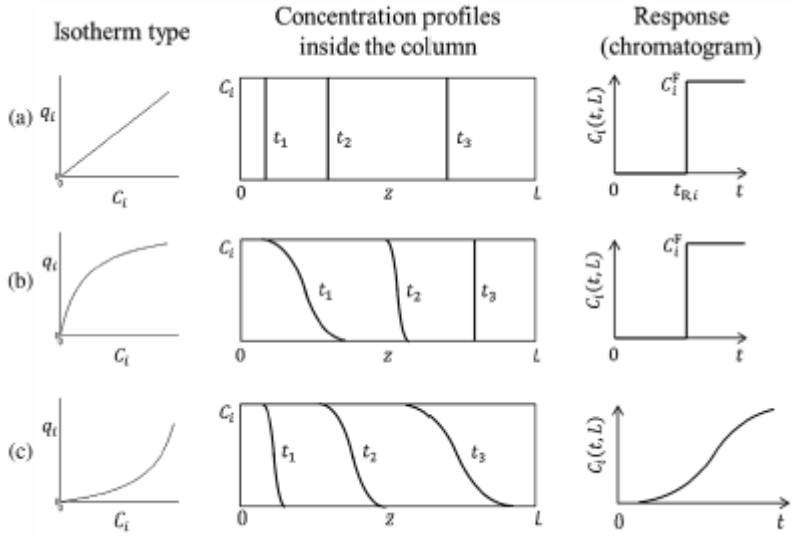

Figure 2.1 – Schematic diagram of concentration profiles inside the column and system responses in the cases of a) linear, b) favorable and c) unfavorable isotherms.[26]

According to Figure 2.1 a), the isotherm derivative is constant and equal to H_i, all concentrations propagate at the same velocity. Regarding Figure 2.1 b), as the concentration increases, the isotherm derivative decreases and higher concentrations move faster. For the last case, Figure 2.1 c), the isotherm derivative increases as the concentration grows and higher concentrations move slower.

2.4. Moment Analysis Method

The moment analysis method is a theoretical strategy that can be employed to obtain thermodynamic and kinetic model parameters (*e.g.* the equilibrium and transport parameters) from the information provided by a chromatogram, transforming it into a small number of temporal moments. These theoretical moments are able to describe, in a simple manner, the essential data supplied by chromatograms and estimate performance parameters of the separation of a mixture and also to optimize more easily the process.[64]

One approach for the kinetic study of chromatography is to analyse the flow rate dependence of the height equivalent to a theoretical plate (HETP).[58] The general case, linear isotherm and noncompressible system, was studied by some authors, such as van Deemter[58,60,61,62]. The moment analysis method is an effective strategy to analyse quantitatively the chromatographic behaviour. Axial dispersion (and in turn, the Peclet

number, Pe (Equation (2.10))) and mass transfer limitation in the film and inside the particle are considered.

$$Pe = \frac{u_{inst} L}{D_{ax}} \tag{2.10}$$

where,

$$u_{inst} = \frac{u_0}{\varepsilon} \tag{2.11}$$

The corresponding equation to the first central moment match the retention time for symmetric peaks (Equation (2.12)).

$$\mu_1 = t_r = (1 + \xi_i)\left(1 + \frac{1}{Pe}\right) \tag{2.12}$$

where ξ_i represents the capacity parameter.

The second central moment (Equation (2.13)) corresponds to the variance:

$$\mu_2 = \sigma^2 = \frac{2}{N_{LDF}} {\xi_i}^2 \left(1 + \frac{1}{Pe}\right) + 2\frac{1 + \xi_i}{Pe} + 3\frac{1 + \xi_i}{Pe^2} \tag{2.13}$$

where N_{LDF} is the number of global mass transfer units.

The third central moment (Equation (2.14)) represents the skewness:

$$\mu_3 = \frac{6}{N_{LDF}^2} {\xi_i}^3 + 6\frac{{\xi_i}^2(1 + \xi_i)}{N_{LDF}^{Pe}}\left(\frac{1}{N_{LDF}}\frac{\xi_i}{1 + \xi_i} + \frac{3}{Pe} + 2\right) + 12\frac{(1 + \xi_i)^3}{Pe^2} + 20\frac{(1 + \xi_i)^3}{Pe^3} \tag{2.14}$$

Equilibrium and mass transfer parameters (H_i and K_{LDF}, respectively) and axial dispersion can be determined through optimization.

The expression for the HETP is derived from the first and second central moments, resulting in Equation (2.15).[51,63]

$$HETP = \frac{L}{N} = \frac{\mu_2 L}{\mu_1^2} \tag{2.15}$$

where the theoretical plate number (N) is given by Equation (2.16).

$$N = 5.545 \left(\frac{t_r}{w_h}\right)^2 \tag{2.16}$$

where w_h is the peak width at half height.

2.5. Analytical Solution for Chromatographic Operations

Chromatographic behaviour, such as separation performance, sample retention or elution peak profile depends on both the equilibrium and mass transfer parameters.[58] In order to design an SMB unit, those parameters must be known.

In analytical chromatography, the pulse signals can be interpreted as two steps separated by a finite time interval. Giorgio Carta[50,59] determined the analytical solution to a partial differential equation model describing mass transfer in an adsorption bed, by applying the LDF approximation, linear isotherms and neglecting axial dispersion. This solution has the form of an infinite series and is rapidly convergent and it is given by:

$$\frac{C_i(t,L)}{C_i^F} =$$

$$= \frac{w_{feed}}{2w} + \frac{2}{\pi}\sum_{m=1}^{\infty}\left[\frac{1}{m} e^{-\frac{m^2 N_{LDF}}{m^2+w^2}} sin\left(\frac{m\pi w_{feed}}{2w}\right) cos\left(\frac{m\theta_f}{w}\right.\right.$$

$$\left.\left. - \frac{m\pi w_{feed}}{2w} - \frac{mN_{LDF}}{w\xi_i} - \frac{m\pi N_{LDF}}{m^2+w^2}\right)\right] \tag{2.17}$$

where,

$$w_{feed} = \frac{K_{LDF}}{\pi H_i} t_{feed} \tag{2.18}$$

$$w = \frac{K_{LDF}}{2\pi H_i} (t_{feed} + t_{elution}) \tag{2.19}$$

$$N_{LDF} = K_{LDF}\frac{1-\varepsilon}{\varepsilon}\boldsymbol{\tau} \tag{2.20}$$

$$\theta_f = \frac{K_{LDF}}{H_i}t \tag{2.21}$$

$$\xi_i = \frac{1-\varepsilon}{\varepsilon}H_i \tag{2.22}$$

where t_{feed} represents the feed pulse duration in Carta's solution and $t_{elution}$ is the duration of elution period in Carta's solution.

Analytic solution for linear chromatography have been presented in the form of convergent series and can be applied directly to the calculation of the response to rectangular feed injection pulses and to steady periodic operations with repeated injections, considering intraparticle and external film mass transfer resistances.[50] The chromatographic model described herein was the one selected for the fitting of the breakthrough curves.

2.6. SMB Modeling and Optimization

This section covers several aspects of the SMB modeling and optimization. All material balances, equilibrium and kinetic equations, initial and boundary conditions, along with the triangle theory and the performance indicators are listed.

2.6.1. SMB Modeling

Assuming axial dispersion plug flow pattern, the material balance for compound *i* in fluid phase of column *j* is represented by Equation (2.23).[7,55]

$$\frac{\partial C_{ij}}{\partial t} = D_{ax,ij}\frac{\partial^2 C_{ij}}{\partial z^2} - u_i\frac{\partial C_{ij}}{\partial z} - \frac{1-\varepsilon}{\varepsilon}\frac{\partial q_{ij}}{\partial t} \tag{2.23}$$

where D_{ax} represents the axial dispersion.

Considering that the internal and external mass transfer resistances are taken in linear driving force (LDF) coefficients, the material balance for compound *i* in solid phase of column *j* can be approximated by[7,55]:

$$\frac{\partial q_{ij}}{\partial t} = K_{LDF,ij}\left(q_{ij}^{*} - q_{ij}\right) \tag{2.24}$$

where K_{LDF} is the global LDF mass transfer coefficient.

In the SMB technology, the solid phase is completely stationary and the countercurrent movement of fluid and solid is simulated by an appropriate flow switching sequence, unlike what happens in TMB, in which solid and fluid phases flow in opposite directions.[7,57] There are several models developed in literature to predict the performance of an SMB separation process. These models can follow two different strategies, simulating the SMB system directly or considering TMB. The main difference is that the TMB strategy embodies a continuous model with steady-state solutions, while the real SMB strategy needs to be solved at the cyclic steady state (CSS).[55]

Considering the inlet and outlet are fixed, the interstitial velocity of liquid in SMB unit is the sum of interstitial velocities of liquid and solid in TMB and it is given by[7,28,55]:

$$v_j^{*} = v_j + u_{solid} \tag{2.25}$$

where v_j^{*} is the interstitial velocity of the fluid in the SMB, v_j is the interstitial velocity of the fluid in the TMB and u_{solid} is the solid velocity in the TMB.

As the solid velocity in TMB is related to the switch time (t^{*}) of SMB, the switch time can be written as[7,28,55]:

$$t^{*} = \frac{L_j}{u_{solid}} \tag{2.26}$$

where *L* is the column length.

The higher the number of columns per section the most accurate is the prediction of an SMB unit performance by equivalent TMB model.

Considering single chromatography column and SMB unit, the combination of the mass balance of component *i* in fluid phase of column *j* (Equation (2.23)) and the mass

balance of component *i* in solid phase of column *j* (Equation (2.24)), can be represented by Equation (2.27).[7,28,55]

$$\frac{\partial C_{ij}}{\partial t} = D_{ax,ij}\frac{\partial^2 C_{ij}}{\partial z^2} - v_j^*\frac{\partial C_{ij}}{\partial z} - \frac{1-\varepsilon}{\varepsilon}K_{LDF,ij}\left(q_{ij}^* - q_{ij}\right) \tag{2.27}$$

The initial time condition for Equation (2.27) is that $C_{ij} = C_{ij,0}$, where $C_{ij,0}$ is the inlet concentration. Regarding the initial and boundary conditions for the position variable, they are as follow:

$$z = 0 \qquad C_{ij} - \frac{D_{ax,ij}}{v_j^*}\frac{\partial C_{ij}}{\partial z} = C_{ij,0} \tag{2.28}$$

$$z = L_j \qquad \frac{\partial C_{ij}}{\partial z} = 0 \tag{2.29}$$

Equations (2.28) and (2.29) represents the famous Danckwerts conditions, imposing no diffusive flux at the end of the column ($z = L_j$) and equals the convective flux of the upstream solution to the convective and diffusive fluxes at the bed entrance.[26]

Considering the isotherm described in Equation (2.1), the initial and boundary conditions are denoted by Equation (2.28) and by[7,26,55]:

$$t = 0 \qquad C_{ij}^{n=0} = 0 \;\; and \;\; q_{ij}^{n=0} = 0 \quad or \quad C_{ij}^{n+1} = C_{ij}^{n} \;\; and \;\; q_{ij}^{n+1} = q_{ij}^{n} \tag{2.30}$$

The component node balances used at end of column *j* (for $z = L_j$) are as follow[7,28,51,55]:

$$Internal\ Nodes: \quad z = L_j \qquad C_{ij} = C_{ij} + 1{,}0 \tag{2.31}$$

$$Eluent\ Node: \quad z = L_j \qquad C_{ij} = \frac{v_I^*}{v_{IV}^*}C_{ij} + 1{,}0 \tag{2.32}$$

$$Feed\ Node: \quad z = L_j \qquad C_{ij} = \frac{v_{III}^*}{v_{II}^*}C_{ij} + 1{,}0 - \frac{v_F^*}{v_{II}^*}C_i^F \tag{2.33}$$

where C_i^F is the feed concentration.

The global balances to the nodes in the SMB are described by[7,28,55]:

$$Eluent\ Node: \qquad v_I^* = v_{IV}^* + v_E \tag{2.34}$$

$$Extract\ Node: \qquad v_{II}^* = v_I^* - v_X \tag{2.35}$$

$$Feed\ Node: \qquad v_{III}^* = v_{II}^* + v_F \tag{2.36}$$

$$Rafinate\ Node: \qquad v_{IV}^* = v_{III}^* - v_R \tag{2.37}$$

To define the flow rates in each section in order to ensure the desired separation, it must be defined some restrictions, allowing the possibility to recover the more retained compound (A) from extract and the less retained compound (B) from raffinate stream. These restrictions are established as shown in the following equations[55]:

$$Section\ I: \qquad \frac{Q_I C_{A,I}}{Q_S q_{A,I}} > 1 \tag{2.38}$$

$$Section\ II: \qquad \frac{Q_{II} C_{B,II}}{Q_S q_{B,II}} > 1 \quad and \quad \frac{Q_{II} C_{A,II}}{Q_S q_{A,II}} < 1 \tag{2.39}$$

$$Section\ III: \qquad \frac{Q_{III} C_{B,III}}{Q_S q_{B,III}} > 1 \quad and \quad \frac{Q_{III} C_{A,III}}{Q_S q_{A,III}} < 1 \tag{2.40}$$

$$Section\ IV: \qquad \frac{Q_{IV} C_{B,IV}}{Q_S q_{B,IV}} < 1 \tag{2.41}$$

where Q_S is the solid flow rate and Q_j is the volumetric flow rate in section j for a TMB unit.

For a binary system with a linear adsorption isotherm, these restrictions can be simplified to the following ones[55]:

$$Section\ I: \qquad \frac{Q_I}{Q_S} > H_A \tag{2.42}$$

$$Section\ II: \qquad \frac{Q_{II}}{Q_S} > H_B \quad and \quad \frac{Q_{II}}{Q_S} < H_A \tag{2.43}$$

$$Section\ III: \qquad \frac{Q_{III}}{Q_S} > H_A \quad and \quad \frac{Q_{III}}{Q_S} < H_B \tag{2.44}$$

$$Section\ IV: \qquad \frac{Q_{IV}}{Q_S} < H_B \tag{2.45}$$

Assuming all of these inequalities are satisfied with the same safety margin β (β>1), the following equations can be written[55]:

$$Section\ I: \qquad \frac{Q_I}{Q_S H_A} = \beta \tag{2.46}$$

$$Section\ II: \qquad \frac{Q_{II}}{Q_S H_B} = \beta \tag{2.47}$$

$$Section\ III: \qquad \frac{Q_{III}}{Q_S H_A} = \frac{1}{\beta} \tag{2.48}$$

$$Section\ IV: \qquad \frac{Q_{IV}}{Q_S H_B} = \frac{1}{\beta} \tag{2.49}$$

It is also possible to establish the global mass balances of the inlet and outlet of the streams of the column[28,55]:

$$Q_E = Q_I - Q_{IV} \tag{2.50}$$

$$Q_X = Q_I - Q_{II} \tag{2.51}$$

$$Q_F = Q_{III} - Q_{II} \tag{2.52}$$

$$Q_R = Q_{III} - Q_{IV} \tag{2.53}$$

The ideal situation corresponds to $\beta = 1$, however, to achieve a complete separation of a binary mixture, β should be higher than 1. This margin reaches a maximum value as shown by[55]:

$$1 < \beta < \sqrt{\frac{H_A}{H_B}} \tag{2.54}$$

The volumetric flow rates in the SMB unit can be determined through the TMB and SMB equivalence[55]:

$$Q_j^* = Q_j + \frac{\varepsilon}{1-\varepsilon} Q_s \tag{2.55}$$

where Q_j^* and Q_j are the volumetric flow rates in the section *j* of a SMB and TMB unit, respectively.

2.6.2. Equilibrium Theory for Linear Isotherms (Triangle Theory)

The triangle theory is commonly used for the optimization and simulation of SMB processes since it is a practical and simplified approach to SMB design. In this approach, it is assumed that the adsorption equilibrium is reached everywhere at every time. Mass transfer resistances are not considered and axial dispersion is neglected.[28,51,55] Based on this theory, the ratio of fluid to solid flow rates (m_j) can be represented through the following equation[51]:

$$m_j = \frac{Q_j^* t^* - \varepsilon_t V_c}{V_c(1-\varepsilon_t)} \qquad j = I, II, III, IV \tag{2.56}$$

where ε_t represents the total porosity of the column and V_c is the column volume.

In the case of a linear isotherm, the restrictions for complete separation are given by[27,28,51]:

$$H_B \leq m_I \tag{2.57}$$

$$H_A < m_{II} \leq H_B \tag{2.58}$$

$$H_A \leq m_{III} \leq H_B \tag{2.59}$$

$$m_{IV} \leq H_A \tag{2.60}$$

Equations (2.58) and (2.59) define a triangular region in the upper half of the (m_{II}, m_{III}) plane which corresponds to the operating conditions, and Equations (2.57) and (2.60) delineate a rectangular region in the upper half of the (m_I, m_{IV}) plane in terms to obtain a complete separation.[27] The projection of both planes are shown in Figure 2.2.

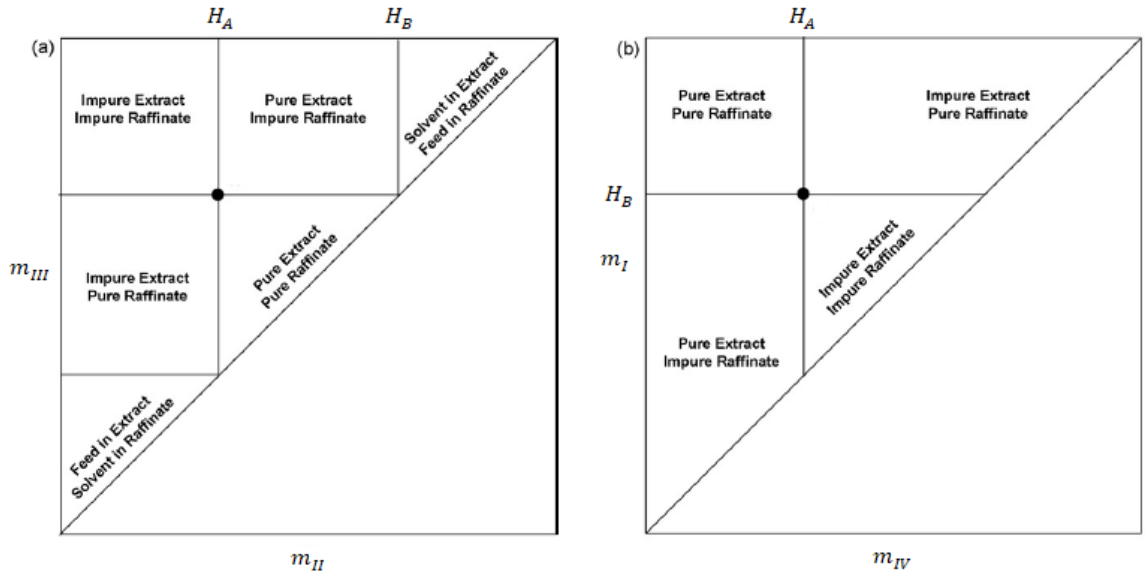

Figure 2.2 – Complete separation region and SMB operation regimes on (a) (m_{II}, m_{III}) plane and (b) (m_I, m_{IV}) plane for the binary separation of A and B considering linear adsorption isotherm (adapted from A. Rajendran et al [27]).

2.6.3. SMB Performance Indicators

In order to analyze the performance of the SMB process, there are a few important parameters that must be taken into account, especially the purity in the raffinate and in the

extract (PuR and PuX, respectively), the recovery in the raffinate and in the extract (RecR and RecX, respectively), the productivity (Prod) and the solvent consumption (SC). The purity can be defined as the ratio between the concentration of the desired component and the total concentration (Equation (2.61) and Equation (2.62)).[26,27,51,55]

$$PuR = 100 \times \frac{C_B^R}{C_A^R + C_B^R} \tag{2.61}$$

$$PuX = 100 \times \frac{C_A^X}{C_A^X + C_B^X} \tag{2.62}$$

Recovery is defined as the ratio of the amount of component in the corresponding product stream and the amount of the same component fed to the system (Equation (2.63) and Equation (2.64)).[26,27,51,55]

$$RecR = 100 \times \frac{Q_R C_B^R}{Q_F C_B^F} \tag{2.63}$$

$$RecX = 100 \times \frac{Q_X C_A^X}{Q_F C_A^F} \tag{2.64}$$

The productivity is the total mass of feed processed per unit volume of the adsorbent and per unit time (Equation (2.65)).[26,27,51,55]

$$Prod = \frac{Q_F(C_A^F + C_B^F)}{V_c} \tag{2.65}$$

Finally, solvent consumption, can be defined as the volume of solvent used per unit mass of the solutes in the feed (Equation (2.66)).[26,27,51,55]

$$SC = \frac{Q_E + Q_F}{Q_F(C_A^F + C_B^F)} \tag{2.66}$$

Chapter 3

Material and Methods

3.1. Chemicals

HPLC grade methanol, water, acetonitrile, ethanol, isopropanol, ethyl acetate and acetone were purchased from Sigma-Aldrich. Betulinic (purity ≥ 98) and oleanolic (purity ≥ 98) acids were supplied from Aktin Chemicals, Inc and suffered no purification prior to their use.

3.2. Equipment

The chromatographic studies were performed in three HPLC equipments: Gilson HPLC system (Gilson, Inc., Middleton, WI, USA) equipped with a 305 isocratic controller pump, a 306 gradient pump, a 805 manometric module, a 811C dynamic mixer and a 118 UV/Vis detector; Gilson HPLC system (Gilson, Inc., Middleton, WI, USA) equipped with a Refractive Index Detector Model 131 and a 307 isocratic pump; and ThermoFisher Scientific UltiMate 3000 UHPLC system equipped with a DIONEX UltiMate 3000 pump, a DIONEX UltiMate 3000 column compartment and a DIONEX UltiMate 3000 diode array detector. A Unipoint Gilson software (Gilson, Inc., Middleton, WI, USA) was used to record automatically all the chromatographic runs in Gilson HPLC equipments and a ThermoFisher Chromeleon 7 software was used to record automatically all the chromatographic runs in UltiMate 3000 UHPLC equipment. To execute the breakthrough experiments were used Azura P 4.1S pumps from Knauer. The Apollo C18 HPLC column was purchased from Grace Davison Discovery Sciences and the Acclaim C30 column was purchased from ThermoFisher Scientific. The characteristics of both columns are presented in Table 3.1.

Table 3.1 – Characteristics of the columns used in the chromatographic assays.

Column	Dimensions ($L \times d_i$, mm)	Particle diameter (d_p, μm)	Column packing
Apollo C18	250 × 4.6	5	octadecylsilyl silica gel
Acclaim C30	250 × 4.6	5	triacontylsilyl silica gel

3.3. Chromatographic pulse experiments

The chromatographic pulse experiments performed in this work consisted of small injection of 20 μL of feed at room temperature (approximately 20 ºC). For the index refractor detector, whenever the chromatographic peaks were not properly visible, the volume of the loop was increased to 100 μL. These assays were conducted to select the best mobile phase for the separation of betulinic and oleanolic acids (*ca.* 100 injections), to analyze the samples gathered during the breakthrough experiments (*ca.* 1500 injections), to study the effect of water addition (*ca.* 200 injections), to apply the moment analysis method (*ca.* 50 injections) and to obtain all necessary calibration curves.

In moment analysis method it was also performed a set of chromatographic pulse experiments. However, they were done resorting to the UltiMate 3000 UHPLC equipment, using the software "Chromeleon 7" to record the chromatographic runs.

All the tested mobile phases and the related operating conditions are presented in Table 3.2. Note that the assessment of the best mobile phase for the separation of betulinic and oleanolic acids was performed in the Acclaim C30 column, the stationary phase under evaluation. The supplementary work was performed on an Apollo C18 column.

Table 3.2 – Operating conditions of HPLC system to perform the chromatographic assays for the test of the mobile phase at room temperature (ca. 20 ºC) using the Acclaim C30 column.

Mobile phase	**Type of detector**	**Q (mL/min)**	**V_{loop} (μL)**	**λ (nm)**	**C_{BA} (mg/mL)**	**C_{OA} (mg/mL)**
MeOH	UV/Vis	0.4	20	210	0.09800	0.1016
MeOH/H_2O 95/5 (%, v/v)						
MeOH/H_2O 90/10 (%, v/v)						
MeOH/ACN 85/15 (%, v/v)						
MeOH/ACN 70/30 (%, v/v)						
MeOH/ACN 50/50 (%, v/v)						
MeOH/ACN 30/70 (%, v/v)						
EtOH	Refractive index			Not Applicable	0.4980	0.5040
EtOH/H_2O 90/10 (%, v/v)						
EtOH/ACN 50/50 (%, v/v)					0.4000	0.4100
EtOH/ACN 85/15 (%, v/v)			100			
Isopropanol					0.5250	0.5250
Isopropanol/ACN 50/50 (%, v/v)					0.2450	0.2500
MeOH/acetone 50/50 (%, v/v)					0.5150	0.5500
Ethyl acetate		0.3			0.5000	0.5000

3.4. System characterization

Reversed phase columns are commonly applied to perform chromatographic assays. When a reversed phase column is employed, the stationary phase is hydrophobic, leading to the capture of hydrophobic molecules and allowing the polar molecules to elute first. Reverse phase packings operate with polar mobile phases, mostly containing organic solvents. For hydrophobic solutes, the retention time increases with the hydrophobic character. The most common reversed phase packings are silicas with surface bonded long chain n-alkyl groups, as both columns presented in this work.

Based on preliminary work performed in EgiChem group with the Acclaim C30, bed porosity was assessed by determining the retention time of uracil, a non-retained tracer. According to Equation (3.1), the retention time of uracil is plotted against L/u_0 (ratio between column length and superficial velocity).

$$t_r = \varepsilon \frac{L}{u_0} \tag{3.1}$$

In the same way, total porosity can be calculated by determining the retention time of blue-dextran and plotting it against L/u_0:

$$t_r = \varepsilon_t \frac{L}{u_0} \tag{3.2}$$

Finally, the particle porosity can be determined by:

$$\varepsilon_p = \frac{\varepsilon_t - \varepsilon}{(1 - \varepsilon)} \tag{3.3}$$

For the Acclaim C30 column, the bed porosity is 0.356, the total porosity is 0.697 and the particle porosity is 0.530.

3.5. Breakthrough curves experiments

The breakthrough experiments were conducted in a chromatographic unit installed in EgiChem laboratory of CICECO. For these assays an analytical Acclaim C30 column was used. The adsorption-desorption experiments were performed using four solutions for

each acid and one solution for the binary mixture. For betulinic acid, the concentrations of the solutions were 0.1991, 0.5973, 1.1946 and 1.9910 mg/mL. Relatively to oleanolic acid, the following concentrations were used: 0.1989, 0.5967, 1.1934 and 1.9890 mg/mL. These solutions should represent the full range of concentrations of each acid considering their solubility in methanol/acetonitrile 50/50 (%, v/v) (consult Table 3.3). For the binary breakthrough experiments the concentration of betulinic acid was 0.6610 mg/mL and the concentration of oleanolic acid was 0.8350 mg/mL, aiming to simulate a real mixture from *E. globulus* extracts, taking into account the mass fraction of betulinic (0.20 wt.) and oleanolic (0.25 wt.) acids in those extracts.[65,66] All solutions were diluted in methanol/acetonitrile 50/50 (%, v/v), the mobile phase chosen to perform the separation of these two triterpenic acids.

To perform the breakthrough experiments, the flow rate required was set and the mobile phase was allowed to flow through the column. Once the system was stabilized, it was switched to the feed pump to start the adsorption stage. To regenerate the column, the mobile phase pump was turned on and the desorption stage begun. Several samples of the outlet stream were collected along time in eppendorfs, that were later analyzed. Calibration curves were performed with a flow rate of 1.20 mL/min, wavelength of 210 nm and at room temperature (*ca.* 20 ºC).

All breakthrough experiments were performed with a flow rate of 1.00 mL/min and at room temperature. The extra column volume (the cumulative volume of non-selective lines and fittings where the liquid is contained) is 0.381 mL.

3.6. Triterpenic acids recovery

To recover the two triterpenic acids from the raffinate and extract, it was performed a solubility study consisting in the addition of water in three distinct mobile phases: methanol/acetonitrile 30/70 (%, v/v), methanol/acetonitrile 50/50 (%, v/v) and methanol/acetonitrile 70/30 (%, v/v). The procedure is the same for all. A saturated solution of each acid was prepared for each mobile phase. Different percentages of water were added in order to evaluate its effect. Samples were then analysed (wavelength of 210 nm and flow rate of 1.20 mL/min). The saturated solutions were prepared based on the solubility of both acids in the mobile phases as detailed in Table 3.3 (previous work performed in EgiChem). Accordingly, the three solutions prepared to accomplish this study

are shown in Table 3.4. To carry out this analysis, water content varied between 10 and 85 %. Note that, *e.g*, when it is said the solution has 10 % of water it means the whole solution is composed by 90 % of the original one and 10 % by water.

Table 3.3 – Solubility (mg/mL) of betulinic and oleanolic acids in methanol/acetonitrile 30/70, 50/50 and 70/30 (%, v/v) mixtures.

	Solubility (mg/mL)	
Mobile phase	Betulinic acid	Oleanolic acid
MeOH/ACN 30/70 (%, v/v)	1.440	1.620
MeOH/ACN 50/50 (%, v/v)	2.380	2.530
MeOH/ACN 70/30 (%, v/v)	3.520	3.660

Table 3.4 – Concentration (mg/mL) of betulinic and oleanolic acids in methanol/acetonitrile 30/70, 50/50 and 70/30 (%, v/v) mixtures.

	Concentration (mg/mL)	
Mobile phase	Betulinic acid	Oleanolic acid
MeOH/ACN 30/70 (%, v/v)	1.424	1.556
MeOH/ACN 50/50 (%, v/v)	2.314	2.464
MeOH/ACN 70/30 (%, v/v)	3.409	3.518

3.7. Moment analysis method

The moment analysis method was executed in order to obtain the transport and mass transfer parameters, such as axial dispersion of both betulinic and oleanolic acids. To perform the moment analysis method two solutions were prepared. The solution of betulinic acid has a concentration of 0.152 mg/mL and the solution of oleanolic acid has a concentration of 0.169 mg/mL. Both solutions were diluted in methanol/acetonitrile 50/50 (%, v/v).

To implement this method, chromatographic experiments were performed at seven different flow rates from 0.13 to 1.00 mL/min. The retention times of both acids were plotted against L/u_{inst} (ratio between column length and interstitial velocity), where the interstitial velocity (u_i) can be calculated by Equation (3.4),

$$u_{inst} = \frac{u_0}{\varepsilon} \tag{3.4}$$

From the chromatograms of each run several parameters were withdrawn, such as the first central moment, the second central moment (σ^2), the third central moment (skewness), the peak width at half height (w_h), the asymmetry (A) (Equation (3.5)), the resolution (R) (Equation (3.6)) and the number of theoretical plates (Equation (2.16)).

$$A = \frac{RW_{5\%} + LW_{5\%}}{2 \times LW_{5\%}} \tag{3.5}$$

$$R = 1.18 \times \left(\frac{t_{ref,peak} - t_r}{w_{h,ref,peak} - w_h} \right) \tag{3.6}$$

The second central moment was plotted against the interstitial velocity. Additionally, it was represented the profile of HETP against the interstitial velocity, to demonstrate the flow rate dependence of HETP. This representation can provide not only certain kinetic parameters, but also the optimum flow rate, *i.e.*, the flow rate that offers the best separation for a binary mixture containing the components under study. This value is obtained from the minimum of the function.

The equilibrium and mass transfer coefficients, such as the axial dispersion, were determined through optimization in MATLAB.

Chapter 4

Results and Discussion

4.1. Elution chromatography assays for mobile phase selection

Preliminary elution experiments were performed with the intent of selecting the most efficient mobile phase for the separation of betulinic and oleanolic acids with the Acclaim C30 column. The retention behavior of C30 stationary phases is strongly dependent on the temperature and the best separation is obtained at lower temperatures.[67,68] Thus, all chromatograms were obtained at approximately 20 ºC. The retention times, retention factors and the respective selectivities for each mobile phase are shown in Table 4.1.

Table 4.1 – Outcomes of the preliminary elution experiments for the selection of mobile phase for the separation of betulinic (BA) and oleanolic (OA) acids with the Acclaim C30 column at 20 ºC.

	t_r (min)		Retention factor, k_i'		Selectivity
Mobile phase	**BA**	**OA**	**BA**	**OA**	$\alpha_{OA/BA}$
MeOH	11.54	12.25	0.59	0.69	1.16
MeOH/H_2O 95/5 (%, v/v)	15.59	17.07	1.15	1.35	1.18
MeOH/H_2O 90/10 (%, v/v)	24.89	28.44	2.43	2.92	1.20
MeOH/ACN 85/15 (%, v/v)	12.26	13.2	0.69	0.82	1.19
MeOH/ACN 70/30 (%, v/v)	13.12	14.38	0.81	0.98	1.22
MeOH/ACN 50/50 (%, v/v)	14.24	15.83	0.96	1.18	1.23
MeOH/ACN 30/70 (%, v/v)	15.405	17.32	1.12	1.39	1.24
EtOH	8.28	8.28	0.14	0.14	1.00
EtOH/H_2O 90/10 (%, v/v)	10.19	10.64	0.40	0.47	1.15
EtOH/ACN 50/50 (%, v/v)	10.55	11.22	0.45	0.55	1.21
EtOH/ACN 85/15 (%, v/v)	8.63	8.84	0.19	0.22	1.15
Isopropanol	8.15	8.15	0.12	0.12	1.00
Isopropanol/ACN 50/50 (%, v/v)	10.25	10.76	0.41	0.48	1.17
Ethyl acetate	10.33	10.33	0.42	0.42	1.00
MeOH/acetone 50/50 (%, v/v)	10.06	10.63	0.39	0.46	1.20

Initially, the chromatographic experiments were performed in a UV/Vis detector to test the mobile phases containing methanol, water and acetonitrile. Since detection of the triterpenic acids is conducted at 210 nm, UV detection can only be used for the solvents mentioned above due to their lower UV cutoff.

The necessity for testing new mobile phases composed of "greener" solvents, led to the use of a refractive index detector, a universal detector based on the difference of the refractive indexes of the analyzed components. The obtained selectivities are available for consultation in Figure 4.1. These assays allow us to understand that the addition of water to methanol and ethanol improves the separation. This phenomenon also occurs in the addition of acetonitrile to methanol, ethanol and isopropanol. In ethanol, isopropanol and ethyl acetate, the triterpenic acids present selectivities of 1, *i.e.*, the retention factors and subsequently the retention times were equal for betulinic and oleanolic acids, displaying that the separation did not occur. The mobile phases with higher selectivities were methanol/acetonitrile 70/30, 50/50 and 30/70 (%, v/v). These three mobile phases exhibited high resolutions, however the solubility of the triterpenic acids varied significatively (see Table 3.3). The mobile phase selected for the following assays was methanol/acetonitrile 50/50 (%, v/v), since it showed better compromise between selectivity, solubility and resolution. The chromatogram obtained with this mobile phase is shown in Figure 4.2, the remaining chromatograms can be found in Appendix A.

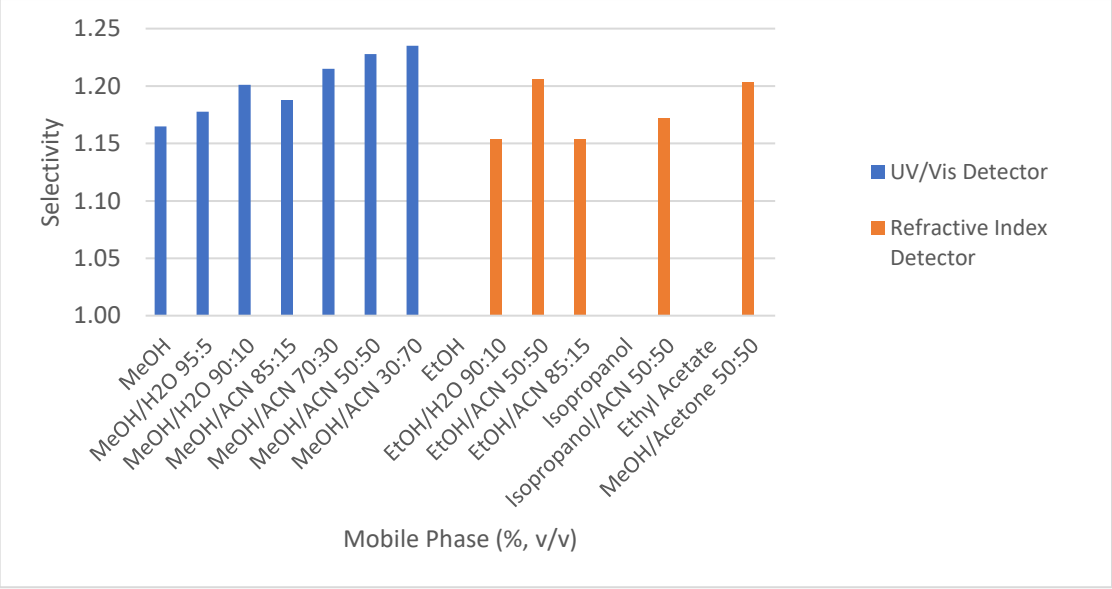

Figure 4.1 – Chromatographic selectivities for the separation of betulinic and oleanolic acids with the Acclaim C30 column.

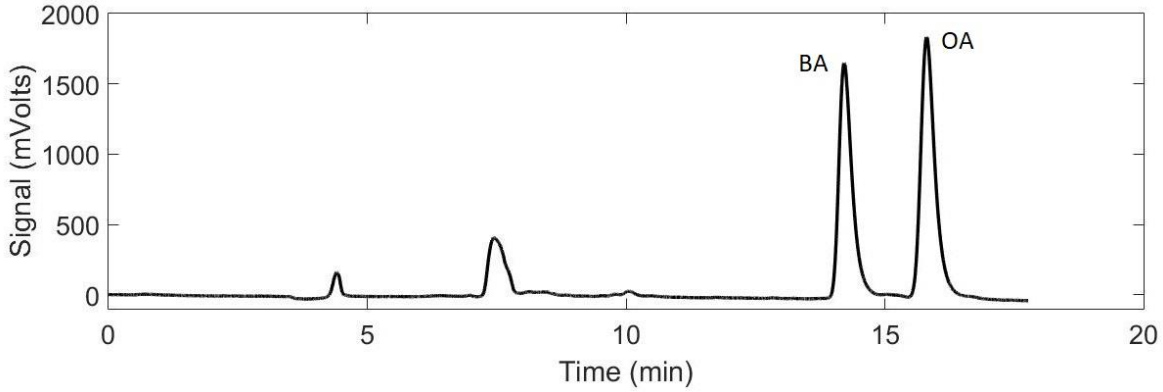

Figure 4.2 – HPLC chromatogram of a binary mixture of betulinic (BA, 0.09800 mg/mL) and oleanolic (OA, 0.1016 mg/mL) acids using an Acclaim C30 column with methanol/acetonitrile 50/50 (%, v/v) as mobile phase. Flow rate of 0.4 mL/min, UV detection at 210 nm, injection volume of 20 µL and 20 ºC.

4.2. Triterpenic acids recovery

The solubility study performed in this section (the recovery of triterpenic acids into a saturated solution of betulinic and oleanolic acids) aims to understand the amount of water necessary to add to a solution in order to recover the triterpenic acids by precipitating. That way, the solute can be recovered, and through distillation, the water can be separated from the mobile phase. The triterpenic acids reveal different behaviors, as displayed in Figures 4.3, 4.4 and 4.5. Note that the points where the percentage of water is zero represent the concentration of the initial saturated solutions. The curves are lines to guide the eyes.

Overall, betulinic acid presents a constant behavior regardless the used mobile phase. The obtained results disclose that a solution containing about 45 % of water (%, v/v) precipitates almost completely this acid (over 98 %). Oleanolic acid exhibits a peculiar behavior since mobile phases containing higher proportions of methanol lead to a quicker precipitation of the acid. (*e.g.* for methanol/acetonitrile 30/70 (%, v/v), the solution needs 30 to 35 % of water (%, v/v) to decrease the acid concentration to half, while for methanol/acetonitrile 50/50 (%, v/v) it is only necessary less than 20 % of water (%, v/v), and for methanol/acetonitrile 70/30 (%, v/v), less than 15 % of water (%, v/v) is sufficient to cut acid concentration to 50%). Nevertheless, for all the mobile phases tested, a solution containing about 50 % (%, v/v) of water precipitates nearly all the oleanolic acid (over 96 %).

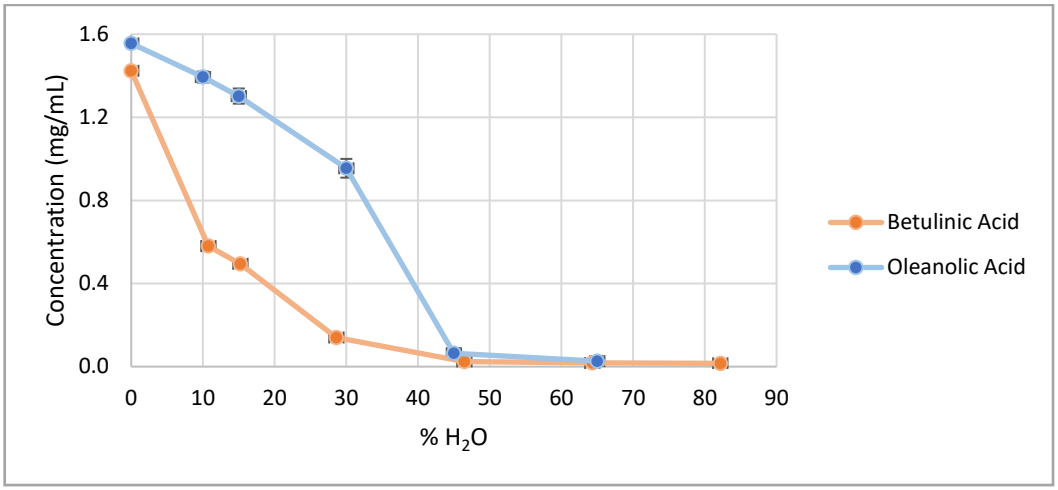

Figure 4.3 – Solubility of betulinic and oleanolic acids in methanol/acetonitrile 30/70 (%, v/v) aqueous mixtures as function of water content (%, v/v) at 20 ºC.

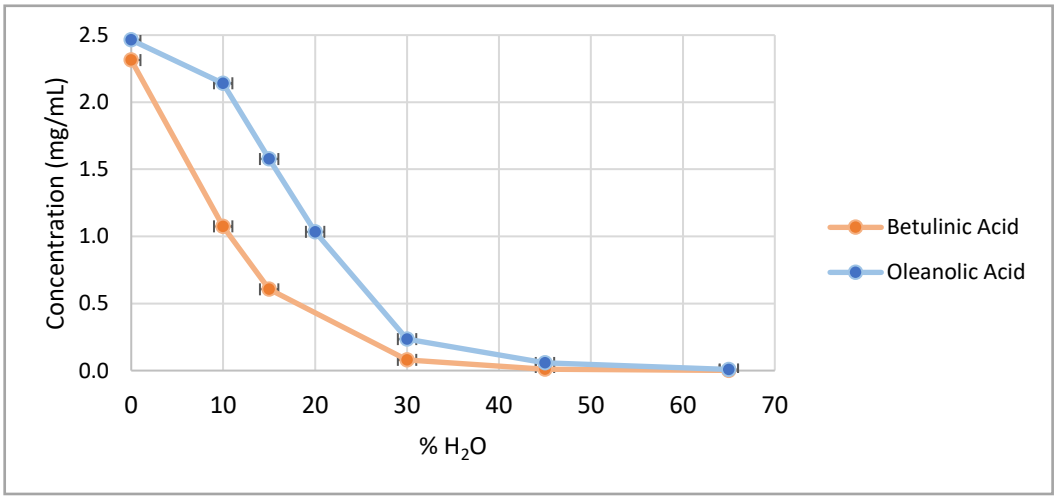

Figure 4.4 – Solubility of betulinic and oleanolic acids in methanol/acetonitrile 50/50 (%, v/v) aqueous mixtures as function of water content (%, v/v) at 20 ºC.

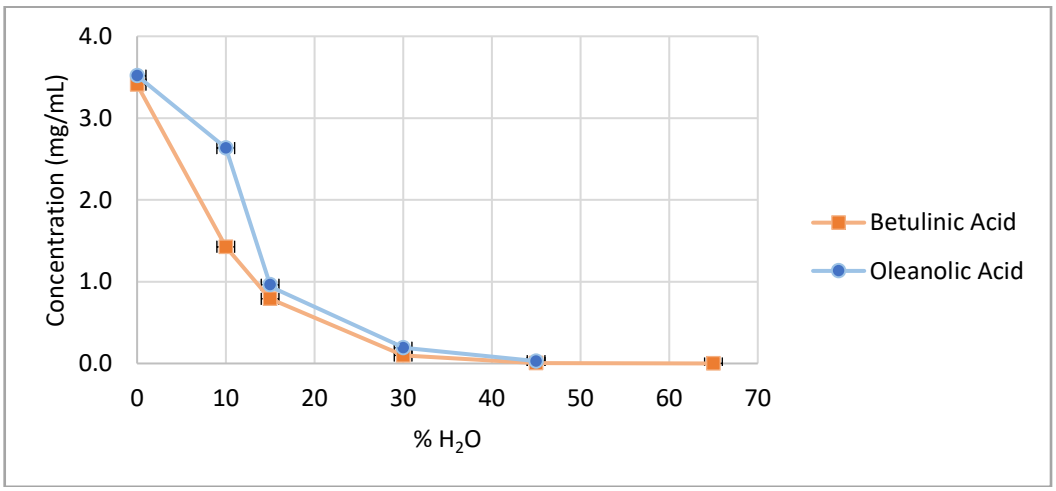

Figure 4.5 – Solubility of betulinic and oleanolic acids in methanol/acetonitrile 70/30 (%, v/v) aqueous mixtures as function of water content (%, v/v) at 20 ºC.

4.3. Breakthrough curves and transport parameters determination

The breakthrough experiments to determine the equilibrium constants and the global linear driving force mass transfer coefficients were performed in the range of 0.20 – 2.00 mg/mL for both acids at a flow rate of 1.00 mL/min and 20 ºC. The experimental breakthrough curves for betulinic and oleanolic acids are exhibited in Figures 4.6 and 4.7, respectively. The chromatographic model used was the Carta's analytical solution, as described in section 2.5. The optimization of the equilibrium constant and the global mass transfer coefficient was performed in MATLAB by fitting Equations (2.17) – (2.22) to the experimental data. The outcomes are shown in Table 4.2. The average absolute relative deviation (AARD) was used as objective function and also to assess the goodness of the fit.

$$AARD = \frac{100}{NDP}\sum_{i=1}^{NDP}\left|\frac{C^{calc} - C^{exp}}{C^{exp}}\right| \tag{4.1}$$

Overall, the results obtained were satisfactory with AARDs below 8 %. These results also disclose that the isotherm is linear in the range of the experimental conditions, as assumed initially. Note the pulse time for all experiments was 29 minutes, except for the breakthrough curve of betulinic acid with a concentration of 1.9910 mg/mL. This means the adsorption stage finishes at 29 minutes, 20 minutes for the exception stated. After this period, the desorption phase begins.

Table 4.2 – Optimized parameters using Carta's analytical solution.

Triterpenic acid	H_i	K_{LDF} (min^{-1})	AARD (%)
Betulinic acid	1.50	520	7.65
Oleanolic acid	1.70	2392	4.33

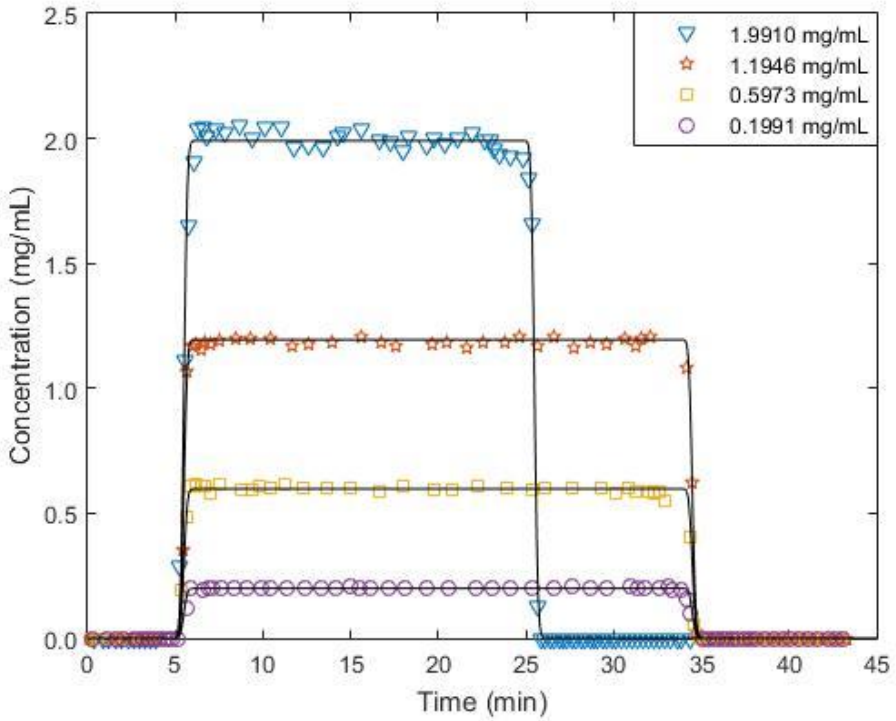

Figure 4.6 – Breakthrough curves of betulinic acid with the Acclaim C30 column and methanol/acetonitrile 50/50 (%, v/v) as mobile phase. Flow rate of 1.00 mL/min, UV detection at 210 nm and 20 ºC. Full line represents Carta's solution.

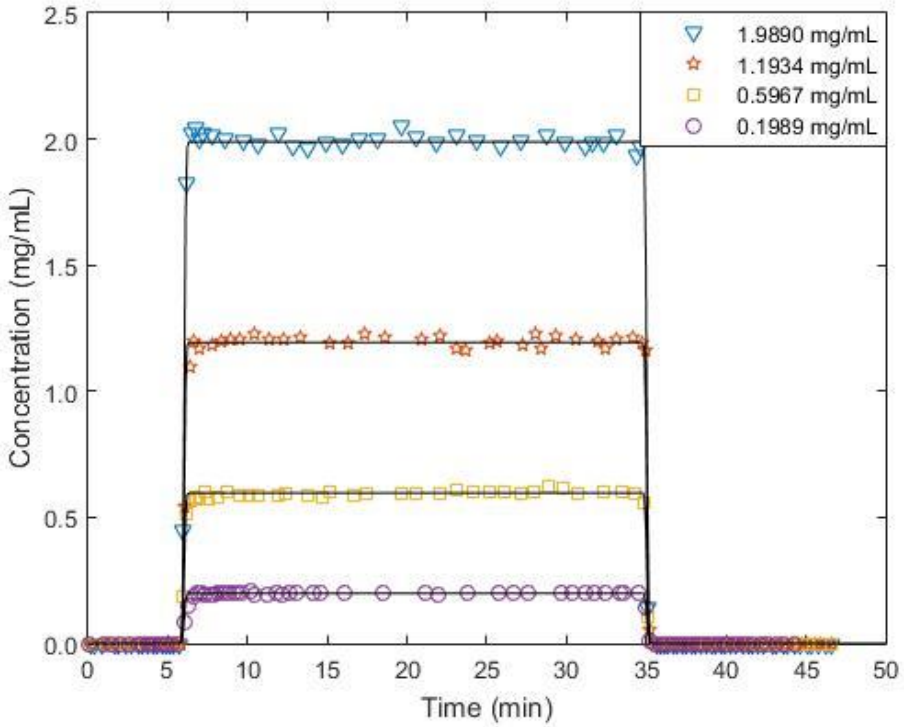

Figure 4.7 – Breakthrough curves of oleanolic acid with the Acclaim C30 column and methanol/acetonitrile 50/50 (%, v/v) as mobile phase. Flow rate of 1.00 mL/min, UV detection at 210 nm and 20 ºC. Full line represents Carta's solution.

4.4. Binary system results

The parameters determined for the pure compounds (consult Table 4.2) were used to predict the behavior of breakthrough curves of binary mixtures of betulinic and oleanolic acids. To validate these parameters, a binary run was conducted as explained in section 3.5. The results for the binary mixture are presented in Figure 4.8. As can be seen, the parameters determined previously for the pure acids were able to predict properly the chromatographic separation with AARDs of 3.69 % and 8.42 % for the betulinic and oleanolic acid breakthrough curves, respectively. The results confirmed the absence of competitive effects and validated the optimized parameters for use in subsequent SMB simulations. The pulse time for this experiment was 29 minutes, so the adsorption stage ends when the time reached 29 minutes, while the desorption stage begun at 29 minutes till the end of the experience.

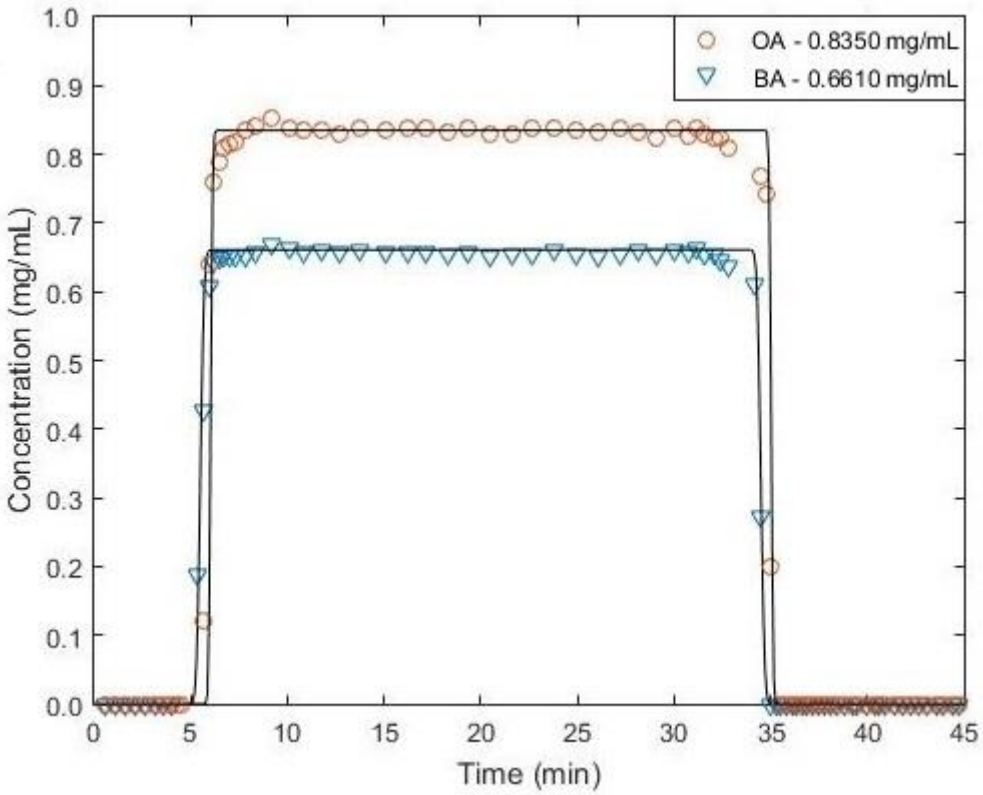

Figure 4.8 – Breakthrough curves of a binary mixture of betulinic and oleanolic acids with the Acclaim C30 column and methanol/acetonitrile 50/50 (%, v/v) as mobile phase. Flow rate of 1.00 mL/min, UV detection at 210 nm and 20 ºC. Full line represents Carta's solution.

4.5. Moment analysis method

In this work, the moment analysis method was implemented in order to analyze quantitatively the chromatographic process and to compare the results obtained with the ones acquired through the fitting of the breakthrough curves, for both acids. This well-established method uses the information condensed in a chromatogram and converts it into a relatively small number of temporal moments, as explained in section 2.4. To perform the chromatographic experiments, the flow rates used were 0.13, 0.20, 0.40, 0.55, 0.70, 0.90 and 1.00 mL/min. The first and second central moments were plotted against L/u_i and u_i, respectively, as shown in Figures 4.9 and 4.10.

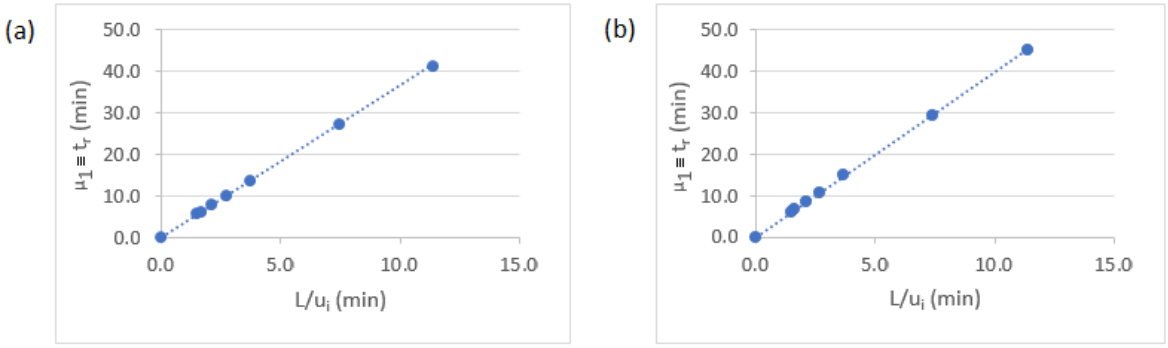

Figure 4.9 – Representation of the first central moment for: (a) betulinic acid; (b) oleanolic acid.

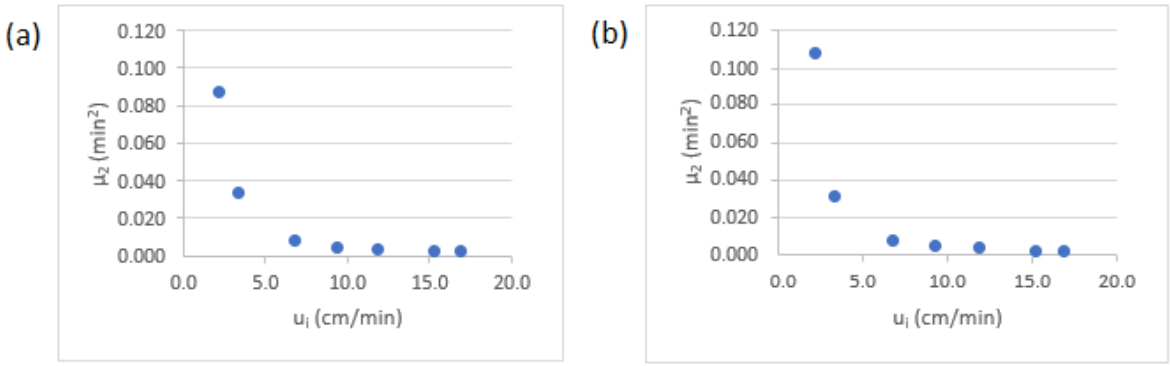

Figure 4.10 – Representation of the second central moment for: (a) betulinic acid; (b) oleanolic acid.

The graphics obtained are as expected, the retention time (representing the first central moment) increases linearly with the decrease of the interstitial velocity (since the column length is constant, the ratio L/u_i increases with the decrease of u_i) and the variance (second central moment) decreases infinitely, tending to zero the higher the interstitial velocity.

Equilibrium constant, global mass transfer coefficient and axial dispersion were optimized in MATLAB by fitting Equations (2.10), (2.12), (2.13), (2.20) and (2.22) to the experimental data shown in Figures 4.9 and 4.10. Results are reported in Table 4.3.

Table 4.3 – Parameters obtained with the moment analysis method.

Triterpenic acid	D_{ax} (cm^2/min)	H_i	K_{LDF} (min^{-1})
Betulinic acid	3.96×10^{-3}	1.47	4578
Oleanolic acid	5.21×10^{-3}	1.64	9974

The H_i values are slightly lower than those obtained before from the chromatographic model, however, they can still represent precisely the behavior of breakthrough curves for both acids. The mass transfer coefficients are larger than the ones shown in Table 4.2. Nevertheless, they are an accurate estimate since K_{LDF} values in that order of magnitude simply mean there is no resistance to mass transfer (*e.g.* when K_{LDF} has a value of 2392 min^{-1} or a value of 9974 min^{-1}, the mass transfer resistance is negligible).

The results from axial dispersion values are also as expected. In Figures 4.11 and 4.12 are show the breakthrough curves of betulinic and oleanolic acids modelled with parameters from Table 4.3 with AARDs of 8.76 % and 9.94 % for the betulinic and oleanolic acid breakthrough curves, respectively.

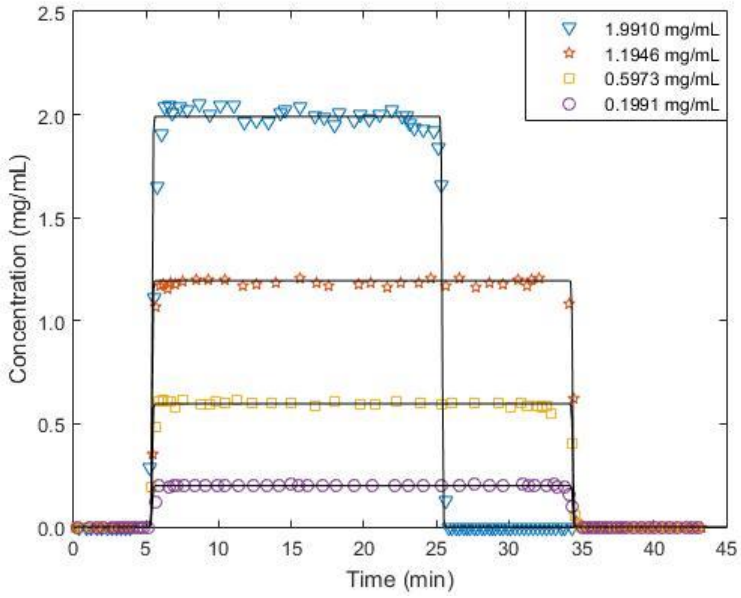

Figure 4.11 – Breakthrough curves of betulinic acid using parameters obtained by moment analysis method with the Acclaim C30 column and methanol/acetonitrile 50/50 (%, v/v) as mobile phase. Flow rate of 1.00 mL/min, UV detection at 210 nm and 20 ºC. Full line represents Carta's solution.

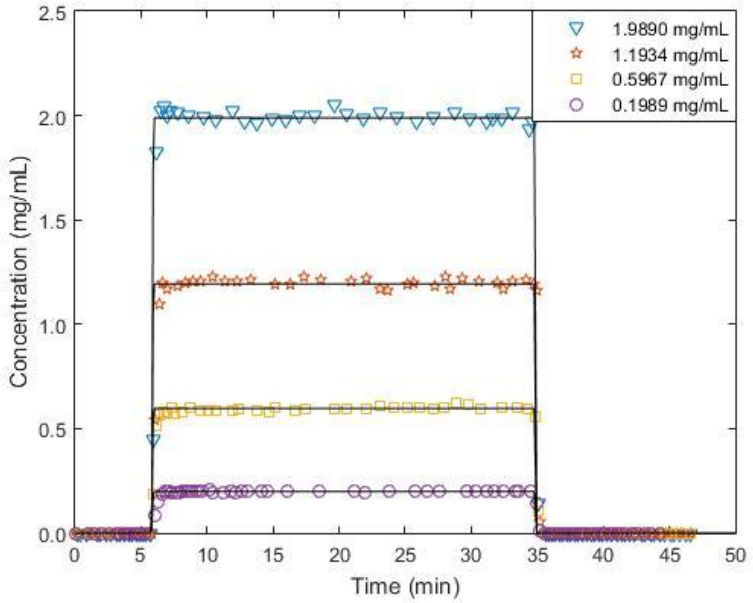

Figure 4.12 – Breakthrough curves of oleanolic acid using parameters obtained by moment analysis method with the Acclaim C30 column and methanol/acetonitrile 50/50 (%, v/v) as mobile phase. Flow rate of 1.00 mL/min, UV detection at 210 nm and 20 ºC. Full line represents Carta's solution.

Finally, in order to demonstrate the flow rate dependence of HETP, it was represented the HETP against the interstitial velocity for both acids, as shown in Figure 4.13. As can be seen, the optimum flow rate to perform separations with betulinic and oleanolic acids is achieved at an interstitial velocity of 6.76 cm/min, which is equivalent to a flow rate of 0.40 mL/min for the Acclaim C30 column.

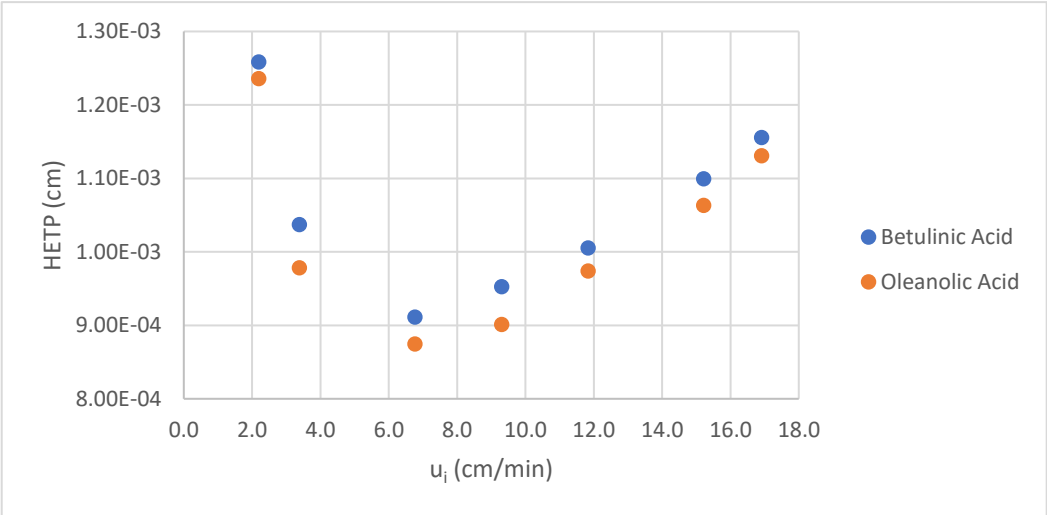

Figure 4.13 – Flow rate dependence of HETP for oleanolic and betulinic acids (Van Deemter plot).

4.6. Simulation of SMB separation of BA/OA mixtures

The separation of betulinic and oleanolic acids was studied *via* SMB simulations, using preparative Acclaim C30 columns using a program developed in EgiChem group. The triangle theory was applied to determine the ideal conditions and the optimal region of binary separation. The transport parameters obtained from the breakthrough assays (see Table 4.2) were used in these simulations. The K_{LDF} values used meet the triangle theory approach, since it does not consider mass transfer resistances. Since the moment analysis method is a reliable method and it gives an accurate estimation of the transport parameters, the values of the axial dispersion coefficient were the ones obtained by this method (see Table 4.3). The composition of the mixture to be fed into the SMB unit was defined taking into consideration the ratio of the triterpenic acids in extracts of *E. globulus* (consult section 3.5.). Consequently, a total concentration of 2.00 mg/mL was established, giving rise to 0.8890 and 1.1110 mg/mL of betulinic and oleanolic acids, respectively.

A total of six different scenarios were studied, employing two different configurations, 1-1-1-1 and 2-2-2-2 column configuration, *i.e.*, one/two columns per section with a total of four sections, where all columns possess the characteristics of an Acclaim C30 column. Different column lengths were studied (10, 15, 20 and 25 cm of column length), where the flow rates in the first section (Q_I^*) are also different. The maximum flow rate allowed was calculated using the Ergun equation (Equation (4.2)), considering the pressure drop limitations of the unit (maximum 30 bar). All necessary parameters for the simulations are listed in Table 4.4.

$$\frac{\Delta P}{L_j} = \frac{150 u_{0,j} \mu_f}{{d_p}^2} \frac{(1-\varepsilon)^2}{\varepsilon^3} + \frac{1.75 \rho_f {u_{0,j}}^2}{d_p} \frac{1-\varepsilon}{\varepsilon^3} \tag{4.2}$$

Table 4.4 – Simulation parameters for the separation of betulinic and oleanolic acids by SMB with Acclaim C30 as adsorbent and methanol/acetonitrile 50/50 (%, v/v) as mobile phase, at 20 ºC.

Parameter	Scenario 1	Scenario 2	Scenario 3	Scenario 4	Scenario 5	Scenario 6
Configuration	2-2-2-2	2-2-2-2	2-2-2-2	2-2-2-2	1-1-1-1	1-1-1-1
L_j **(cm)**	10	15	20	25	10	25
d_i **(cm)**	2.2	2.2	2.2	2.2	2.2	2.2
d_p **(μm)**	5	5	5	5	5	5
Q_I^* **(mL/min)**	27.49	18.33	13.75	11.00	27.49	11.00
ε	0.356	0.356	0.356	0.356	0.356	0.356
C_{BA}^F **(mg/mL)**	0.889	0.889	0.889	0.889	0.889	0.889
C_{OA}^F **(mg/mL)**	1.111	1.111	1.111	1.111	1.111	1.111
H_{BA}	1.50	1.50	1.50	1.50	1.50	1.50
H_{OA}	1.70	1.70	1.70	1.70	1.70	1.70
$K_{LDF,BA}$ **(min^{-1})**	340	340	340	340	340	340
$K_{LDF,OA}$ **(min^{-1})**	335	335	335	335	335	335
$D_{ax,BA}$ **(cm^2/min)** $\times 10^{-3}$	3.96	3.96	3.96	3.96	3.96	3.96
$D_{ax,OA}$ **(cm^2/min)** $\times 10^{-3}$	5.21	5.21	5.21	5.21	5.21	5.21
β	1.000	1.000	1.000	1.000	Variable	Variable

For each scenario the productivity was maximized by defining a minimum purity of 99 %. From scenarios 1 to 4 it was always possible to operate at maximum productivity (represented by the triangle vertex, where β equals 1), as the purities in the extract and raffinate were always above 99 %. The separation region for scenarios 1 to 4 is represented by the triangle theory in Figure 4.14 and the ultimate set of optimum conditions applied to the SMB unit, for these scenarios, are displayed in Table 4.5.

Table 4.5 – Simulation outcomes for the SMB separation of betulinic and oleanolic acids using Acclaim C30 columns as adsorbent and methanol/acetonitrile 50/50 (%, v/v) as mobile phase, at 20 ºC.

Parameter	Scenario 1	Scenario 2	Scenario 3	Scenario 4
t^* (min)	2.01	4.51	8.02	10.03
CSS initial cycle	20	20	20	20
Number of cycles	25	25	25	25
m_{II}	1.50	1.50	1.50	1.50
m_{III}	1.70	1.70	1.70	1.70
Q_{II}^* (mL/min)	25.02	16.68	12.52	10.01
Q_{III}^* (mL/min)	27.49	18.33	13.75	11.00
Q_{IV}^* (mL/min)	25.02	16.68	12.52	10.01
Q_F^* (mL/min)	2.47	1.65	1.23	0.99
Q_E^* (mL/min)	2.47	1.65	1.23	0.99
Q_X^* (mL/min)	2.47	1.65	1.23	0.99
Q_R^* (mL/min)	2.47	1.65	1.23	0.99
SC (m^3/kg)	1.00	1.00	1.00	1.00
RecX (%)	96.15	97.28	97.85	98.01
RecR (%)	96.58	97.57	98.05	98.19
PuX (%)	99.60	99.97	99.98	100.00
PuR (%)	99.27	99.91	100.00	99.99
Prod ($kg/(m^3_{adsorbent}$ day))	23.37	10.39	5.85	4.68

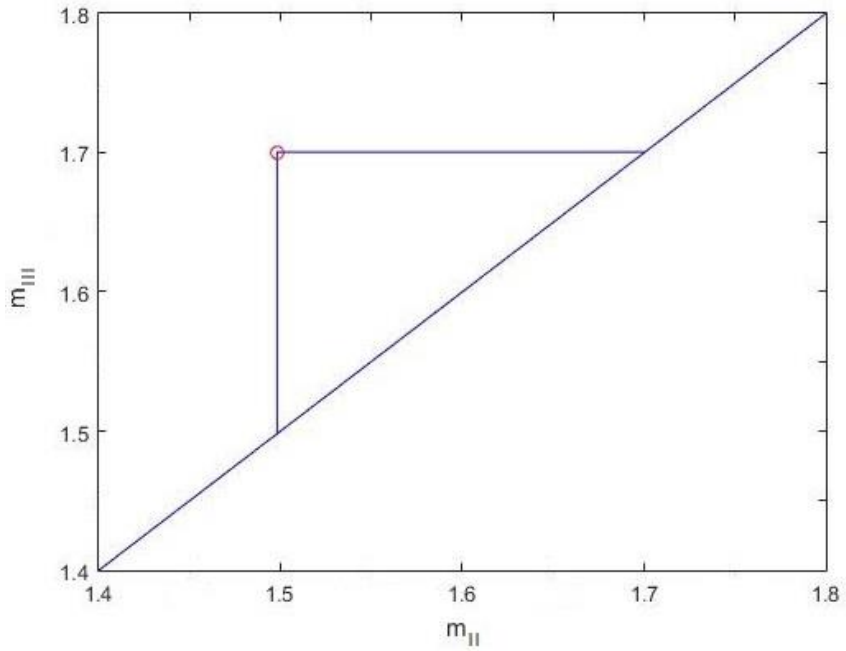

Figure 4.14 – Location of the optimum separation region (red circle) in terms of purities in the (m_{II}, m_{III}) plane for scenarios 1, 2, 3 and 4 for the SMB separation of betulinic and oleanolic acids using Acclaim C30 columns as adsorbent and methanol/acetonitrile 50/50 (%, v/v) as mobile phase, at 20 ºC.

Regarding scenarios 5 and 6, a design of experiments (DoE) was conducted to optimize the separation of the two triterpenic acids, consisting of two continuous factors, the flow rates in section II and III. This method aimed to maximizing the productivity and achieving purities in the extract and raffinate above 99 %. The results of the simulations are presented in Table 4.6 and the optimization domain is represented in Figures 4.15 and 4.16 for scenario 5 and scenario 6, respectively.

Table 4.6 – DoE for the optimization of the SMB separation of betulinic and oleanolic acids using Acclaim C30 columns as adsorbent and methanol/acetonitrile 50/50 (%, v/v) as mobile phase, at 20 ºC.

Scenario	β	m_{II}	m_{III}	PuX (%)	PuR (%)	Prod (kg/($m^3_{adsorbent}$ day))
Scenario 5	1.000	1.50	1.70	93.58	89.76	46.75
	1.020	1.53	1.67	98.90	98.17	31.64
	1.025	1.54	1.66	99.27	98.73	27.98
	1.030	1.54	1.65	99.49	99.08	24.37
	1.050	1.57	1.62	99.85	99.68	10.34
Scenario 6	1.000	1.50	1.70	97.04	96.24	7.48
	1.010	1.51	1.68	99.62	99.14	6.26
	1.020	1.53	1.67	100.00	99.66	5.06
	1.030	1.54	1.65	100.00	99.83	3.90

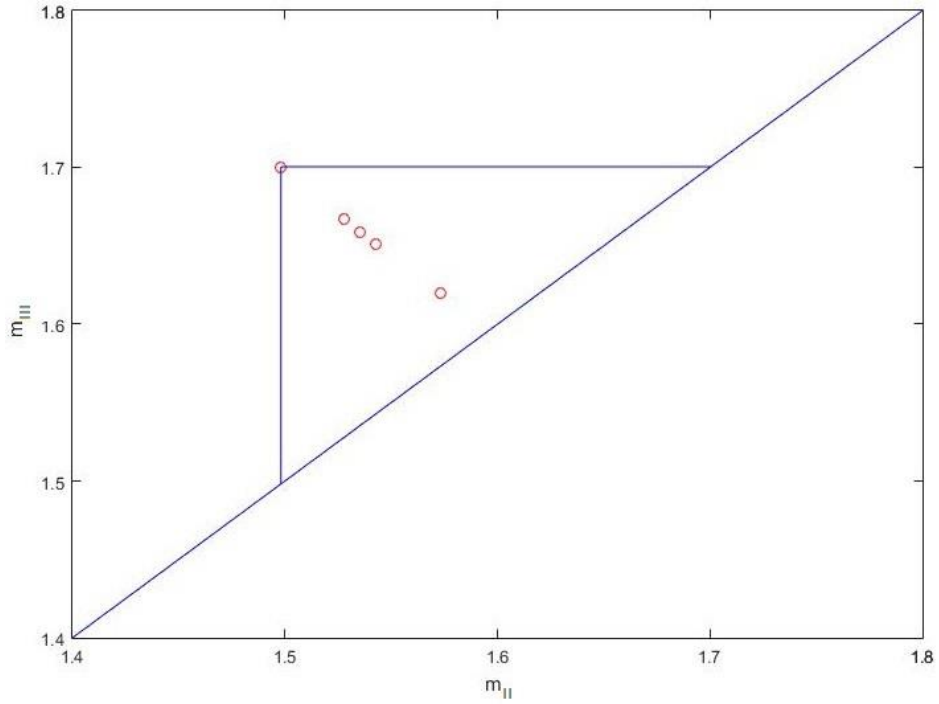

Figure 4.15 – Optimization domain for scenario 5 for SMB separation of betulinic and oleanolic acids using Acclaim C30 columns as adsorbent and methanol/acetonitrile 50/50 (%, v/v) as mobile phase, at 20 ºC. The red circles represent the simulations conducted.

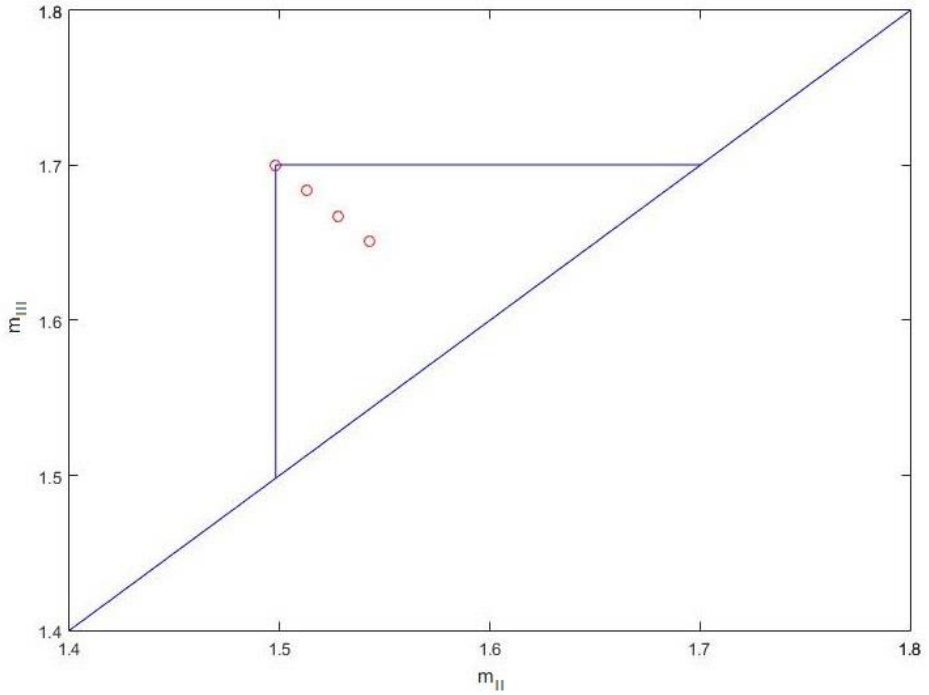

Figure 4.16 – Optimization domain for scenario 6 for SMB separation of betulinic and oleanolic acids using Acclaim C30 columns as adsorbent and methanol/acetonitrile 50/50 (%, v/v) as mobile phase, at 20 ºC. The red circles represent the simulations conducted.

The concentration profiles of betulinic and oleanolic acids in scenarios 2 to 6 such as the concentration histories in the raffinate and extract streams are displayed in Appendix B, for all the SMB simulations conducted. As example, for scenario 1, the concentration profiles of betulinic and oleanolic acids are represented in Figure 4.17 and the concentration histories in the raffinate and extract streams are represented in Figures 4.18 and 4.19, respectively.

As can be noticed in Table 4.5, scenarios 1 to 4 allow the separation of betulinic and oleanolic acid with purities higher than 99.60 % in the extract and higher than 99.25 % in the raffinate. The bigger the column length, the greater the purity, the minor the productivity and the smaller the flow rate in section I. Also, the productivity undergoes a decrease of almost 5 times when the column length increases from 10 cm to 25 cm. Taking these results into account, the smaller columns (10 cm of column length) are the most viable choice since they allow lower adsorbent costs and lower pressure drop.

Concerning scenario 5, where the configuration was 1-1-1-1 with column length of 10 cm, the DoE study permitted to reach the optimum productivity for purities above 99 % both in extract and raffinate through the simulation conducted with β equal to 1.030. For scenario 6, the simulation performed with β equal to 1.010 achieved the maximum productivity, giving purities of 99.62 % and 99.14 % in the extract and in the raffinate, respectively.

Contemplating the results of all scenarios and aiming to lower costs and purities above 99 % in the extract and raffinate, the best outcome was found for a 1-1-1-1 configuration with column lengths of 10 cm. The productivity achieved assumed a value of 24.37 kg/($m^3_{adsorbent}$ day) with a purity of 99.49 % in extract and 99.08 % in the raffinate.

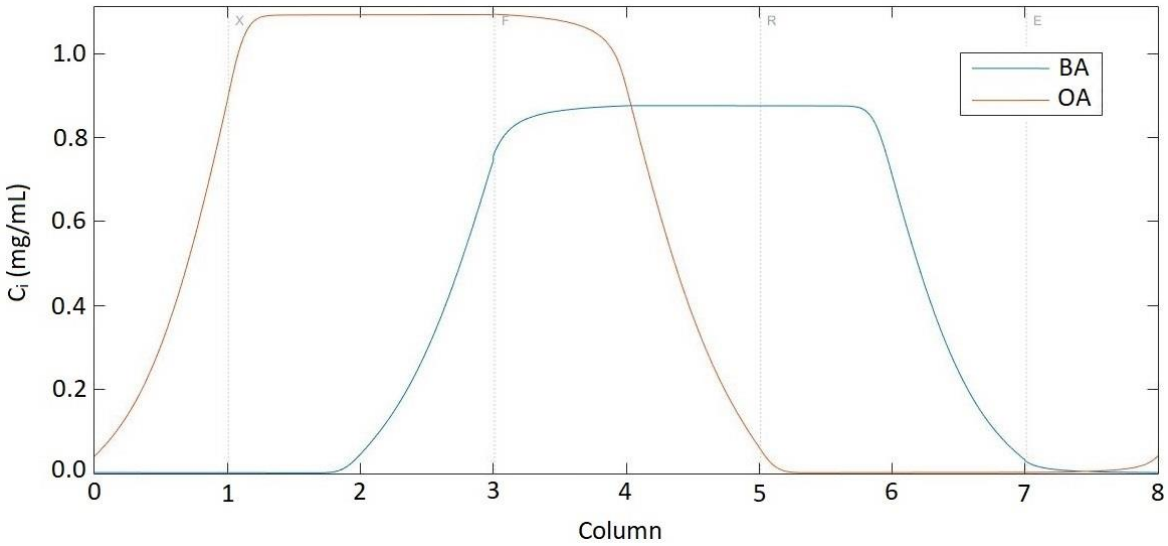

Figure 4.17 – Concentration profiles of betulinic and oleanolic acids for simulations with configuration 2-2-2-2 and column lengths of 10 cm (β equal to 1.000).

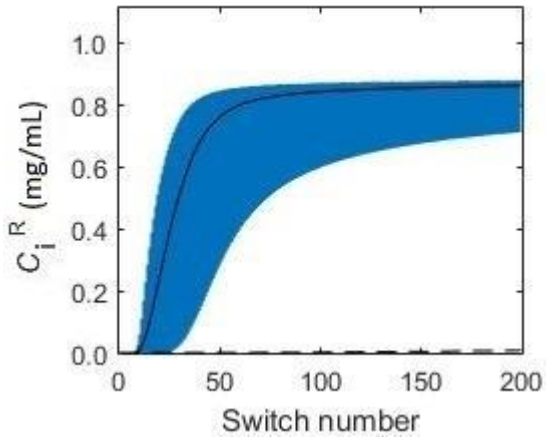

Figure 4.18 – Switch time average concentrations in the raffinate and betulinic acid concentration history (blue) for simulations with configuration 2-2-2-2 and column lengths of 10 cm (β equal to 1.000). Full black line represents the average concentration of betulinic acid and dashed line represents the average concentration of oleanolic acid.

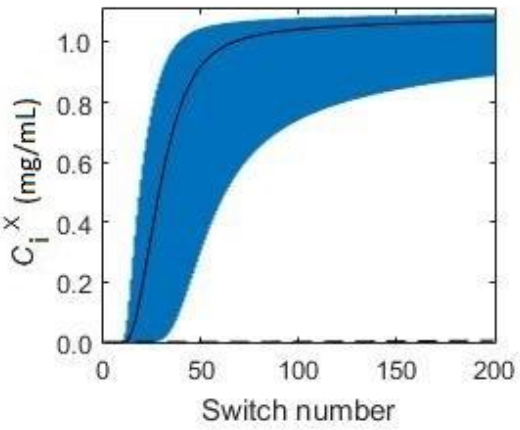

Figure 4.19 – Switch time average concentrations in the extract and oleanolic acid concentration history (blue) for simulations with configuration 2-2-2-2 and column lengths of 10 cm (β equal to 1.000). Full black line represents the average concentration of oleanolic acid and dashed line represents the average concentration of betulinic acid.

Chapter 5

Conclusion and Future Perspectives

Conclusions

The separation of two naturally occurring triterpenic acids, betulinic and oleanolic acids, was studied with the objective of implementing their continuous separation using an SMB technology. Elution chromatography assays were conducted in an Acclaim C30 column to choose the most suitable mobile phase. A mobile phase containing methanol/acetonitrile 50/50 (%, v/v) was selected as it was a good compromise between selectivity and solubility of the target molecules. Afterwards, breakthrough experiments of pure acids solutions were run to determine equilibrium and mass transfer coefficients, since both were necessary to perform simulations of an SMB unit with a feed mixture representative of a natural extract of *E. globulus*. These parameters were then successfully validated in the prediction of a breakthrough curve of binary mixtures of betulinic and oleanolic acids. The moment analysis method was explored and validated, achieving consistent values with the ones obtained from the breakthrough curves. The SMB simulations were accomplished by varying the column lengths from 10 to 25 cm with two different configurations, 1-1-1-1 and 2-2-2-2. It was demonstrated that the SMB unit can achieve purities of at least 99 % in the raffinate and extract streams, for all the scenarios presented. Concerning the simulations with configuration 2-2-2-2, although scenario 1 presents the lowest purities (though always above 99 %), the achieved productivity is higher, due to the smaller column length. However, the best result comes from a simulation with configuration 1-1-1-1, where the purities are higher than 99 % for extract and raffinate, and the productivity presents a value of 24.37 kg/($m^3_{adsorbent}$ day). Additionally, aiming at the recovery of the pure betulinic and oleanolic acids from the raffinate and extract streams, it was performed a solubility study where the solubility of betulinic and oleanolic acids in solvent mixtures of increasing water concentration was experimentally measured and discussed.

Future Perspectives

Hereafter, it is also worth exploring even more solvents to act as mobile phase and different stationary phases. It is important to perform tests in preparative columns in order to compare and evaluate the parameters achieved with the analytical column. Moreover, it is envisioned to expand the SMB simulations to a real unit in order to optimize the operating conditions and to validate the results presented throughout this work.

References

(1) Höök, M.; Tang, X. Depletion of Fossil Fuels and Anthropogenic Climate Change. *Energy Policy* **2013**, *52*, 797–809.

(2) Field, C. B.; Campbell, J. E.; Lobell, D. B. Biomass Energy: The Scale of the Potential Resource. *Trends Ecol. Evol.* **2008**, *23* (2), 65–72.

(3) Aniceto, J. P. S.; Portugal, I.; Silva, C. M. Biomass-Based Polyols through Oxypropylation Reaction. *ChemSusChem* **2012**, *5* (8), 1358–1368.

(4) Cherubini, F. The Biorefinery Concept: Using Biomass Instead of Oil for Producing Energy and Chemicals. *Energy Convers. Manag.* **2010**, *51* (7), 1412–1421.

(5) Barbosa-Filho, J. M.; Do Nascimento Júnior, F. A.; De Andrade Tomaz, A. C.; De Athayde-Filho, P. F.; Da Silva, M. S.; Da Cunha, E. V. L.; De De Souza, M. F. V.; Batista, L. M.; Diniz, M. F. F. M. Natural Products with Antileprotic Activity. *Brazilian J. Pharmacogn.* **2007**, *17* (1), 141–148.

(6) Maier, M. E. Design and Synthesis of Analogues of Natural Products. *Org. Biomol. Chem.* **2015**, *13* (19), 5302–5343.

(7) Aniceto, J. P. S.; Azenha, I. S.; Domingues, F. M. J.; Mendes, A.; Silva, C. M. Design and Optimization of a Simulated Moving Bed Unit for the Separation of Betulinic, Oleanolic and Ursolic Acids Mixtures: Experimental and Modeling Studies. *Sep. Purif. Technol.* **2018**, *192*, 401–411.

(8) De Carvalho, C. C. C. R.; Da Fonseca, M. M. R. Biotransformation of Terpenes. *Biotechnol. Adv.* **2006**, *24* (2), 134–142.

(9) ICNF, I. Áreas dos usos do solo e das espécies florestais de Portugal continental em 1995, 2005 e 2010. http://www2.icnf.pt/portal/florestas/ifn/resource/doc/ifn/ifn6-res-prelimv1-1 (accessed Jun 3, 2019).

(10) Domingues, R. M. A.; Patinha, D. J. S.; Sousa, G. D. A.; Villaverde, J. J.; Silva, C. M.; Freire, C. S. R.; Silvestre, A. J. D.; Pascoal Neto, C. *Eucalyptus* Biomass Residues from Agro-Forest and Pulping Industries as Sources of High-Value Triterpenic Compounds. *Cellul. Chem. Technol.* **2011**, *45* (7–8), 475–481.

(11) Freire, C. S. R.; Silvestre, A. J. D.; Neto, C. P.; Cavaleiro, J. A. S. Lipophilic Extractives of the Inner and Outer Barks of *Eucalyptus Globulus*. *Holzforschung* **2002**, *56* (4), 372–379.

(12) Laszczyk, M. N. Pentacyclic Triterpenes of the Lupane, Oleanane and Ursane

Group as Tools in Cancer Therapy. *Planta Med.* **2009**, *75* (15), 1549–1560.

(13) Fulda, S. Betulinic Acid for Cancer Treatment and Prevention. *Int. J. Mol. Sci.* **2008**, *9* (6), 1096–1107.

(14) Ghaffari Moghaddam, M.; Bin H. Ahmad, F.; Samzadeh-Kermani, A. Biological Activity of Betulinic Acid: A Review. *Pharmacol. & Pharm.* **2012**, *03* (02), 119–123.

(15) Del Carmen Recio, M.; Giner, R. M.; Manez, S.; Gueho, J.; Julien, H. R.; Hostettmann, K.; Rios, J. L. Investigations on the Steroidal Anti-Inflammatory Activity of Triterpenoids from *Diospyros Leucomelas*. *Planta Med.* **1995**, *61* (1), 9–12.

(16) De Sá, M. S.; Costa, J. F. O.; Krettli, A. U.; Zalis, M. G.; De Azevedo Maia, G. L.; Sette, I. M. F.; De Amorim Câmara, C.; Filho, J. M. B.; Giulietti-Harley, A. M.; Ribeiro Dos Santos, R.; et al. Antimalarial Activity of Betulinic Acid and Derivatives in Vitro against *Plasmodium Falciparum* and in Vivo in P. Berghei-Infected Mice. *Parasitol. Res.* **2009**, *105* (1), 275–279.

(17) Yogeeswari, P.; Sriram, D. Betulinic Acid and Its Derivatives: A Review on Their Biological Properties. *Curr. Med. Chem.* **2010**, *12* (6), 657–666.

(18) Enwerem, N. M.; Okogun, J. I.; Wambebe, C. O.; Okorie, D. A.; Akah, P. A. Anthelmintic Activity of the Stem Bark Extracts of *Berlina Grandiflora* and One of Its Active Principles, Betulinic Acid. *Phytomedicine* **2001**, *8* (2), 112–114.

(19) Tolstikova, T. G.; Sorokina, I. V.; Tolstikov, G. A.; Tolstikov, A. G.; Flekhter, O. B. Biological Activity and Pharmacological Prospects of Lupane Terpenoids: II. Semisynthetic Lupane Derivatives. *Bioorganicheskaia khimiia.* **2006**, *32* (3), 291–307.

(20) Liu, J. Oleanolic Acid and Ursolic Acid: Research Perspectives. *J. Ethnopharmacol.* **2005**, *100* (1–2), 92–94.

(21) Fontanay, S.; Grare, M.; Mayer, J.; Finance, C.; Duval, R. E. Ursolic, Oleanolic and Betulinic Acids: Antibacterial Spectra and Selectivity Indexes. *J. Ethnopharmacol.* **2008**, *120* (2), 272–276.

(22) Liu, J. Pharmacology of Oleanolic Acid and Ursolic Acid. *J. Ethnopharmacol.* **1995**, *49* (2), 57–68.

(23) Gutiérrez-Rebolledo, G. A.; Siordia-Reyes, A. G.; Meckes-Fischer, M.; Jiménez-

Arellanes, A. Hepatoprotective Properties of Oleanolic and Ursolic Acids in Antitubercular Drug-Induced Liver Damage. *Asian Pac. J. Trop. Med.* **2016**, *9* (7), 644–651.

(24) Martelanc, M.; Vovk, I.; Simonovska, B. Separation and Identification of Some Common Isomeric Plant Triterpenoids by Thin-Layer Chromatography and High-Performance Liquid Chromatography. *J. Chromatogr. A* **2009**, *1216* (38), 6662–6670.

(25) Henner, S.-T. *Preparative Chromatography of Fine Chemicals and Pharmaceutical Agents*; 2005.

(26) Aniceto, J. P. S.; Silva, C. M. Preparative Chromatography: Batch and Continuous. *Anal. Sep. Sci.* **2015**, 1207–1313.

(27) Rajendran, A.; Paredes, G.; Mazzotti, M. Simulated Moving Bed Chromatography for the Separation of Enantiomers. *J. Chromatogr. A* **2009**, *1216* (4), 709–738.

(28) Aniceto, J. P. S.; Silva, C. M. Simulated Moving Bed Strategies and Designs: From Established Systems to the Latest Developments. *Sep. Purif. Rev.* **2014**, *44* (1), 41–73.

(29) Broughton, D. B.; Gerhold, C. G. US Patent 2,985,589, 1961.

(30) Wiśniewski, Ł.; Antošová, M.; Polakovič, M. Simulated Moving Bed Chromatography Separation of Galacto-Oligosaccharides. *Acta Chim. Slovaca* **2013**, *6* (2), 206–210.

(31) Sá Gomes, P.; Minceva, M.; Rodrigues, A. E. Simulated Moving Bed Technology: Old and New. *Adsorption* **2006**, *12* (5–6), 375–392.

(32) Adam, P.; Nicoud, R. N.; Bailly, M.; Ludermann-Houbourger. US Patent 6,136,198. **1985**.

(33) Zhang, Z.; Mazzotti, M.; Morbidelli, M. PowerFeed Operation of Simulated Moving Bed Units: Changing Flow-Rates during the Switching Interval. *J. Chromatogr. A* **2003**, *1006* (1–2), 87–99.

(34) Schramm, H.; Kienle, A.; Kaspereit, M.; Seidel-Morgenstern, A. Improved Operation of Simulated Moving Bed Processes by Cyclic Modulation of the Feed Concentration. *Chemie Ing. Tech.* **2002**, 1151–1155.

(35) Schramm, H.; Kaspereit, M.; Kienle, A.; Seidel-Morgenstern, A. Simulated Moving Bed Process with Cyclic Modulation of the Feed Concentration. *J. Chromatogr. A*

2003, *1006* (1–2), 77–86.

(36) Application, F.; Data, P.; Nicoud, R.; Adam, P.; Ludemann-hombourger, O. US Patent No. WO2004039468, 2004.

(37) Abdelmoumen, S.; Muhr, L.; Bailly, M.; Ludemann-Hombourger, O. The M3C Process: A New Multicolumn Chromatographic Process Integrating a Concentration Step. I - The Equilibrium Model. *Sep. Sci. Technol.* **2006**, *41* (12), 2639–2663.

(38) Paredes, G.; Rhee, H. K.; Mazzotti, M. Design of Simulated-Moving-Bed Chromatography with Enriched Extract Operation (EE-SMB): Langmuir Isotherms. *Ind. Eng. Chem. Res.* **2006**, *45* (18), 6289–6301.

(39) Jin, S. H.; Wankat, P. C. New Design of Simulated Moving Bed (SMB) for Ternary Separations. *Ind. Eng. Chem. Res.* **2005**, *44* (6), 1906–1913.

(40) Hur, J. S.; Wankat, P. C. Two-Zone SMB/Chromatography for Center-Cut Separation from Ternary Mixtures: Linear Isotherm Systems. *Ind. Eng. Chem. Res.* **2006**, *45* (4), 1426–1433.

(41) Araújo, J. M. M.; Rodrigues, R. C. R.; Mota, J. P. B. Use of Single-Column Models for Efficient Computation of the Periodic State of a Simulated Moving Bed Process. *Ind. Eng. Chem. Res.* **2006**, *45* (15), 5314–5325.

(42) Abunasser, N.; Wankat, P. C.; Kim, Y. S.; Koo, Y. M. One-Column Chromatograph with Recycle Analogous to a Four-Zone Simulated Moving Bed. *Ind. Eng. Chem. Res.* **2003**, *42* (21), 5268–5279.

(43) Sá Gomes, P.; Leão, C. P.; Rodrigues, A. E. Simulation of True Moving Bed Adsorptive Reactor: Detailed Particle Model and Linear Driving Force Approximations. *Chem. Eng. Sci.* **2007**, *62* (4), 1026–1041.

(44) Kim, J. K.; Abunasser, N.; Wankat, P. C. Use of Two Feeds in Simulated Moving Beds for Binary. *Korean J. Chem. Eng.* **2005**, *22* (4), 619–627.

(45) Gomes, P. S.; Rodrigues, A. E. Outlet Streams Swing (OSS) and MultiFeed Operation of Simulated Moving Beds. *Sep. Sci. Technol.* **2007**, *42* (2), 223–252.

(46) Kurup, A. S.; Hidajat, K.; Ray, A. K. Comparative Study of Modified Simulated Moving Bed Systems at Optimal Conditions for the Separation of Ternary Mixtures of Xylene Isomers. *Ind. Eng. Chem. Res.* **2006**, *45* (18), 6251–6265.

(47) da Silva, E. A. B.; Rodrigues, A. E. Design of Chromatographic Multicomponent Separation by a Pseudo-Simulated Moving Bed. *Am. Inst. Chem. Eng.* **2006**.

(48) Martínez Cristancho, C. A.; Peper, S.; Johannsen, M. Supercritical Fluid Simulated Moving Bed Chromatography for the Separation of Ethyl Linoleate and Ethyl Oleate. *J. Supercrit. Fluids* **2012**, *66*, 129–136.

(49) Faria, R. P. V.; Rodrigues, A. E. Instrumental Aspects of Simulated Moving Bed Chromatography. *J. Chromatogr. A* **2015**, *1421*, 82–102.

(50) Carta, G. Exact Analytic Solution of a Mathematical Model for Chromatographic Operations. *Chem. Eng. Sci.* **1988**, *43* (10), 2877–2883.

(51) Li, M.; Bao, Z.; Xing, H.; Yang, Q.; Yang, Y.; Ren, Q. Simulated Moving Bed Chromatography for the Separation of Ethyl Esters of Eicosapentaenoic Acid and Docosahexaenoic Acid under Nonlinear Conditions. *J. Chromatogr. A* **2015**, *1425*, 189–197.

(52) Seidel-Morgenstern, A. Experimental Determination of Single Solute and Competitive Adsorption Isotherms. *J. Chromatogr. A* **2004**, *1037* (1–2), 255–272.

(53) Andrzejewska, A.; Kaczmarski, K.; Guiochon, G. Theoretical Study of the Accuracy of the Pulse Method, Frontal Analysis, and Frontal Analysis by Characteristic Points for the Determination of Single Component Adsorption Isotherms. *J. Chromatogr. A* **2009**, *1216* (7), 1067–1083.

(54) Golshan-Shirazi, S.; Guiochon, G. Analytical Solution of the Ideal Model of Elution Chromatography in the Case of a Binary Mixture with Competitive Langmuir Isotherms. II. Solution Using the h-Transform. *J. Chromatogr. A* **1989**, *484* (C), 125–151.

(55) Rodrigues, A. E.; Pereira, C.; Minceva, M.; Pais, L. S.; Ribeiro, A. M.; Ribeiro, A.; Silva, M.; Graça, N.; Santos, J. C. *Principles of Simulated Moving Bed*; 2015.

(56) Devault, D. De. The Theory of Chromatography. *J. Am. Chem. Soc.* **1943**, *65*, 532–540.

(57) Pais, L. S.; Loureiro, J. M.; Rodrigues, A. E. Modeling Strategies for Enantiomers Separation by SMB Chromatography. *AIChE J.* **1998**, *44* (3), 561–569.

(58) Miyabe, K. Moment Analysis of Chromatographic Behavior in Reversed-Phase Liquid Chromatography. *J. Sep. Sci.* **2009**, *32* (5–6), 757–770.

(59) Carta, G.; Pigford, R. L. Analytical Solution for Cycling Zone Adsorption. *Chem. Eng. Sci.* **1986**, *41* (3), 511–517.

(60) Klinkenberg, A.; Zuiderweg, F. J.; van Deemter, J. J. Longitudinal Diffusion and

Resistance to Mass Transfer as Causes of Nonideality in Chromatography. *Chem. Eng. Sci.* **1956**, *5* (6), 271–289.

(61) Villermaux, J. Chemical Engineering Approach to Dynamic Modelling of Linear Chromatography. A Flexible Method for Representing Complex Phenomena from Simple Concepts. *J. Chromatogr. A* **1987**, *406* (C), 11–26.

(62) Rasmuson, A. The Effect of Particles and Properties of Variable Size, Shape and Properties on the Dynamics of Fixed Beds. *Chem. Eng. Sci.* **1985**, *40* (4), 621–629.

(63) Golshan-shirazi, S.; Guiochon, G. Analytical Solution for the Ideal Model of Chromatography in the Case of a Langmuir Isotherm. *Anal. Chem.* **1988**, *60* (21), 2364–2374.

(64) Qamar, S.; Seidel-Morgenstern, A. Extending the Potential of Moment Analysis in Chromatography. *TrAC - Trends Anal. Chem.* **2016**, *81*, 87–101.

(65) Domingues, R. M. A.; De Melo, M. M. R.; Oliveira, E. L. G.; Neto, C. P.; Silvestre, A. J. D.; Silva, C. M. Optimization of the Supercritical Fluid Extraction of Triterpenic Acids from *Eucalyptus Globulus* Bark Using Experimental Design. *J. Supercrit. Fluids* **2013**, *74*, 105–114.

(66) Melo, M. M. R. De; Oliveira, E. L. G.; Silvestre, A. J. D.; Silva, C. M. Supercritical Fluid Extraction of Triterpenic Acids from *Eucalyptus Globulus* Bark. *J. Supercrit. Fluids* **2012**, *70*, 137–145.

(67) Pursch, M.; Strohschein, S.; Ha, H.; Albert, K. Temperature-Dependent Behavior of C 30 Interphases. A Solid-State NMR and LC - NMR Study. *Anal. Chem.* **1996**, 386–393.

(68) Albert, K. Correlation between Chromatographic and Physicochemical Properties of Stationary Phases in HPLC: C30 Bonded Reversed-Phase Silica. *TrAC - Trends Anal. Chem.* **1998**, *17* (10), 648–658.

Appendices

Appendix A

This appendix contains all chromatograms obtained with Acclaim C30 column in the preliminary pulse experiments of the study of the separation of betulinic and oleanolic acids by SMB. The chromatograms achieved using a UV/Vis detector are available from Figure A.1 to Figure A.7. Concerning the chromatograms accomplished using a refractive index detector, these are presented from Figure A.8 to Figure A.17.

Mobile phase: methanol

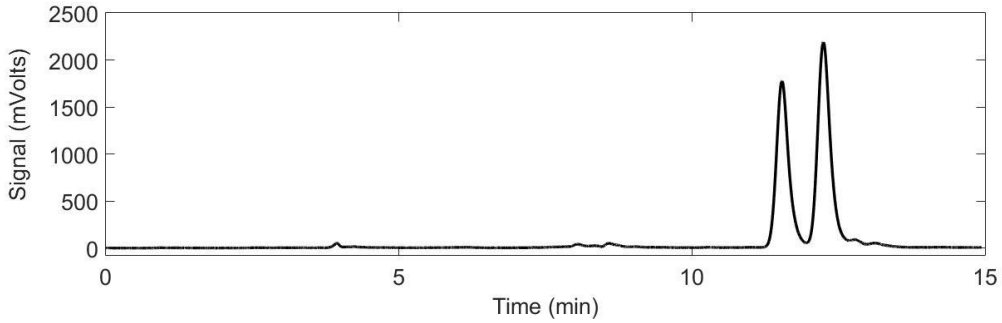

Figure A.1 – HPLC chromatogram of a binary mixture of betulinic (BA, 0.09800 mg/mL) and oleanolic (OA, 0.1016 mg/mL) acids using an Acclaim C30 column with methanol as mobile phase. Flow rate of 0.4 mL/min, UV detection at 210 nm, loop volume of 20 µL, and 20 ºC.

Mobile phase: methanol/water 95/5 (%, v/v)

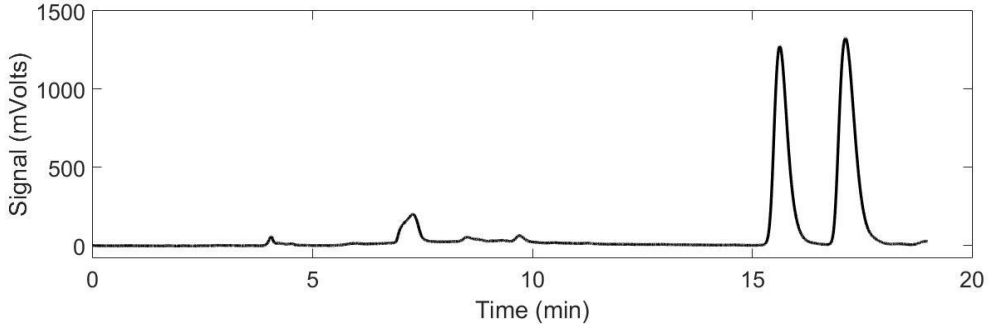

Figure A.2 – HPLC chromatogram of a binary mixture of betulinic (BA, 0.09800 mg/mL) and oleanolic (OA, 0.1016 mg/mL) acids using an Acclaim C30 column with methanol/water 95/5 (%, v/v) as mobile phase. Flow rate of 0.4 mL/min, UV detection at 210 nm, loop volume of 20 µL, and 20 ºC.

Mobile phase: methanol/water 90/10 (%, v/v)

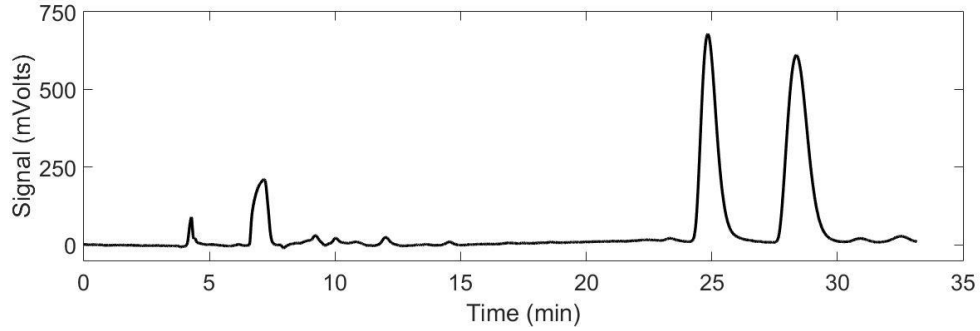

Figure A.3 – HPLC chromatogram of a binary mixture of betulinic (BA, 0.09800 mg/mL) and oleanolic (OA, 0.1016 mg/mL) acids using an Acclaim C30 column with methanol/water 90/10 (%, v/v) as mobile phase. Flow rate of 0.4 mL/min, UV detection at 210 nm, loop volume of 20 µL, and 20 ºC.

Mobile phase: methanol/acetonitrile 85/15 (%, v/v)

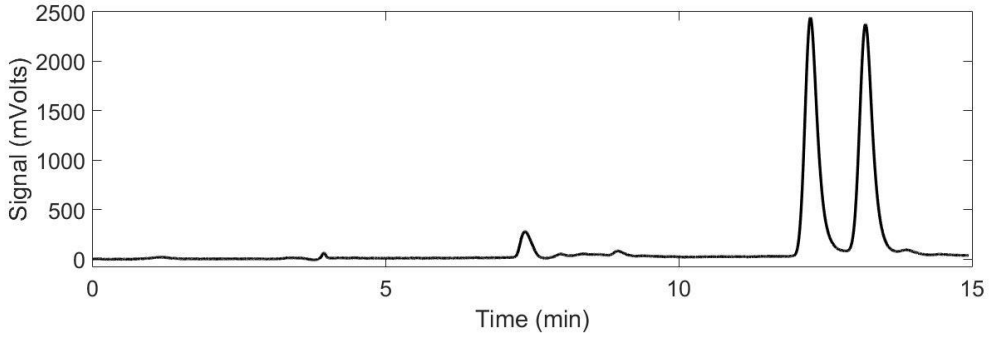

Figure A.4 – HPLC chromatogram of a binary mixture of betulinic (BA, 0.09800 mg/mL) and oleanolic (OA, 0.1016 mg/mL) acids using an Acclaim C30 column with methanol/acetonitrile 85/15 (%, v/v) as mobile phase. Flow rate of 0.4 mL/min, UV detection at 210 nm, loop volume of 20 µL, and 20 ºC.

Mobile phase: methanol/acetonitrile 70/30 (%, v/v)

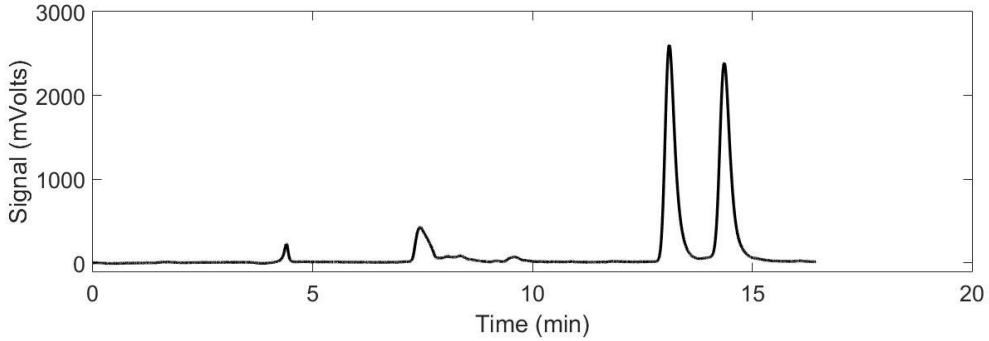

Figure A.5 – HPLC chromatogram of a binary mixture of betulinic (BA, 0.09800 mg/mL) and oleanolic (OA, 0.1016 mg/mL) acids using an Acclaim C30 column with methanol/acetonitrile 70/30 (%, v/v) as mobile phase. Flow rate of 0.4 mL/min, UV detection at 210 nm, loop volume of 20 µL, and 20 ºC.

Mobile phase: methanol/acetonitrile 50/50 (%, v/v)

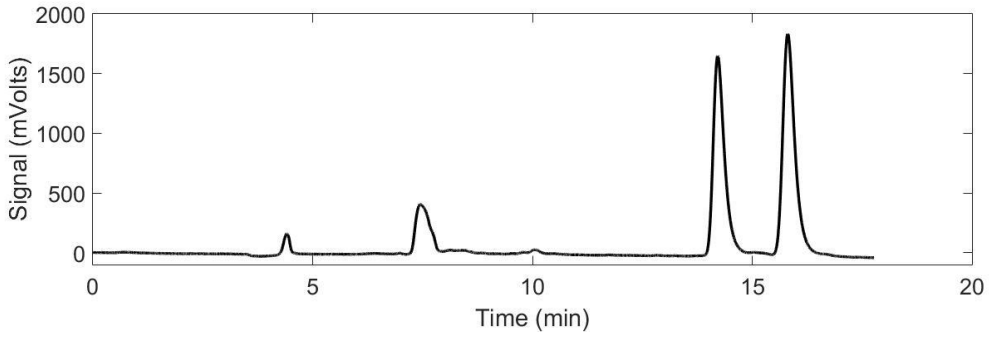

Figure A.6 – HPLC chromatogram of a binary mixture of betulinic (BA, 0.09800 mg/mL) and oleanolic (OA, 0.1016 mg/mL) acids using an Acclaim C30 column with methanol/acetonitrile 50/50 (%, v/v) as mobile phase. Flow rate of 0.4 mL/min, UV detection at 210 nm, loop volume of 20 µL, and 20 ºC.

Mobile phase: methanol/acetonitrile 30/70 (%, v/v)

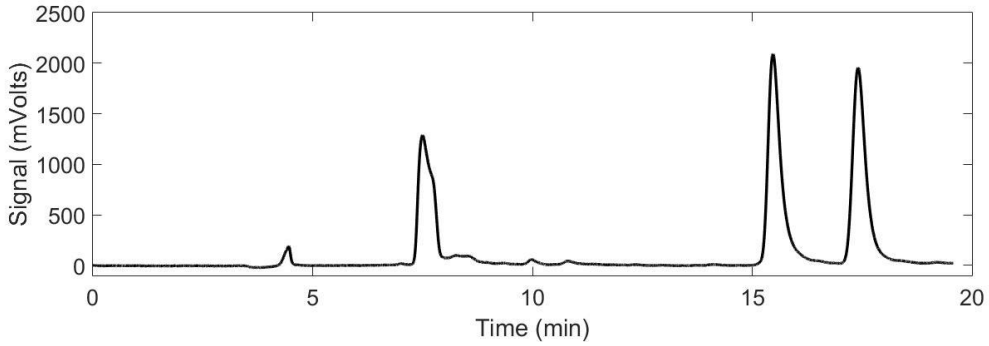

Figure A.7 – HPLC chromatogram of a binary mixture of betulinic (BA, 0.09800 mg/mL) and oleanolic (OA, 0.1016 mg/mL) acids using an Acclaim C30 column with methanol/acetonitrile 30/70 (%, v/v) as mobile phase. Flow rate of 0.4 mL/min, UV detection at 210 nm, loop volume of 20 µL, and 20 ºC.

Mobile phase: ethanol

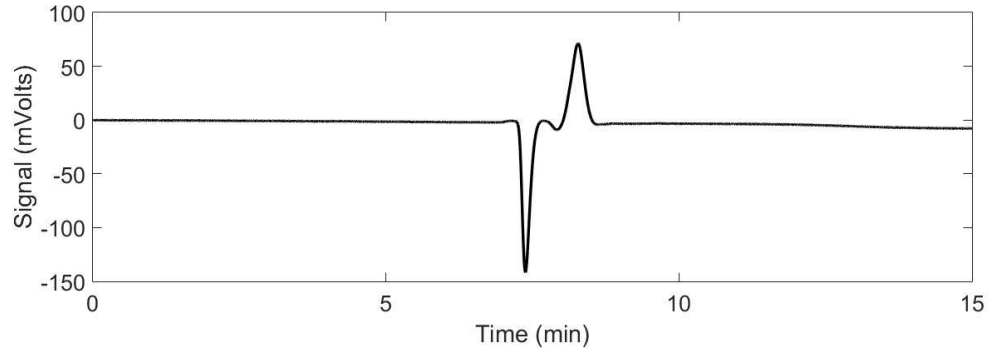

Figure A.8 – HPLC chromatogram of a binary mixture of betulinic (BA, 0.4980 mg/mL) and oleanolic (OA, 0.5040 mg/mL) acids using an Acclaim C30 column with ethanol as mobile phase. Flow rate of 0.4 mL/min, loop volume of 20 µL, and 20 ºC.

Mobile phase: ethanol/water 90/10 (%, v/v)

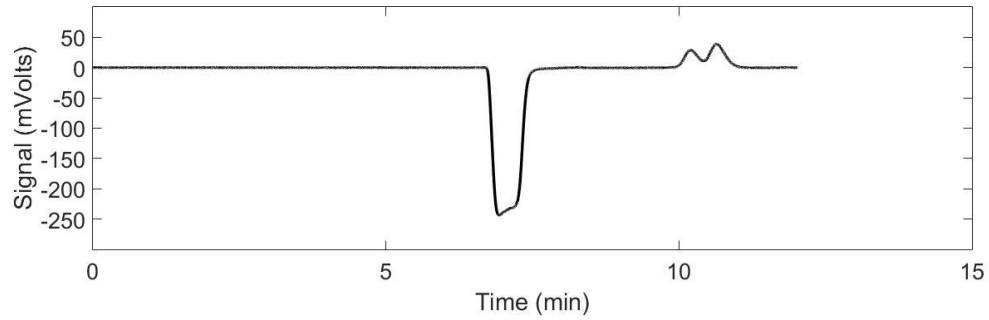

Figure A.9 – HPLC chromatogram of a binary mixture of betulinic (BA, 0.4980 mg/mL) and oleanolic (OA, 0.5040 mg/mL) acids using an Acclaim C30 column with ethanol/water 90/10 (%, v/v) as mobile phase. Flow rate of 0.4 mL/min, loop volume of 20 µL, and 20 ºC.

Mobile phase: ethanol/water 90/10 (%, v/v)

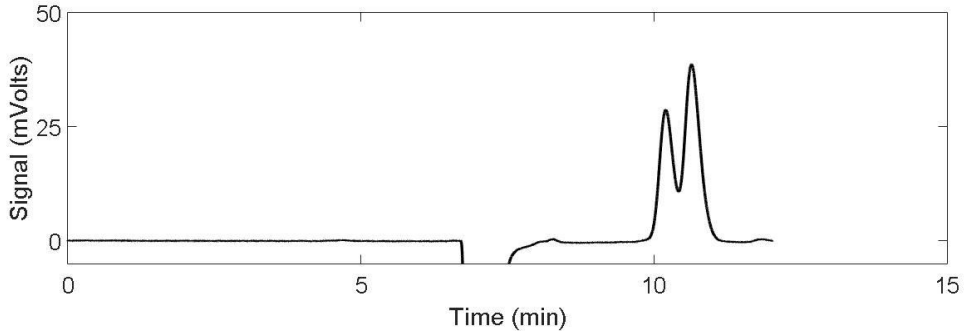

Figure A.10 – Extended HPLC chromatogram of a binary mixture of betulinic (BA, 0.4980 mg/mL) and oleanolic (OA, 0.5040 mg/mL) acids using an Acclaim C30 column with ethanol/water 90/10 (%, v/v) as mobile phase. Flow rate of 0.4 mL/min, loop volume of 20 µL, and 20 ºC.

Mobile phase: ethanol/acetonitrile 85/15 (%, v/v)

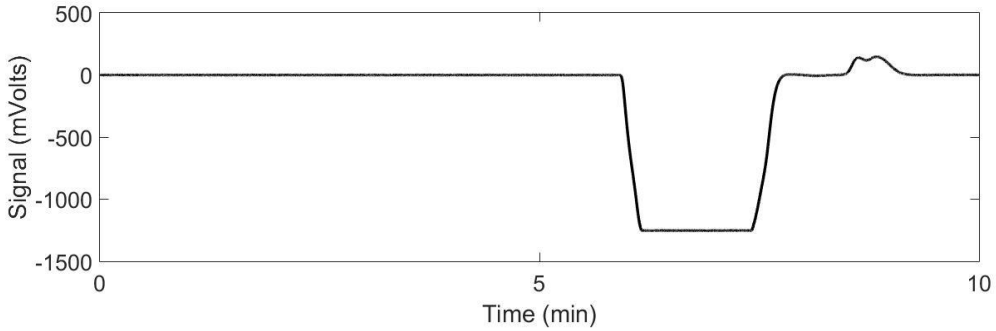

Figure A.11 – HPLC chromatogram of a binary mixture of betulinic (BA, 0.4000 mg/mL) and oleanolic (OA, 0.4100 mg/mL) acids using an Acclaim C30 column with ethanol/acetonitrile 85/15 (%, v/v) as mobile phase. Flow rate of 0.4 mL/min, loop volume of 100 µL, and 20 ºC.

Mobile phase: ethanol/acetonitrile 85/15 (%, v/v)

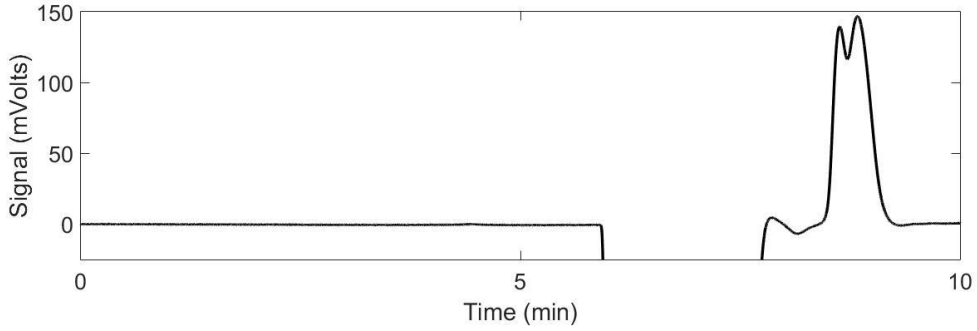

Figure A.12 – Extended HPLC chromatogram of a binary mixture of betulinic (BA, 0.4000 mg/mL) and oleanolic (OA, 0.4100 mg/mL) acids using an Acclaim C30 column with ethanol/acetonitrile 85/15 (%, v/v) as mobile phase. Flow rate of 0.4 mL/min, loop volume of 100 µL, and 20 ºC.

Mobile phase: ethanol/acetonitrile 50/50 (%, v/v)

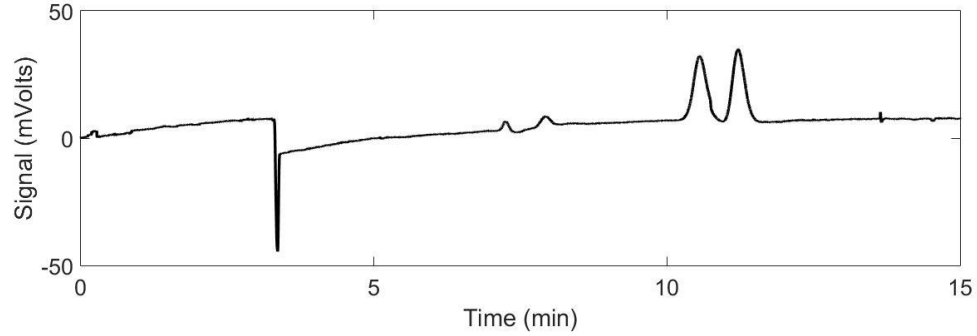

Figure A.13 – HPLC chromatogram of a binary mixture of betulinic (BA, 0.4000 mg/mL) and oleanolic (OA, 0.4100 mg/mL) acids using an Acclaim C30 column with ethanol/acetonitrile 50/50 (%, v/v) as mobile phase. Flow rate of 0.4 mL/min, loop volume of 20 µL, and 20 ºC.

Mobile phase: isopropanol

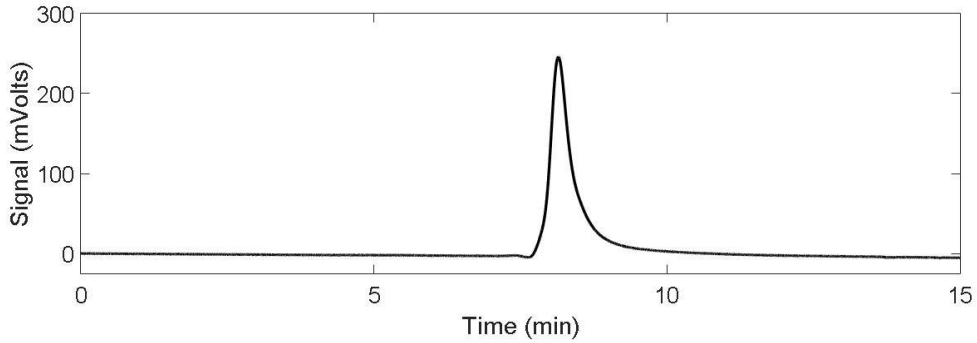

Figure A.14 – HPLC chromatogram of a binary mixture of betulinic (BA, 0.5250 mg/mL) and oleanolic (OA, 0.5250 mg/mL) acids using an Acclaim C30 column with isopropanol as mobile phase. Flow rate of 0.4 mL/min, loop volume of 100 µL, and 20 ºC.

Mobile phase: isopropanol/acetonitrile 50/50 (%, v/v)

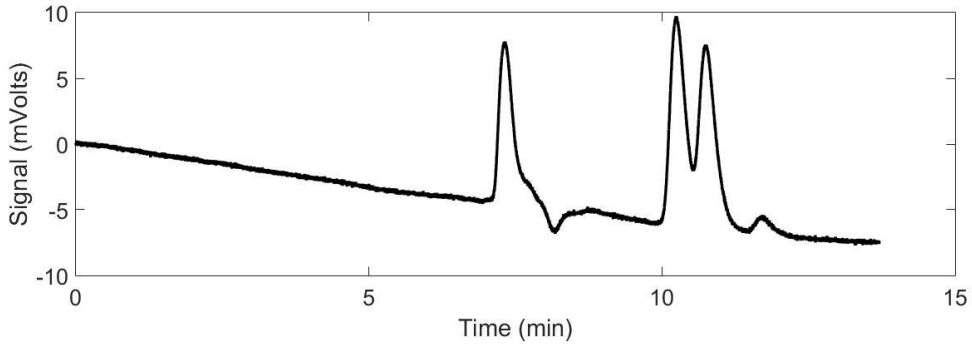

Figure A.15 – HPLC chromatogram of a binary mixture of betulinic (BA, 0.2450 mg/mL) and oleanolic (OA, 0.2500 mg/mL) acids using an Acclaim C30 column with isopropanol/acetonitrile 50/50 (%, v/v) as mobile phase. Flow rate of 0.4 mL/mi, loop volume of 100 µL, and 20 ºC.

Mobile phase: ethyl acetate

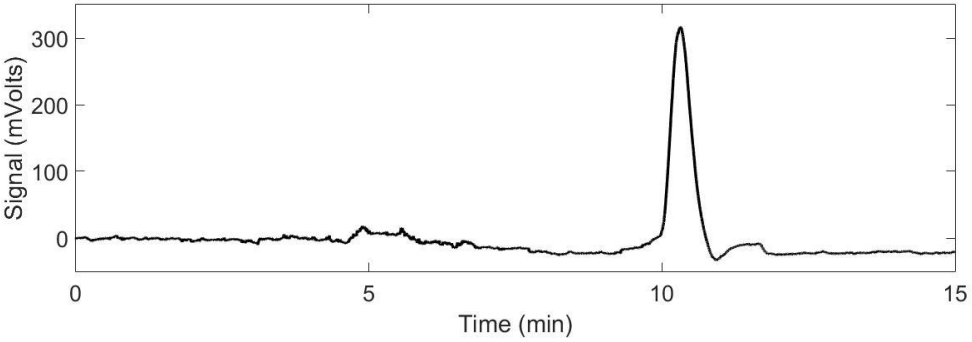

Figure A.16 – HPLC chromatogram of a binary mixture of betulinic (BA, 0.5000 mg/mL) and oleanolic (OA, 0.5000 mg/mL) acids using an Acclaim C30 column with ethyl acetate as mobile phase. Flow rate of 0.3 mL/min, loop volume of 100 µL, and 20 ºC.

Mobile phase: methanol/acetone 50/50 (%, v/v)

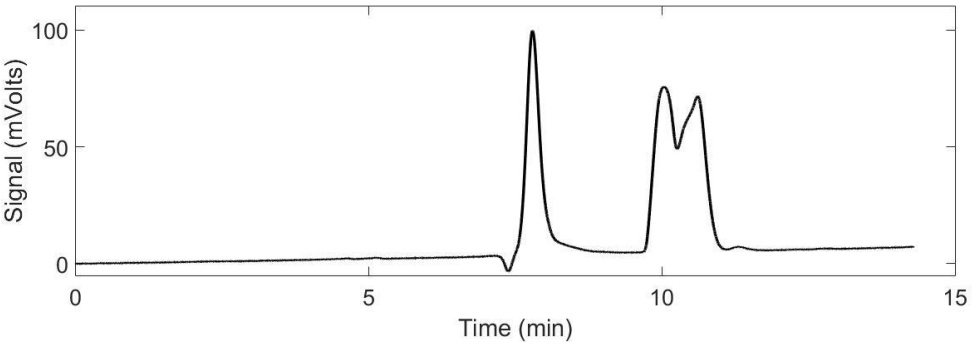

Figure A.17 – HPLC chromatogram of a binary mixture of betulinic (BA, 0.5150 mg/mL) and oleanolic (OA, 0.5500 mg/mL) acids using an Acclaim C30 column with methanol/acetone 50/50 (%, v/v) as mobile phase. Flow rate of 0.4 mL/min, loop volume of 100 µL, and 20 ºC.

Appendix B

Concentration profiles of betulinic and oleanolic acids in the SMB unit obtained by simulations

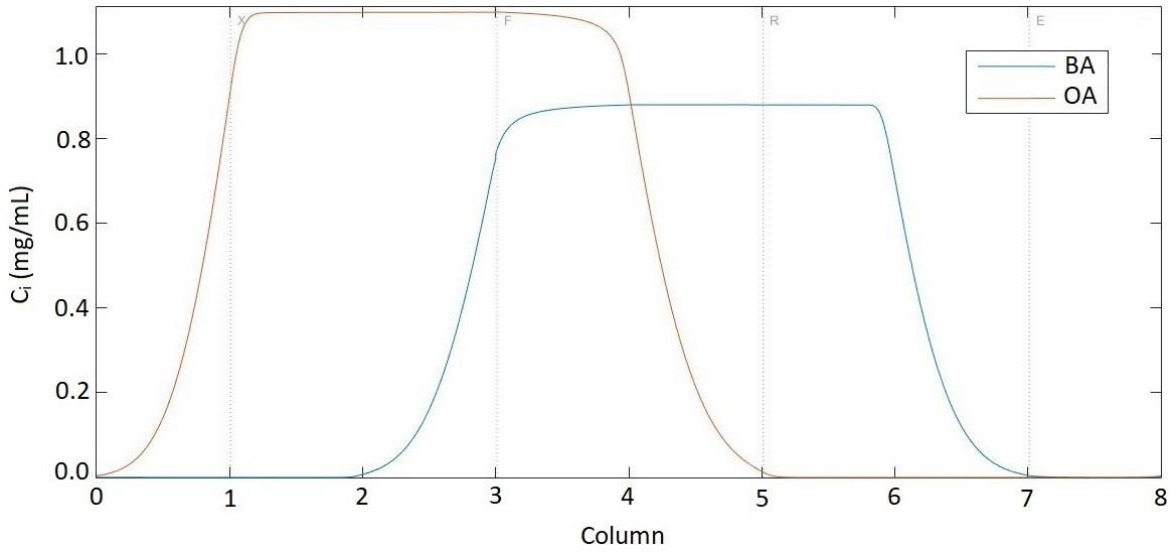

Figure B.1 – Concentration profiles of betulinic and oleanolic acids for simulations with configuration 2-2-2-2, column lengths of 15 cm (β equal to 1.000), at 20 ºC.

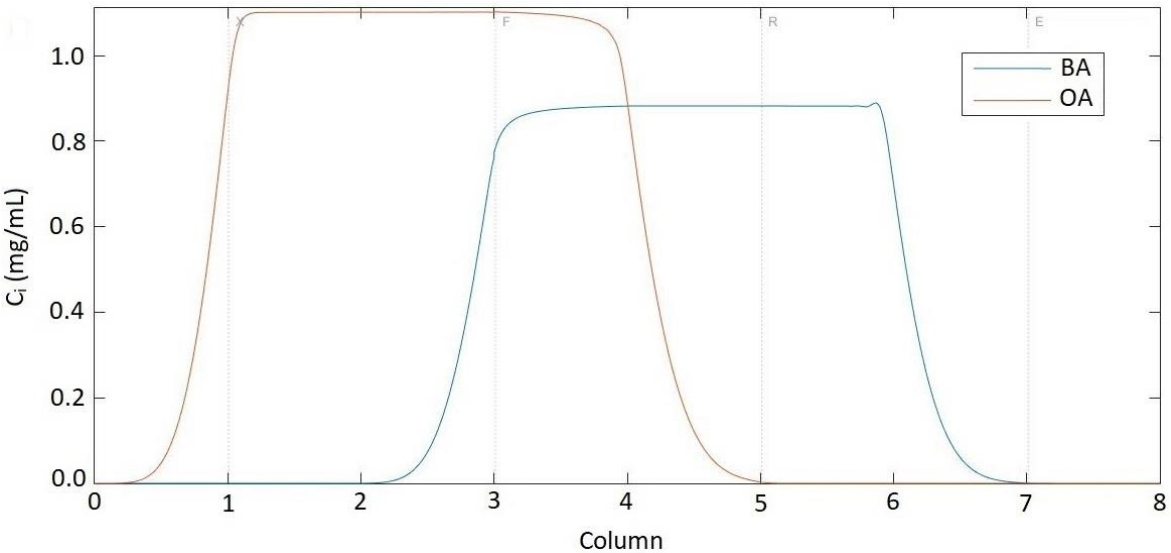

Figure B.2 – Concentration profiles of betulinic and oleanolic acids for simulations with configuration 2-2-2-2, column lengths of 20 cm (β equal to 1.000), at 20 ºC.

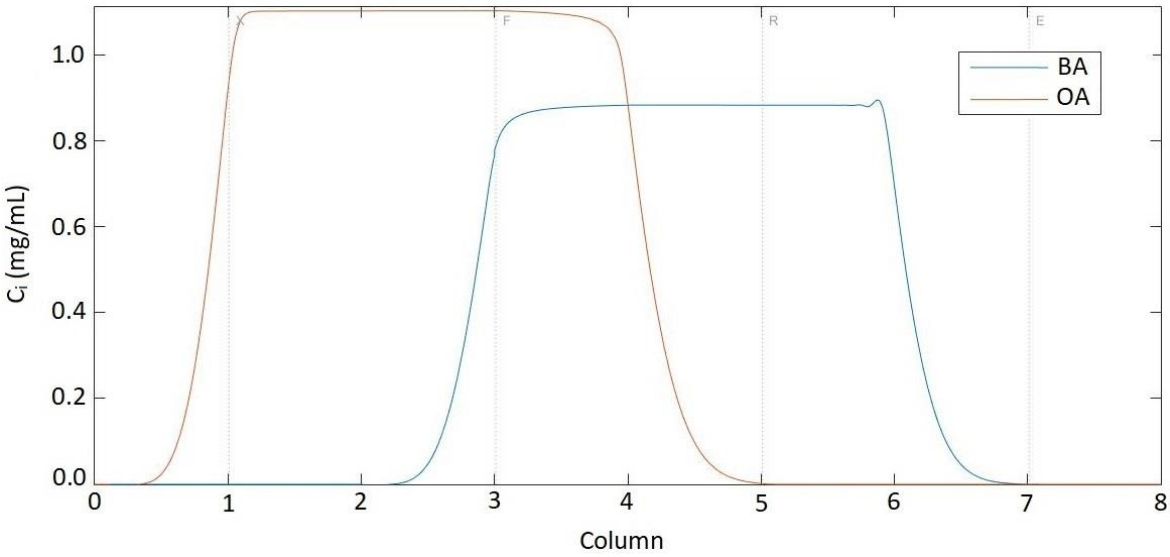

Figure B.3 – Concentration profiles of betulinic and oleanolic acids for simulations with configuration 2-2-2-2, column lengths of 25 cm (β equal to 1.000), at 20 ºC.

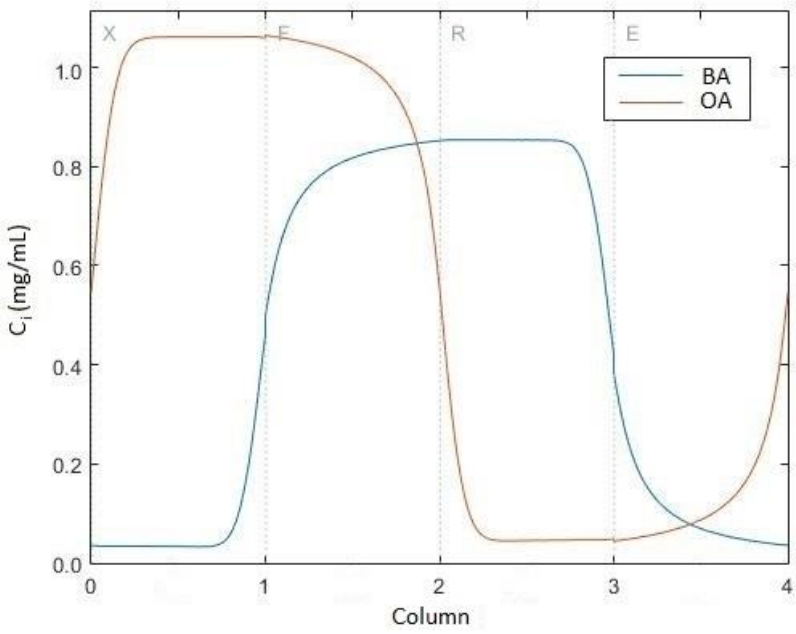

Figure B.4 – Concentration profiles of betulinic and oleanolic acids for simulations with configuration 1-1-1-1, column lengths of 10 cm (β equal to 1.000), at 20 ºC.

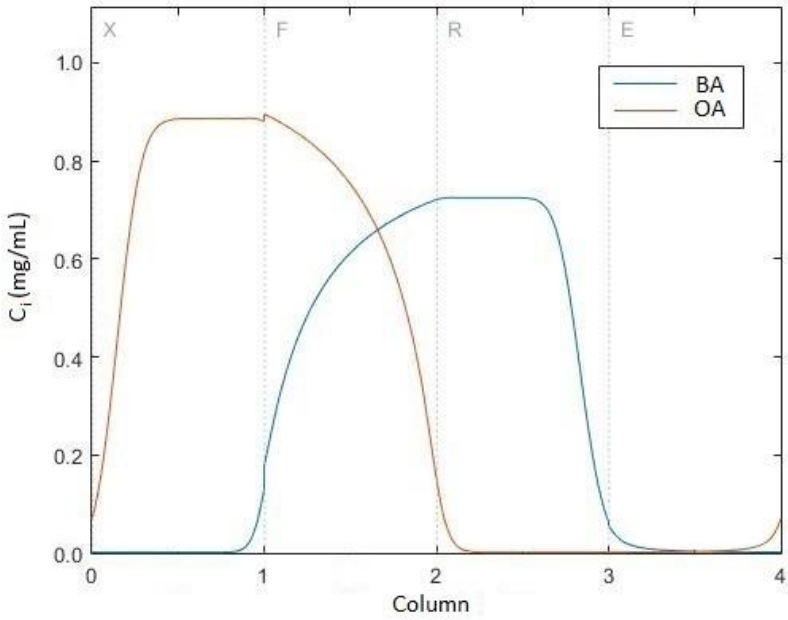

Figure B.5 – Concentration profiles of betulinic and oleanolic acids for simulations with configuration 1-1-1-1, column lengths of 10 cm (β equal to 1.020), at 20 ºC.

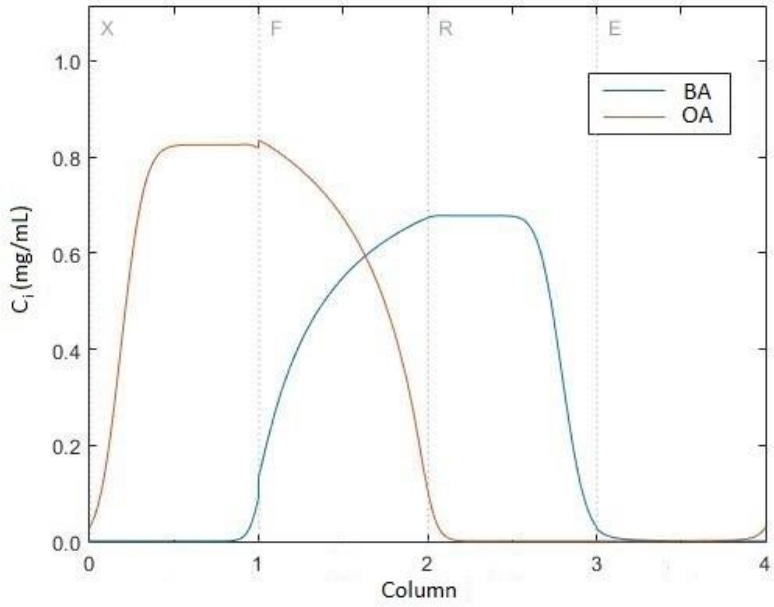

Figure B.6 – Concentration profiles of betulinic and oleanolic acids for simulations with configuration 1-1-1-1, column lengths of 10 cm (β equal to 1.025), at 20 ºC.

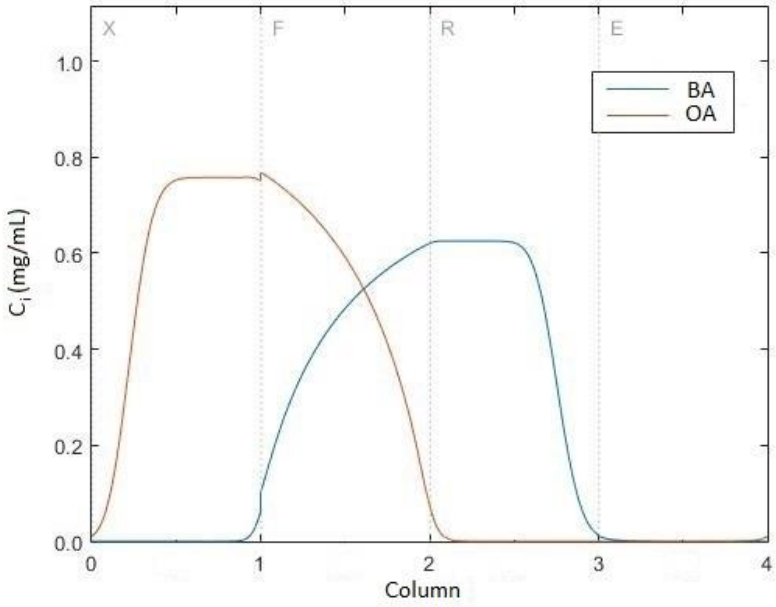

Figure B.7 – Concentration profiles of betulinic and oleanolic acids for simulations with configuration 1-1-1-1, column lengths of 10 cm (β equal to 1.030), at 20 ºC.

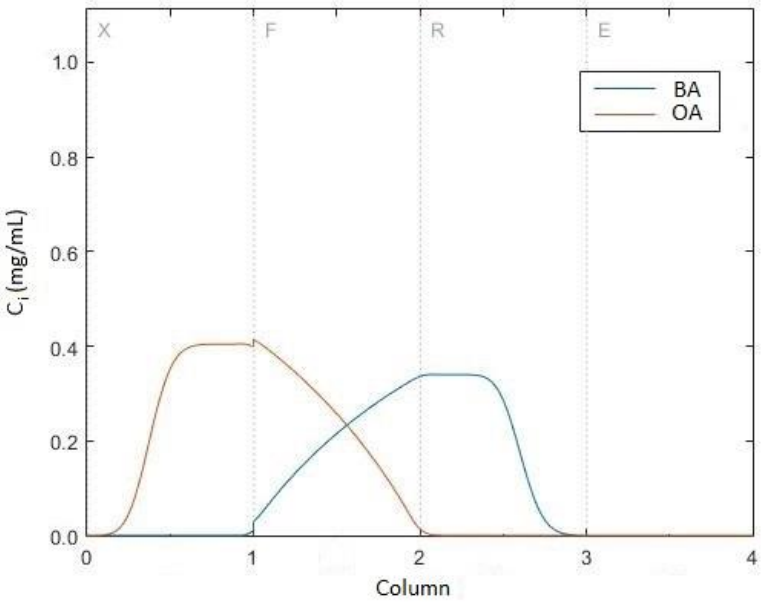

Figure B.8 – Concentration profiles of betulinic and oleanolic acids for simulations with configuration 1-1-1-1, column lengths of 10 cm (β equal to 1.050), at 20 ºC.

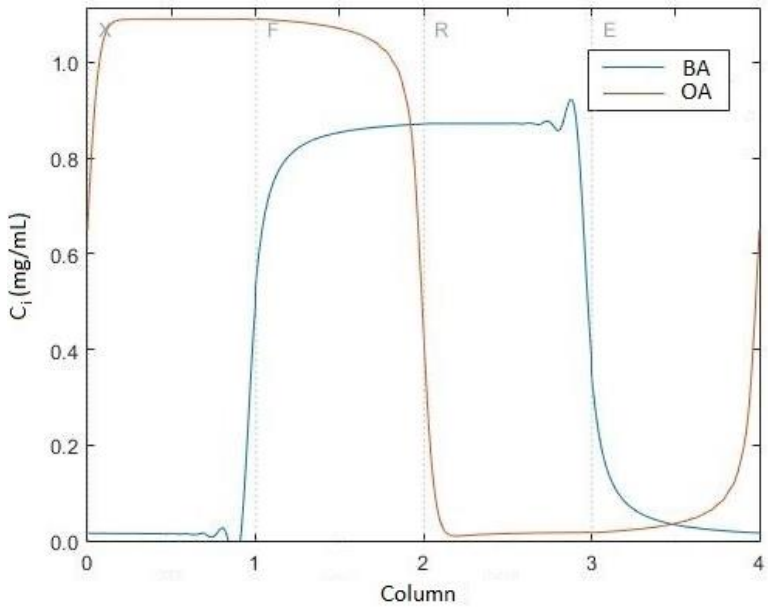

Figure B.9 – Concentration profiles of betulinic and oleanolic acids for simulations with configuration 1-1-1-1, column lengths of 25 cm (β equal to 1.000), at 20 ºC.

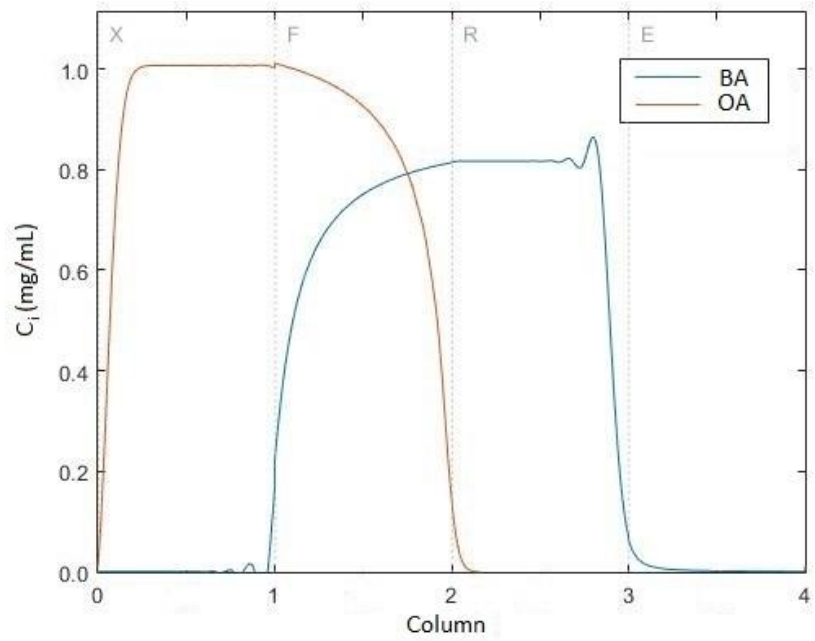

Figure B.10 – Concentration profiles of betulinic and oleanolic acids for simulations with configuration 1-1-1-1, column lengths of 25 cm (β equal to 1.010), at 20 ºC.

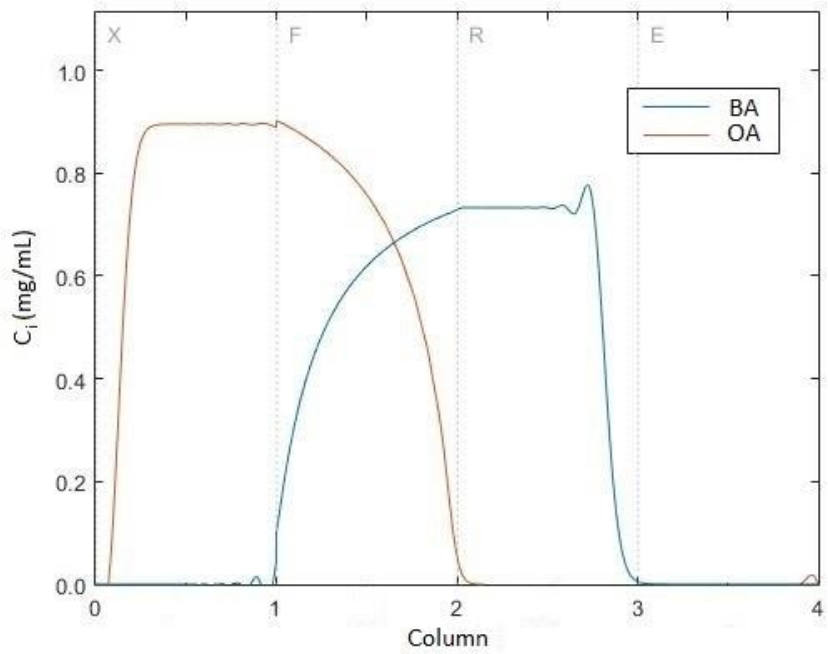

Figure B.11 – Concentration profiles of betulinic and oleanolic acids for simulations with configuration 1-1-1-1, column lengths of 25 cm (β equal to 1.020), at 20 ºC.

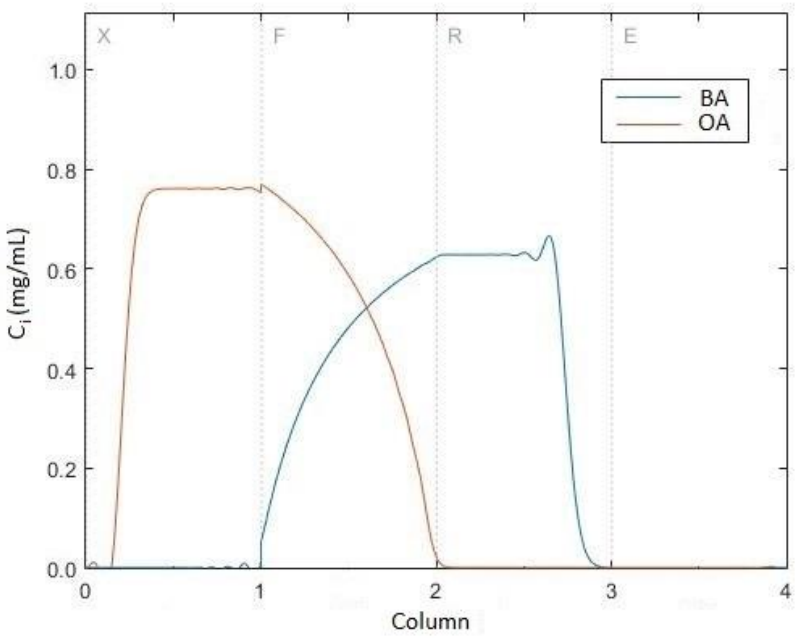

Figure B.12 – Concentration profiles of betulinic and oleanolic acids for simulations with configuration 1-1-1-1, column lengths of 25 cm (β equal to 1.030), at 20 ºC.

Concentration history of the raffinate stream of the SMB unit obtained by simulation

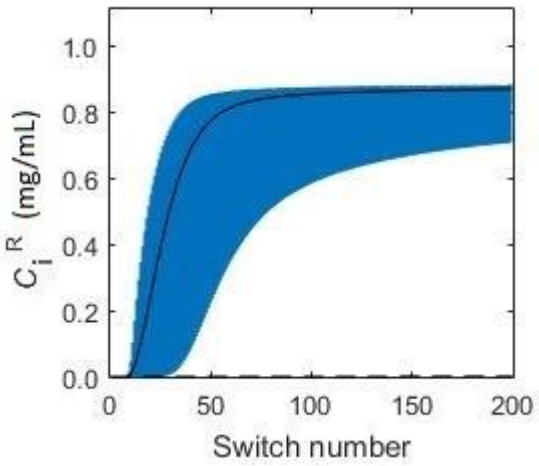

Figure B.13 – Switch time average concentrations in the raffinate and betulinic acid concentration history (blue) for simulations with configuration 2-2-2-2, column lengths of 15 cm (β equal to 1.000), and 20 ºC. Full black line represents the average concentration of betulinic acid and dashed line represents the average concentration of oleanolic acid.

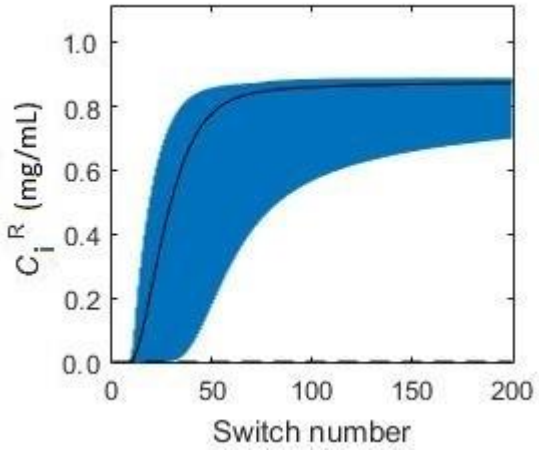

Figure B.14 – Switch time average concentrations in the raffinate and betulinic acid concentration history (blue) for simulations with configuration 2-2-2-2, column lengths of 20 cm (β equal to 1.000), and 20 ºC. Full black line represents the average concentration of betulinic acid and dashed line represents the average concentration of oleanolic acid.

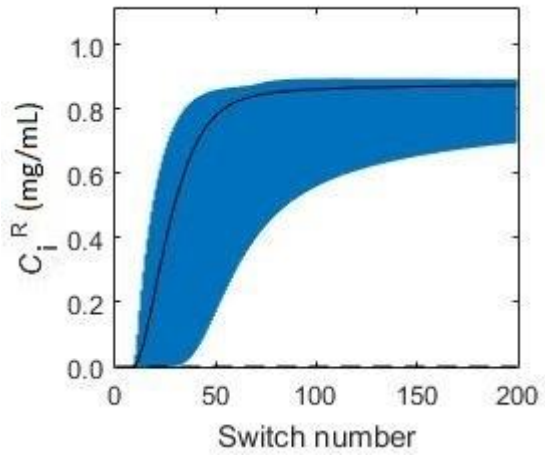

Figure B.15 – Switch time average concentrations in the raffinate and betulinic acid concentration history (blue) for simulations with configuration 2-2-2-2, column lengths of 25 cm (β equal to 1.000), and 20 ºC. Full black line represents the average concentration of betulinic acid and dashed line represents the average concentration of oleanolic acid.

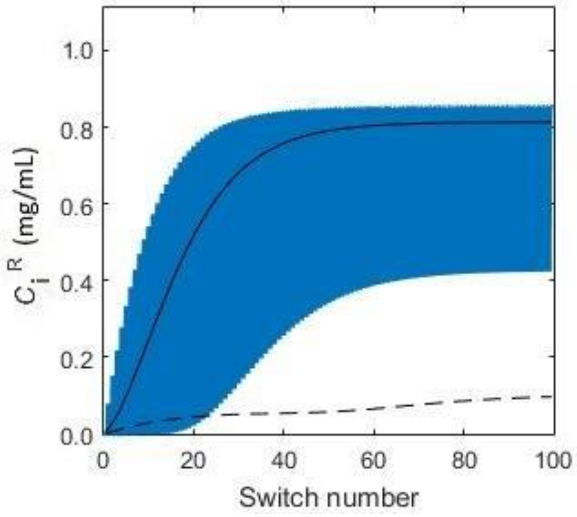

Figure B.16 – Switch time average concentrations in the raffinate and betulinic acid concentration history (blue) for simulations with configuration 1-1-1-1, column lengths of 10 cm (β equal to 1.000), and 20 ºC. Full black line represents the average concentration of betulinic acid and dashed line represents the average concentration of oleanolic acid.

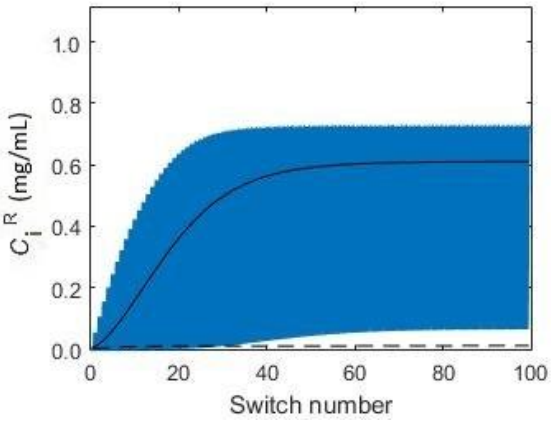

Figure B.17 – Switch time average concentrations in the raffinate and betulinic acid concentration history (blue) for simulations with configuration 1-1-1-1, column lengths of 10 cm (β equal to 1.020), and 20 ºC. Full black line represents the average concentration of betulinic acid and dashed line represents the average concentration of oleanolic acid.

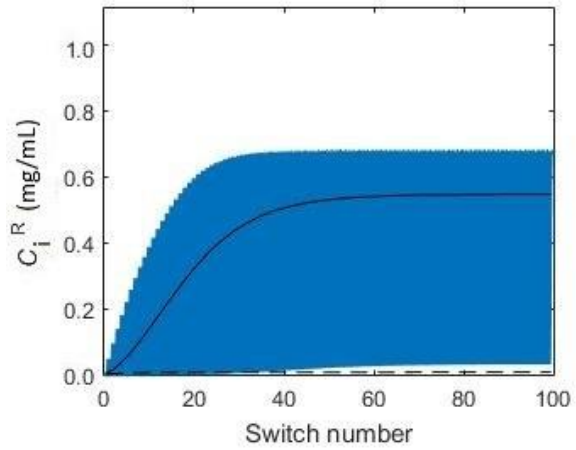

Figure B.18 – Switch time average concentrations in the raffinate and betulinic acid concentration history (blue) for simulations with configuration 1-1-1-1, column lengths of 10 cm (β equal to 1.025), and 20 ºC. Full black line represents the average concentration of betulinic acid and dashed line represents the average concentration of oleanolic acid.

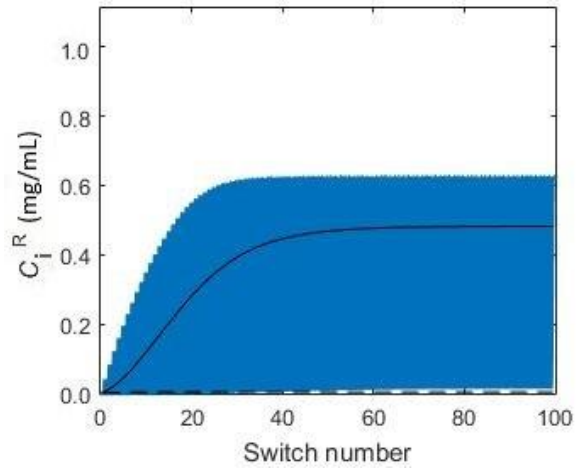

Figure B.19 – Switch time average concentrations in the raffinate and betulinic acid concentration history (blue) for simulations with configuration 1-1-1-1, column lengths of 10 cm (β equal to 1.030), and 20 ºC. Full black line represents the average concentration of betulinic acid and dashed line represents the average concentration of oleanolic acid.

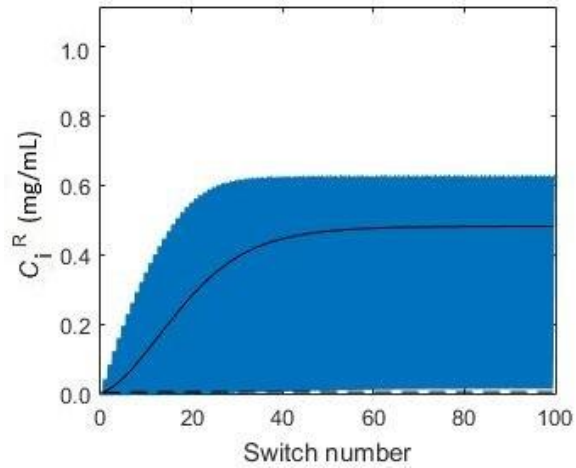

Figure B.20 – Switch time average concentrations in the raffinate and betulinic acid concentration history (blue) for simulations with configuration 1-1-1-1, column lengths of 10 cm (β equal to 1.050), and 20 ºC. Full black line represents the average concentration of betulinic acid and dashed line represents the average concentration of oleanolic acid.

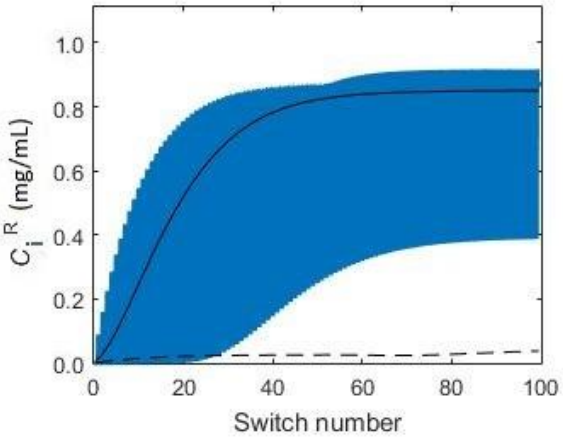

Figure B.21 – Switch time average concentrations in the raffinate and betulinic acid concentration history (blue) for simulations with configuration 1-1-1-1, column lengths of 25 cm (β equal to 1.000), and 20 ºC. Full black line represents the average concentration of betulinic acid and dashed line represents the average concentration of oleanolic acid.

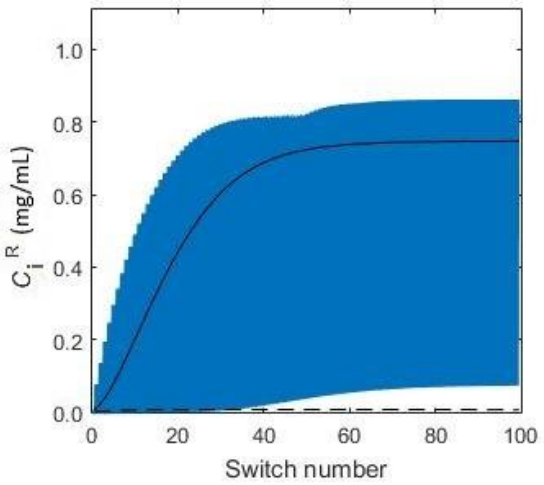

Figure B.22 – Switch time average concentrations in the raffinate and betulinic acid concentration history (blue) for simulations with configuration 1-1-1-1, column lengths of 25 cm (β equal to 1.010), and 20 ºC. Full black line represents the average concentration of betulinic acid and dashed line represents the average concentration of oleanolic acid.

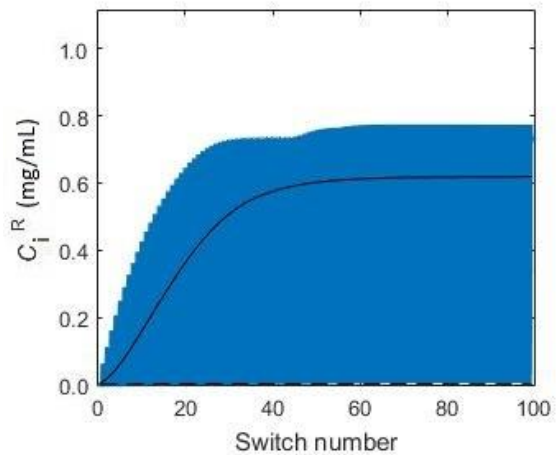

Figure B.23 – Switch time average concentrations in the raffinate and betulinic acid concentration history (blue) for simulations with configuration 1-1-1-1, column lengths of 25 cm (β equal to 1.020), and 20 ºC. Full black line represents the average concentration of betulinic acid and dashed line represents the average concentration of oleanolic acid.

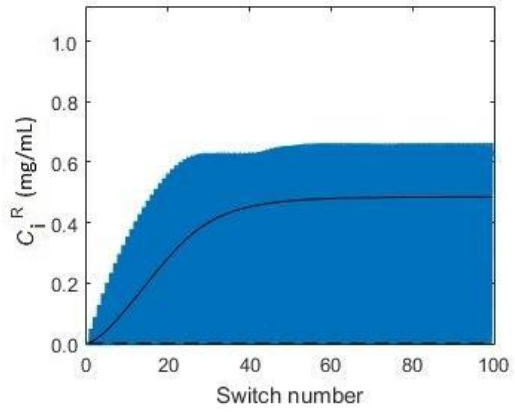

Figure B.24 – Switch time average concentrations in the raffinate and betulinic acid concentration history (blue) for simulations with configuration 1-1-1-1, column lengths of 25 cm (β equal to 1.030), and 20 ºC. Full black line represents the average concentration of betulinic acid and dashed line represents the average concentration of oleanolic acid.

Concentration history of the extract stream of the SMB unit obtained by simulation

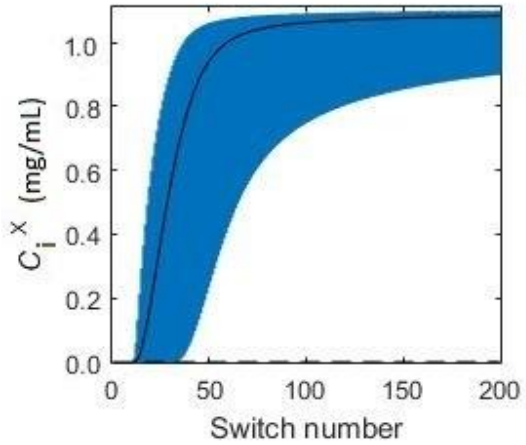

Figure B.25 – Switch time average concentrations in the extract and oleanolic acid concentration history (blue) for simulations with configuration 2-2-2-2, column lengths of 15 cm (β equal to 1.000), and 20 ºC. Full black line represents the average concentration of oleanolic acid and dashed line represents the average concentration of betulinic acid.

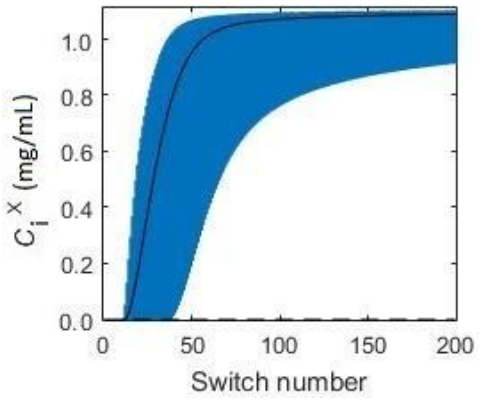

Figure B.26 – Switch time average concentrations in the extract and oleanolic acid concentration history (blue) for simulations with configuration 2-2-2-2, column lengths of 20 cm (β equal to 1.000), and 20 ºC. Full black line represents the average concentration of oleanolic acid and dashed line represents the average concentration of betulinic acid.

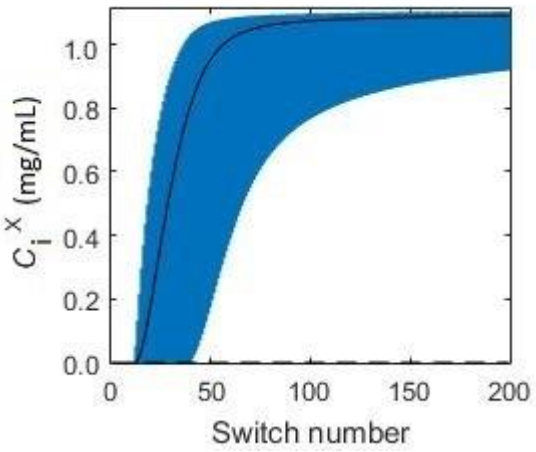

Figure B.27 – Switch time average concentrations in the extract and oleanolic acid concentration history (blue) for simulations with configuration 2-2-2-2, column lengths of 25 cm (β equal to 1.000), and 20 ºC. Full black line represents the average concentration of oleanolic acid and dashed line represents the average concentration of betulinic acid.

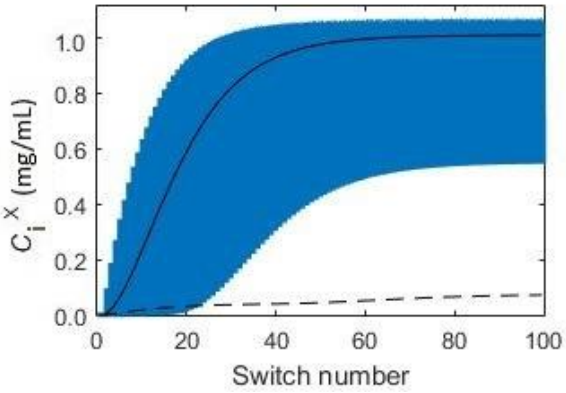

Figure B.28 – Switch time average concentrations in the extract and oleanolic acid concentration history (blue) for simulations with configuration 1-1-1-1, column lengths of 10 cm (β equal to 1.000), and 20 ºC. Full black line represents the average concentration of oleanolic acid and dashed line represents the average concentration of betulinic acid.

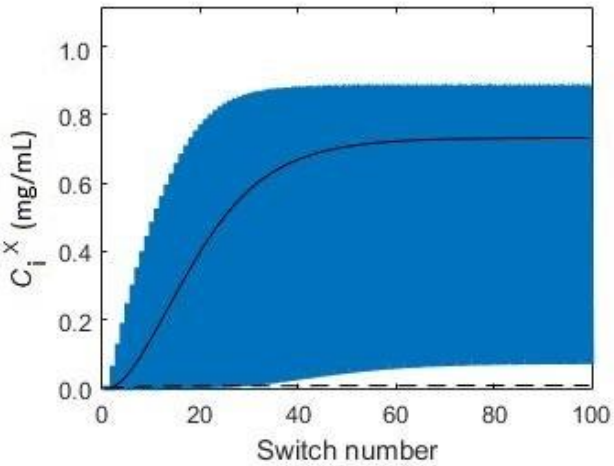

Figure B.29 – Switch time average concentrations in the extract and oleanolic acid concentration history (blue) for simulations with configuration 1-1-1-1, column lengths of 10 cm (β equal to 1.020), and 20 ºC. Full black line represents the average concentration of oleanolic acid and dashed line represents the average concentration of betulinic acid.

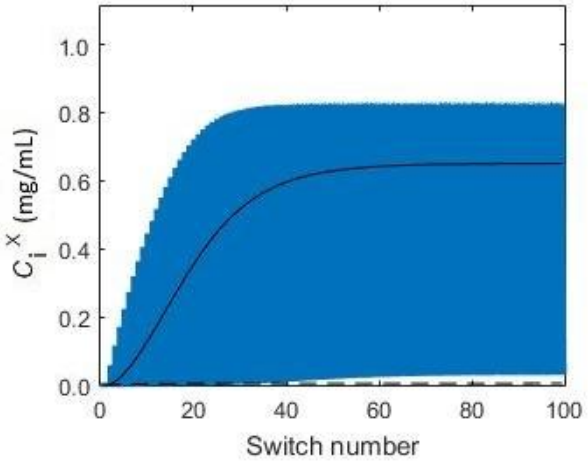

Figure B.30 – Switch time average concentrations in the extract and oleanolic acid concentration history (blue) for simulations with configuration 1-1-1-1, column lengths of 10 cm (β equal to 1.025), and 20 ºC. Full black line represents the average concentration of oleanolic acid and dashed line represents the average concentration of betulinic acid.

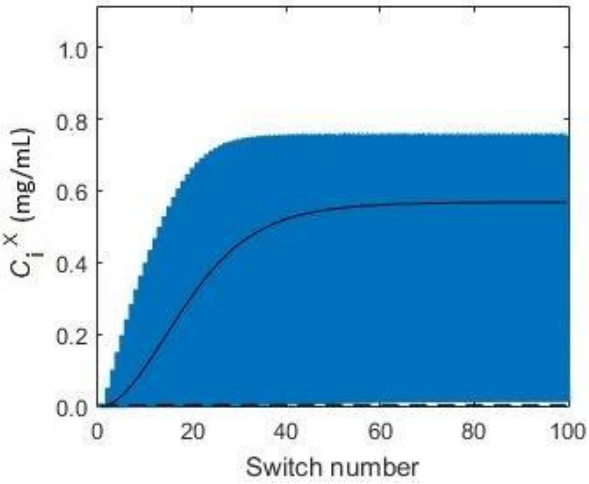

Figure B.31 – Switch time average concentrations in the extract and oleanolic acid concentration history (blue) for simulations with configuration 1-1-1-1, column lengths of 10 cm (β equal to 1.030), and 20 ºC. Full black line represents the average concentration of oleanolic acid and dashed line represents the average concentration of betulinic acid.

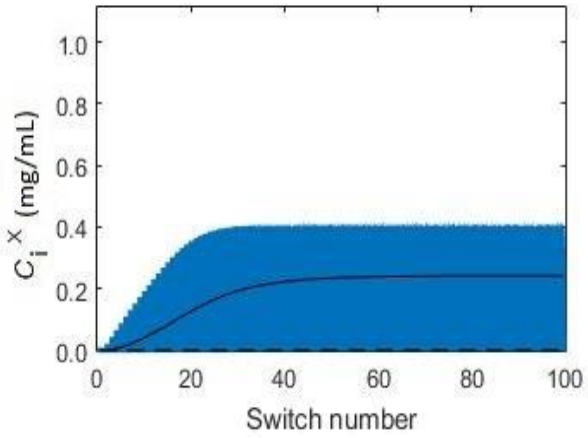

Figure B.32 – Switch time average concentrations in the extract and oleanolic acid concentration history (blue) for simulations with configuration 1-1-1-1, column lengths of 10 cm (β equal to 1.050), and 20 ºC. Full black line represents the average concentration of oleanolic acid and dashed line represents the average concentration of betulinic acid.

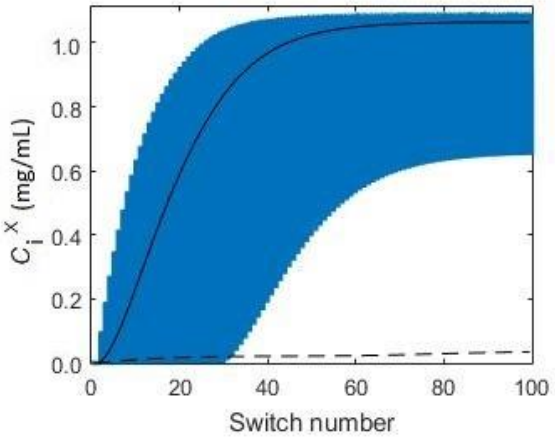

Figure B.33 – Switch time average concentrations in the extract and oleanolic acid concentration history (blue) for simulations with configuration 1-1-1-1, column lengths of 25 cm (β equal to 1.000), and 20 ºC. Full black line represents the average concentration of oleanolic acid and dashed line represents the average concentration of betulinic acid.

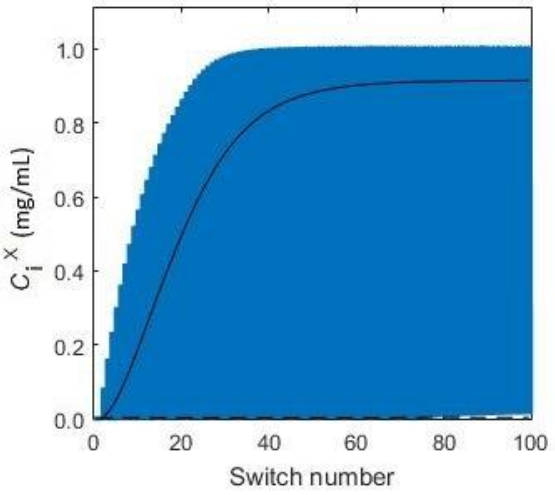

Figure B.34 – Switch time average concentrations in the extract and oleanolic acid concentration history (blue) for simulations with configuration 1-1-1-1, column lengths of 25 cm (β equal to 1.010), and 20 ºC. Full black line represents the average concentration of oleanolic acid and dashed line represents the average concentration of betulinic acid.

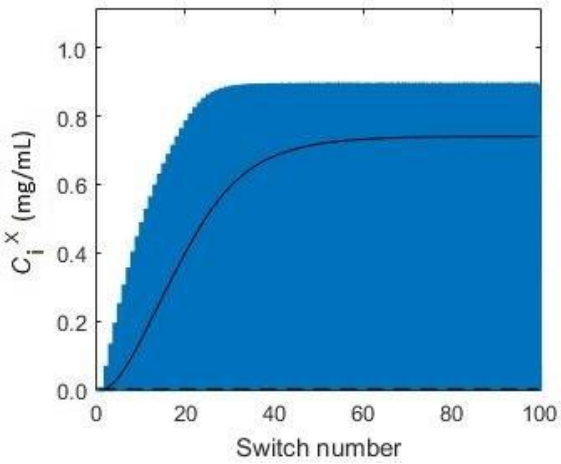

Figure B.35 – Switch time average concentrations in the extract and oleanolic acid concentration history (blue) for simulations with configuration 1-1-1-1, column lengths of 25 cm (β equal to 1.020), and 20 ºC. Full black line represents the average concentration of oleanolic acid and dashed line represents the average concentration of betulinic acid.

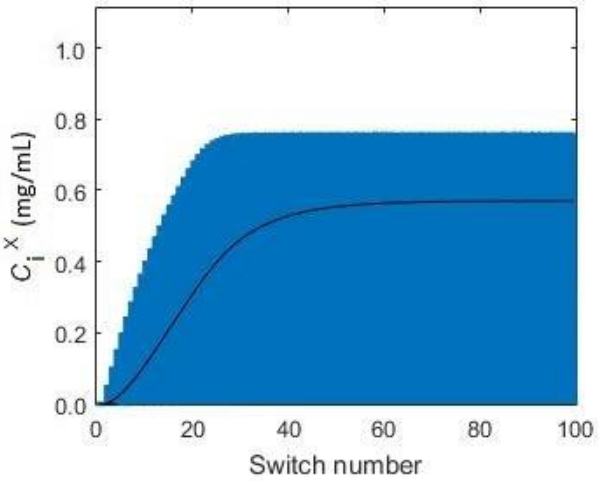

Figure B.36 – Switch time average concentrations in the extract and oleanolic acid concentration history (blue) for simulations with configuration 1-1-1-1, column lengths of 25 cm (β equal to 1.030), and 20 ºC. Full black line represents the average concentration of oleanolic acid and dashed line represents the average concentration of betulinic acid.